Omega-P, Inc.
291 Whitney Avenue – Suite 401
New Haven, CT 06511

COAXIAL TWO-CHANNEL DIELECTRIC WAKE FIELD ACCELERATOR

J. L. Hirshfield, Principal Investigator
tel: (203) 789-1164, e-mail: jay@omega-p.com

Final Report on Phase II DoE SBIR grant DE-SC000 924
Topic 38a: ADVANCED CONCEPTS & TECHNOLOGY FOR HIGH ENERGY ACCELERATORS

ABSTRACT: Theory, computations, and experimental apparatus are presented that describe and are intended to confirm novel properties of a coaxial two-channel dielectic wake field accelerator. In this configuration, an annular drive beam in the outer coaxial channel excites multimode wakefields which, in the inner channel, can accelerator a test beam to an energy much higher than the energy of the drive beam. This high transformer ratio is the result of judicious choice of the dielectric structure parameters, and of the phase separation between drive bunches and test bunches. A structure with cm-scale wakefields has been built for tests at the Argonne Wakefield Accelerator Laboratory, and a structure with mm-scale wakefields has been built for tests at the SLAC FACET facility. Both tests await scheduling by the respective facilities.

TABLE OF CONTENTS

Work on this project was carried out Dr. Thomas C. Marshall and Dr. Gennadi Sotnikov of Omega-P, Inc.; Dr. Sergey Shchelkunov of Yale University working under a sub-grant from Omega-P, Inc.; and J. L. Hirshfield of Omega-P, Inc. serving as Principal Investigator. Dr. Hirshfield edited this report.

April 30, 2013

I. PHASE I RESULTS

Ia. Introduction

In this section we describe the technical accomplishments of the Phase I Coaxial Dielectric Wakefield Accelerator project (CDWA). First among these was the publication of a paper in *Physical Review Special Topics -- Accelerators and Beams* [1] which presents an analytic theory of this structure and compares results of theory with numerical simulations, specifically for a design of our anticipated experiment at Argonne Wakefield Accelerator (AWA) Laboratory, and for a THz design relevant to a future collider application. This published paper provides the theoretical and computational basis for what follows, and for the examples. In this section we summarize results that were goals of our Phase I project. These are divided into three parts, as follows. In Section Ib, we present the design for the AWA experiment, its construction, and the characterization of an annular drive bunch and an axially-moving witness bunch that trails the drive bunch. This apparatus is be used to perform the experiments during Phase II. In Section Ic, we describe a high-gradient THz design that could typify a modular component in a future TeV collider. In Section Id we present results on the stability of bunch motion in the THz unit, and consider what alignment accuracy is needed for reliable bunch transport along the structure.

Ib. Design for AWA Experiment and Related Studies

The AWA facility is to provide individual drive bunches with a charge up to 50 nC and energy of 14 MeV, so the design described here uses the appropriate charge, energy, and dimensions of these bunches, and the equipment is designed to be accommodated in a test chamber compatible with AWA beamline hardware. The CDWA unit fits into the same vacuum chamber and on the same adjustable mount that was built for our two-channel DWA experiment that has a *rectangular* configuration. The dominant modes excited by the bunch in our new structure are at a frequency ~ 28 GHz. The structure uses two nested thin cylinders of Alumina, obtained from Ortech Ceramics, the outer of which is to be coated with UHV deposited copper. An annular drive bunch sets up a wakefield which is directed onto the common cylinder axis where a suitably-delayed witness bunch having small charge is to be accelerated. An "exploded" view of the structure is shown in Fig. 1. The front and rear aligners hold the ceramic tubes, and are spaced apart on the mounting platform (purple). The aligners space and support the suspended inner dielectric cylinder by three narrow vanes made of stainless steel. While these vanes intercept narrow portions of the annular drive bunch, this should cause little trouble for the experiment, as it is only 10 cm in length. The drive bunch is intercepted by a beam stop at the exit end of the unit, while the witness bunch is diverted into diagnostic hardware, chiefly an energy analyzer (not shown). Also not shown is the hardware for positioning and aligning the unit in its vacuum chamber. Table I lists the parameters of the structure and the bunch; the Ortech ceramic cylinders closely match the dimensions listed. A preliminary version of this structure has been built and assembled at AWA. [See photos in Section II, Figs. 4 and 5.] The results we describe in this section depend on assumptions we have made about the drive bunch charge and its charge distribution. For this, we have used parameters provided by AWA. The radial distribution of charge in the bunch has been simplified to a box distribution.

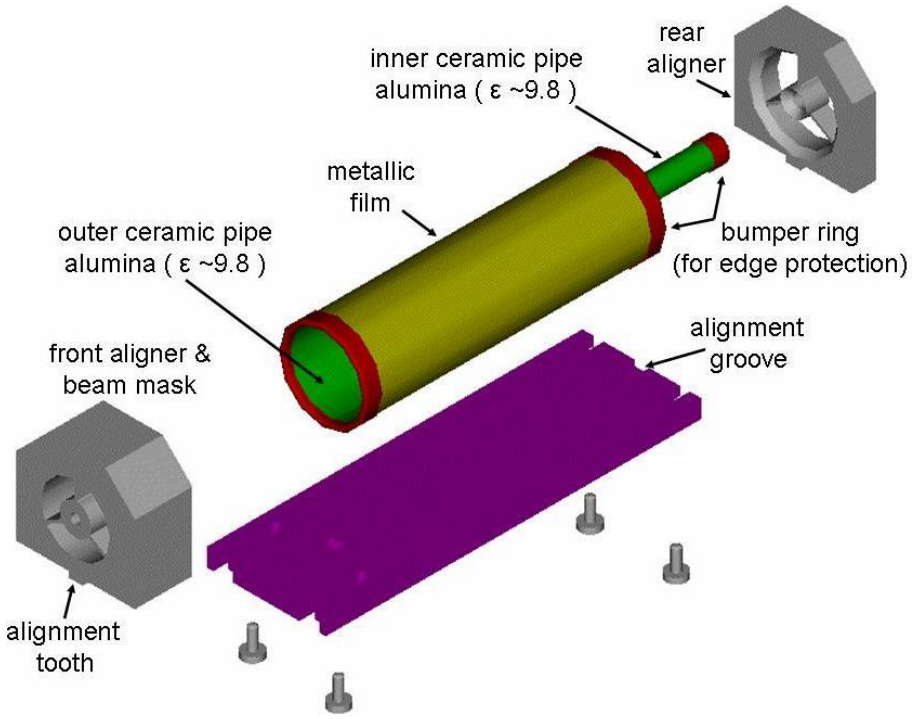

Fig. 1. Exploded view of the CDWA hardware. Photos of the hardware are shown in Section II.

Table I. Parameters for a two-beam channel Coaxial structure (Alumina)

Design mode	~? GHz
Boundary condition	Electric
Surrounding space	PEC+10mm FS r.e.
External radius of outer coaxial cylinder R_e	15.08 mm
Inner radius of outer coaxial waveguide R_i	13.5mm
Accl. channel radius (inner radius of inner coaxial cylinder) a	2.4 mm
External radius of inner coaxial cylinder b	4.0 mm
Relative dielectric constant ε	9.8
Bunch axial RMS dimension $2\sigma_z$ (Gaussian charge distributition)	2.0 mm
Full bunch length (=2 cutoff length of bunch)	5 mm
Outer drive bunch radius (Box charge distributition)	10.75mm
Inner drive bunch radius	6.75 mm
Bunch energy	14 MeV
Bunch charge	50 nC
Number of bunches	1

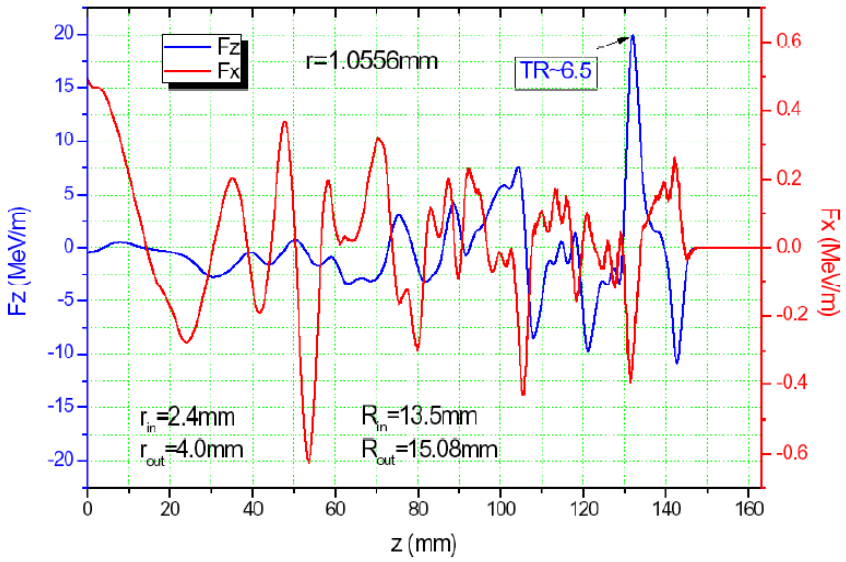

Fig. 2. Axial and transverse forces on the witness bunch; bunches move left to right.

Figure 2 shows the computed accelerating force acting upon the witness bunch along the axis, and the transverse force acting on bunch electrons that are located approximately 1 mm off this axis. The drive bunch head has moved to z = 149 mm here, and the witness bunch is to be located where the arrow indicates a computed transformer ratio of 6.5:1 (~17 mm behind the head of the drive bunch). Notice this transverse force is focusing ($F_x < 0$ for x = +1mm). The jumble of waves behind this location has to do with the quenching wave interfering with the wakefield; the quenching wave extends from $0 < z < 125$ mm.

A map of the axial electric field is shown in Fig. 3. As one can see at the extreme left of Fig. 3 where the drive bunch is located, the fields are uniform across the drive bunch channel.

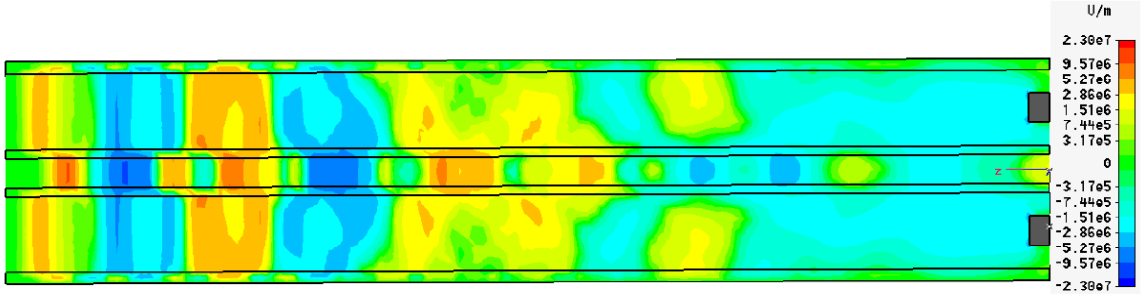

Fig. 3.B.3. Map (*x*,*z*) of the axial electric field (force) set up by the drive bunch travelling from right to left, and here located at the far left; the witness bunch would be located on-axis in the region of the intense blue spot about 17 mm behind the head of the drive bunch. Outlines of the dielectric cylinders are shown as black horizontal lines. Note how the quenching wave wipes out the periodic wake field after about two wake periods.

This effect may account for the excellent behavior of the drive bunch motion. The plot also shows the orderly wakefields being disrupted by the quenching wave as one follows the trailing fields set up by the drive bunch farther downstream (right).

Numerical studies have been made for bunch production at the AWA RF photocathode gun and transport through the AWA beam-line system downstream leading to the location of our structure. In the past these numerical tools have proved to be successful in

guiding experimental work at AWA including our work with the rectangular DWA. Fig. 4a shows the two bunches after they have been created at the cathode, and Fig. 4b shows them at and passing through our structure. This demonstrates that an annular drive bunch containing ~30 nC followed by a small, delayed witness bunch can be created and successfully transported through our structure. Transport is assisted by the use of three solenoid coils (borrowed from Yale Beam Physics Lab) positioned along the beamline. The initial radius of the annular bunch at the RF photocathode is ~ 5mm, and the code shows this bunch can be transported at least 4 m to the structure and then passed along the entire 10 cm length of the CDWA, without intercepting its walls. As the structure is supported in this design by three vanes, there should be no problem with passing the bunch into the unit or aligning the central dielectric cylinder (such as might have been the case for a foil suspension technique). In these simulations, the halo mask in front of the structure is ignored, so some of the electron macroparticles can stray into the dielectric elements and are counted as lost.

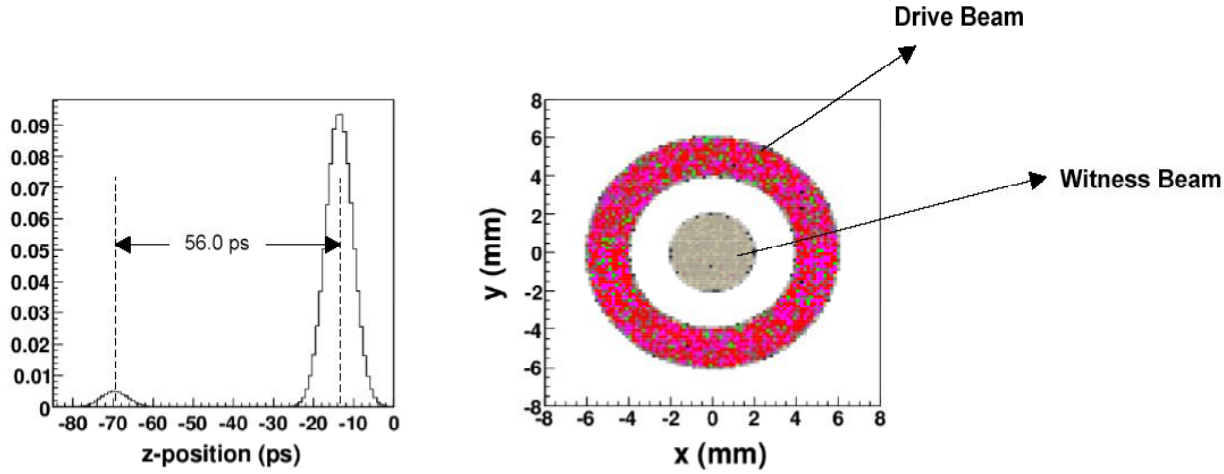

Fig. 4a. Drive and witness bunches after the photocathode (simulation by Dr. Daniel Mihalcea, AWA). Drive bunch energy = 14.8 MeV; witness bunch energy = 12.8 MeV, energy spread = 0.5 MeV RMS. Witness bunch delay is 1.7 cm behind drive bunch.

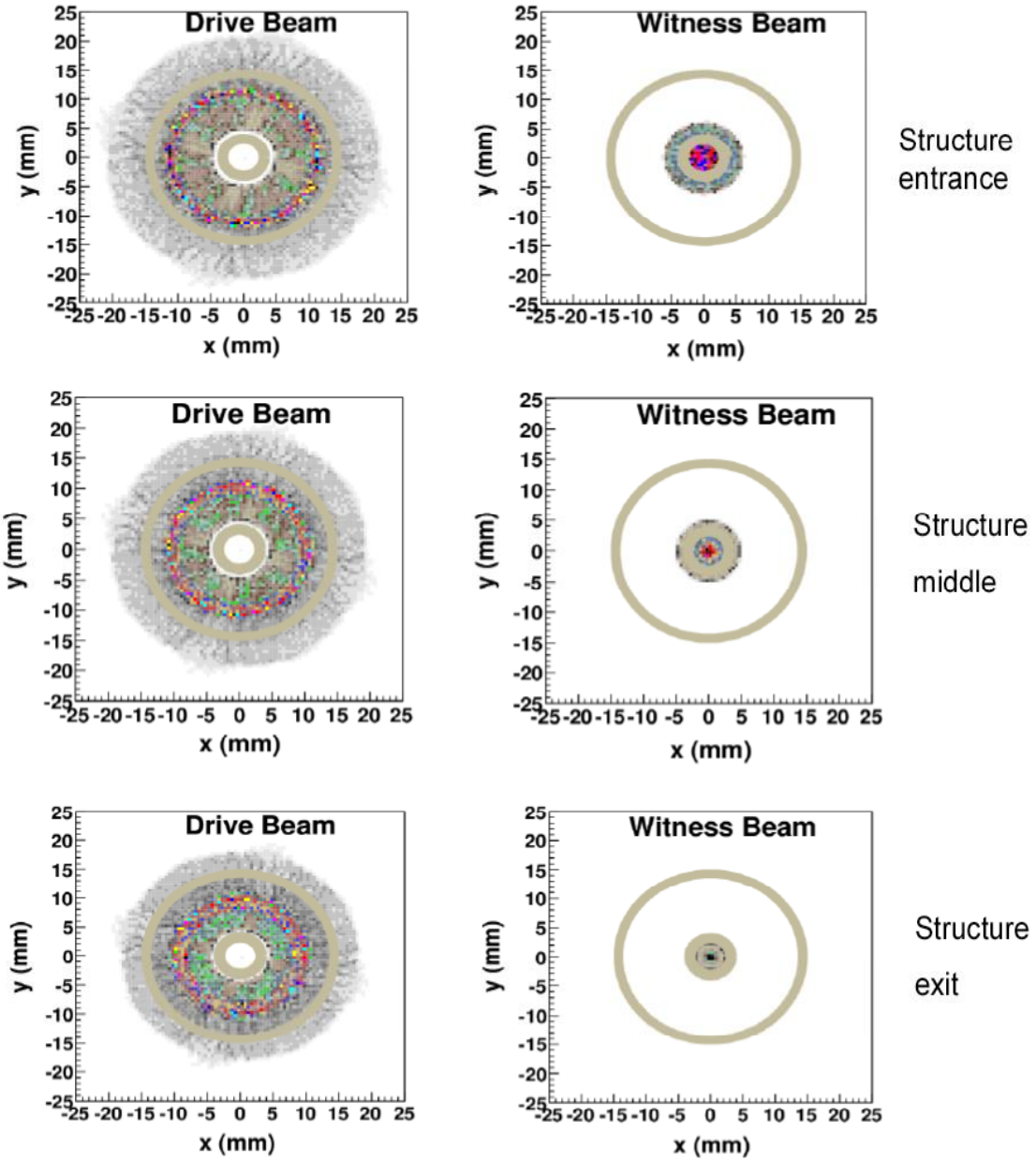

Fig. 4b. Transverse portraits of drive and witness bunch transverse as they move through our structure. Charge passed through the structure: drive bunch = 36 nC (76%); witness bunch = 0.6 nC (24%); no drive bunch/witness bunch contamination. The Yale coils provide transport for 95% of the charge from the photocathode to the entrance of the structure. Tan rings are the dielectric shells.

Our wake field codes can also compute the distribution of energies of the drive and witness bunches. The latter is shown in Fig. 5. The predicted energy gain above the 14 MeV input is approximately 0.5 MeV. There is a spread of energies because the witness bunch has finite length and a Gaussian shape assumption, and the ~ 1cm periodic wakefield accelerating force varies over the length of the bunch.

We have studied acceleration of the witness bunch as its charge is varied. Too much "loading" will cause a reduction in the gradient. Results are shown in Fig. 6 (corresponding data are to be obtained from our tests at AWA). This computation uses a less optimum design than the one described by Table I, which accounts for the lower value of acceleration. The head of the witness bunch, which has no cumulative charge, suffers little energy degradation

with increasing bunch charge, but its energy increment is small because it is placed at a location where the gradient is less than at the middle of the bunch. This figure suggests that to maintain good acceleration, the witness bunch charge should be a few percent of the drive bunch charge, depending on the transformer ratio. In an accelerator where several modules are used to achieve overall large energy gain, the variation of bunch energy over its length can be partly compensated by changing the wakefield period slightly between modules, so that particles at a certain position in the bunch that do not receive enough energy gain in one module can receive more energy in the next, and vice-versa; a more nearly monoenergetic bunch should thereby result. This concept would be an alternating detuned CDWA.

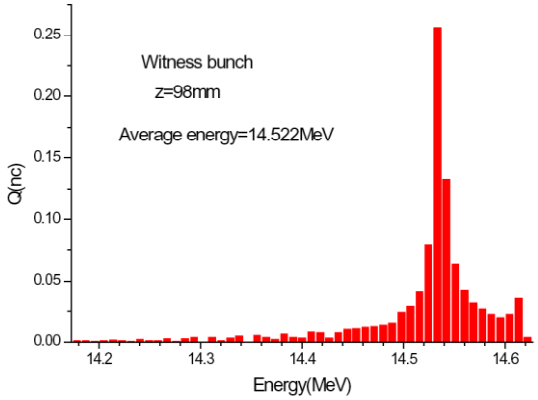

Fig. 5. Distribution of electron energies in the witness bunch, measured near the end of the unit. Input energy of witness bunch is taken to be 14MeV, zero width.

An issue that has been brought up by past reviewers of this work has to do with acceptable alignment accuracies. This is most important in a collider application where each module would be ~ 1 m in length. What are the effects of misalignments? There are several possibilities, but all have to do with one or more components having its axis not aligned with the others. Thus, the drive bunch may not be centered, or perhaps one of the dielectric cylinders. Another misalignment is current asymmetry in the drive bunch. We shall show here an example of each and its effect. In Fig. 7 we show the effect of moving the drive bunch 0.5mm (~5%) off the axis of symmetry. No instability is produced by moving the drive bunch off the axis of symmetry, but in so doing, the forces on the witness bunch are no longer symmetrical, and some minor deflection of the witness bunch in the opposite direction occurs. In the figure, the light gray outline is that of the cathode mount from which the witness bunch is emitted by the software. Thus it is important to maintain alignment symmetry, but we find that a misalignment of ~5 -10% in this design would not cause loss of witness particles in a travel distance of 15cm. The same effect occurs when one of the shells is displaced from the axis of symmetry.

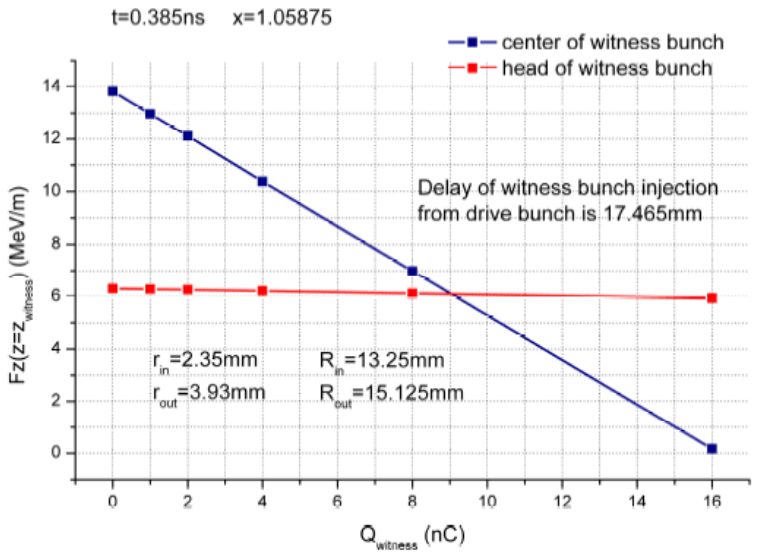

Fig. 6. Reduction of witness bunch accelerating force at the drive bunch center, and at its leading edge, as its charge increases. Radii listed pertain to the two alumina cylinders used for this computation.

Another case is that of asymmetric current in the drive bunch. As an example we show an "m = 1" case, in which the currents in two quadrants of the drive bunch are unequal (Fig. 3.B.8) by +/- 5%. Once again, the witness bunch is slightly deflected. It is interesting to observe that in both of these examples above that the bunch remains focused and the deflecting forces are not large enough to appreciably distort the shape of the witness bunch. However, that will not occur when the asymmetry becomes large, e.g., ~20% for this case. These studies establish that a program of research is possible in Phase II that will permit experimental exploration of the alignment problems (non-concentricity) that will be encountered in this new acceleration concept.

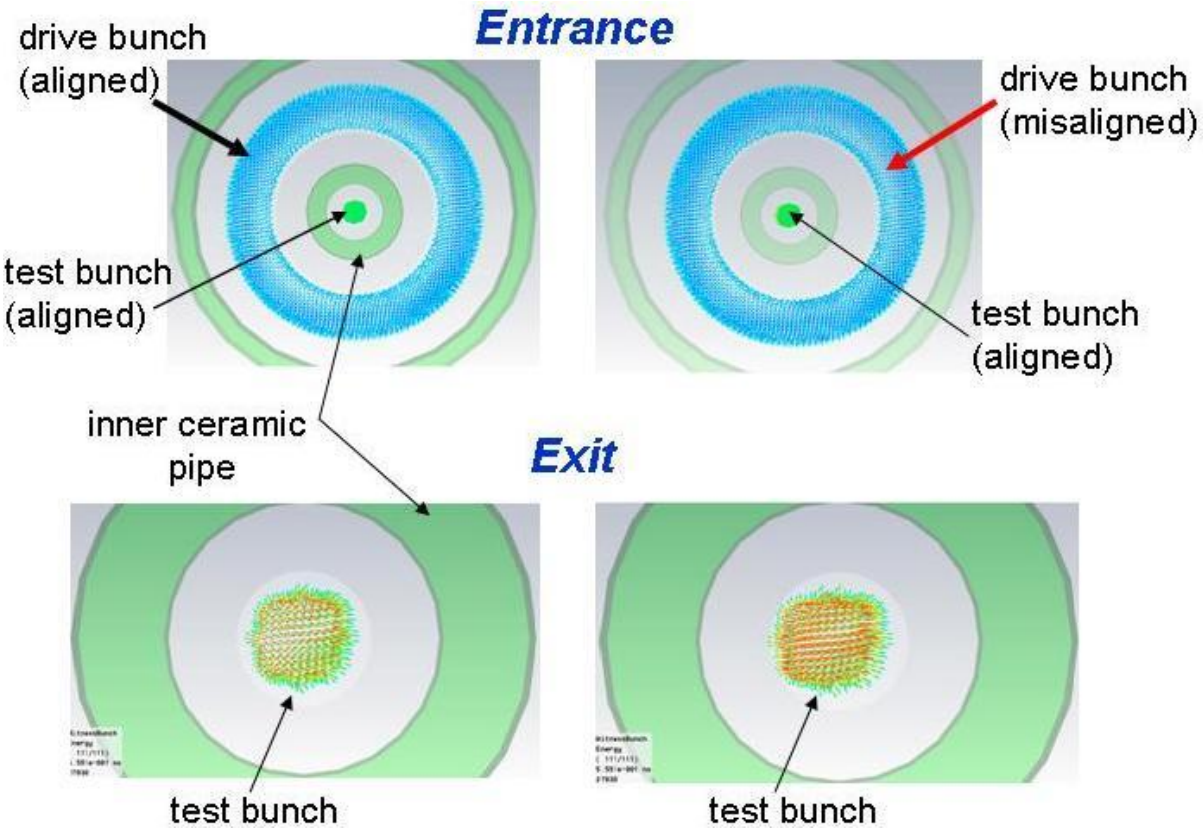

Fig. 7. Left side of diagram: drive bunch aligned, witness bunch at end of unit. Right side of diagram: drive bunch shifted 0.5mm to right, witness bunch deflected to left at the end of the structure.

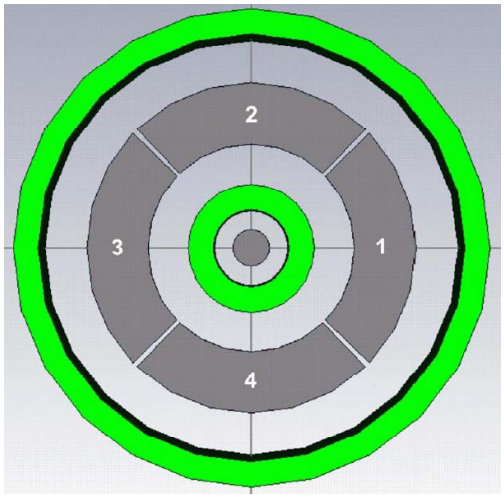

Fig. 8. Drive bunch configured as four sectors, separated by non-emitting spacers. The currents in sectors 2 and 4 are equal, while the current in sector 1 is 95% of #2 and the current in sector 3 is 105% of #2.

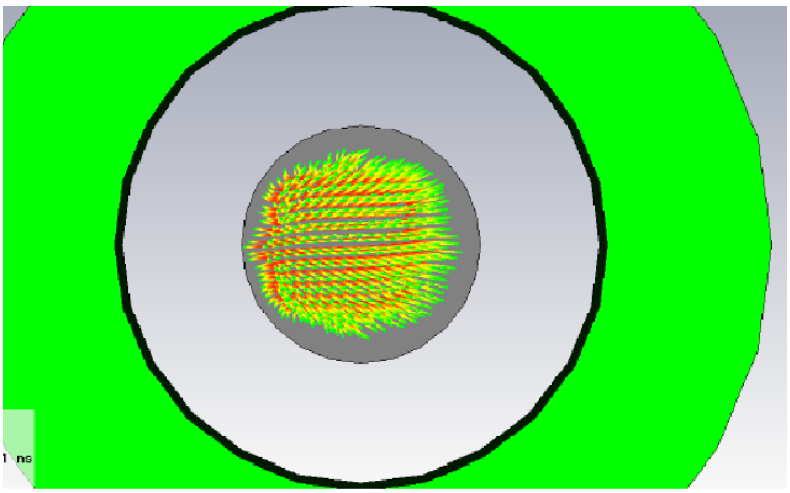

Fig. 9. The witness bunch, deflected by the anisotropic current in the drive bunch, after it has traveled 15cm. Cathode outline is dark gray, first alumina cylinder is green.

Ic. High Gradient THz Design

A design has been carried out for a THz-range coaxial DWA that could have relevance to a future collider application. This has been described in some detail in [1], so we shall only summarize it here. The purpose of this work is to determine if this technology can open a path towards a more affordable TeV machine, and identify where advantages and potential problems occur. Table II provides a list of parameters that we have chosen; note the radius of the structure is ~1mm. The important wakefield modes, which have wavelengths ~ 400μm, are excited to different degrees by the passage of a single 6nC, 5GeV annular drive bunch, such as might be provided by a "conventional" efficient rf linac accelerator. Scale lengths here are not dissimilar from those for some high-gradient laser/plasma wakefield schemes. The radii and thicknesses of the dielectric cylinders determine the size of the on-axis wakefield longitudinal gradient that would accelerate to higher energy but for a lower charge, co-moving, delayed witness bunch. We begin by summarizing our initial findings, and then continue to discuss specific issues that have already been studied.

Design mode	~912 GHz
Boundary condition	Electric + open r.e.
Surrounding space	Vacuum
Outer radius of copper waveguide	1160.5 μm
Inner radius of copper waveguide	1060.5 μm
Conductivity of the copper, σ	$5.8 \cdot 10^7$ S/m
External radius of outer coaxial cylinder R_e	1060.5 μm
Inner radius of outer coaxial waveguide R_i	1047.5 μm
Accl. channel radius (inner radius of inner coaxial cylinder) a	50.0 μm
External radius of inner coaxial cylinder b	89.5 μm
Real part of relative dielectric constant ε'	5.7
Tangent delta of dielectric losses at frequency 170 GHz	0.00013
Bunch axial RMS dimension $2\sigma_z$ (Gaussian charge distributition)	69.28 μm
Full bunch length (=2 cutoff length of bunch)	173.2 μm
Outer drive bunch radius (Box charge distributition)	718.5 μm
Inner drive bunch radius	418.5 μm
Drive bunch energy	5 GeV
Witness bunch energy	5 GeV
Witness bunch charge	0.01 nC
Number of bunches	1

Table II. Parameters of the THz CDWA design unit.

We begin by showing in Fig. 10 a radial profile of the more important wakefield modes excited by the annular drive bunch. The results shown in this figure and the following one are obtained from analytic theory, which omits the quenching wave. A very flat profile is obtained. Fig. 11 shows the longitudinal profile of the composite acceleration force on axis of the device; this force is ~ 600 MeV/m at select locations behind the drive bunch. This large field is obtained by the constructive superposition of three modes; indeed, we have found that a different choice [1] of radii and thicknesses of the dielectric tubes can provide a gradient of 1200 MeV/m. The analytic theory finds the radial force near the axis of the structure is in quadrature with respect to the axial force, so it is nearly zero at the peak of the axial force where the witness bunch is placed.

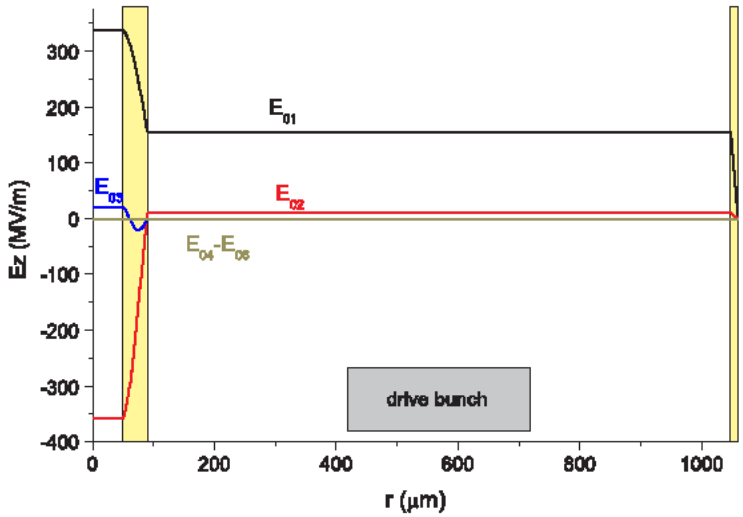

Fig. 9. Transverse profiles $E_z(r)$ for the first six TM-modes, with E_{02} being the operating mode. Location of the two dielectric shells is highlighted in yellow, and location and width of

the 5-GeV drive bunch is shown in gray. Notice the large ratio of field amplitudes in the witness/drive channels, and the flat radial profile that favors uniform acceleration.

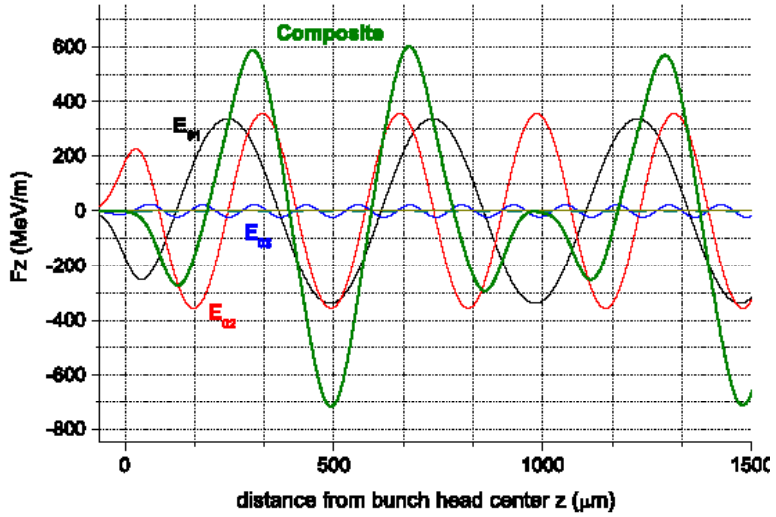

Fig. 10. Axial profiles of the longitudinal individual and composite forces of the E_z 0,m modes acting on a test electron along the center of the accelerating channel. The drive bunch moves from right to left and its center (maximum charge) is located at z=0.

The PIC code reveals some different physics introduced by the quenching wave, which originates from the entrance where the boundary condition is imposed (the analytic theory neglects the entrance, thus it assumes the structure is infinitely long). Unlike the wakefield whose speed is ~*c*, the quenching wave travels at approximately the group velocity of waves in the structure, and lags progressively farther behind the bunch as the travel distance of the latter increases. We first look at the map of the accelerating field (Fig. 11) that develops behind the drive bunch after it has moved approximately 4 mm into the structure. At this time, the quenching wave shows appreciable interference with the wakefields for z < 3.3mm. A plot of the accelerating force on the axis and the radial force near the axis is shown in Fig. 12. There are three things to observe here. First, the accelerating force is 520MeV/m—close to that predicted by the analytic theory (~600MeV/m)—where the witness bunch would be positioned; only one wakefield accelerating peak has emerged from the quenching wave interference. This occurs because the group velocity of the waves is close to *c* in this over-moded structure. Second, the radial force acting on an electron slightly off the axis of symmetry has a focusing sign (the force is negative where the displacement is positive). This effect is caused by the quenching wave, and has been found in other designs, including those at microwave frequency [1]. This focusing effect follows the bunch along the device (we have seen its effect already in the previous section. The betatron period of stable oscillation driven by this force is approximately 0.9 m here. Third, the axial force profile across the witness bunch is flat, which is helpful in maintaining uniform acceleration of the electrons in the witness bunch. This was not the case for the rectangular cross-section DWA we have been studying. The cylindrical geometry also provides a higher gradient acceleration per unit drive bunch charge than the rectangular.

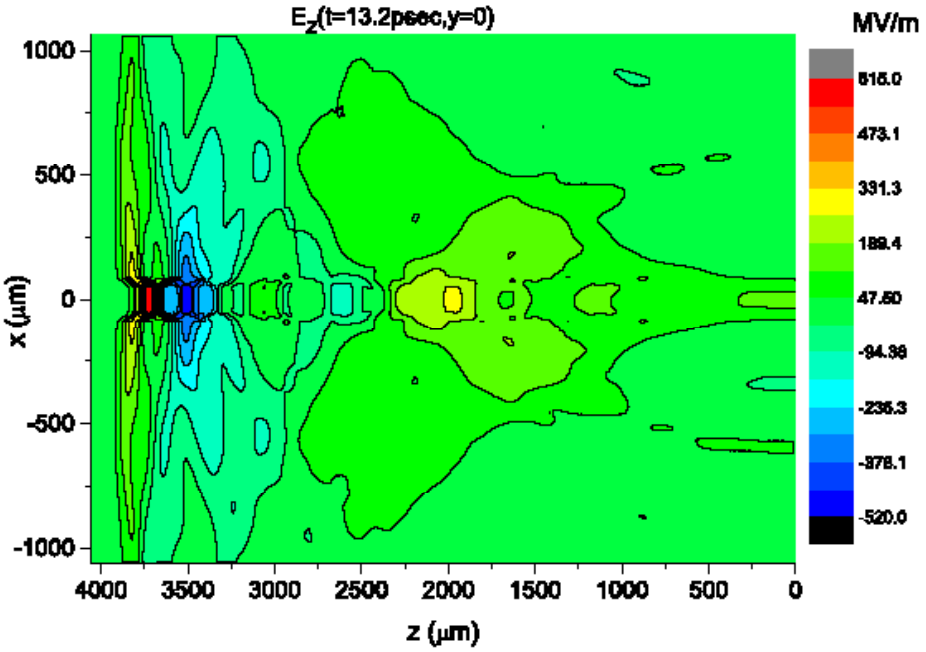

Fig. 11. Map of the axial electric component of wakefield when the drive bunch has moved 13.2 psec and is found at z = 3.88mm from the entrance (z = 0). The witness bunch would be located at the central blue zone of high E_z field.

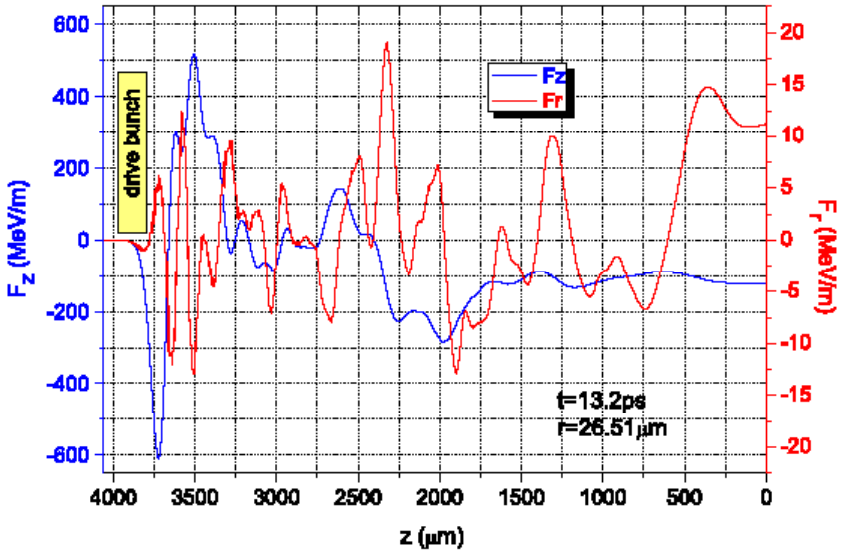

Fig. 12. Axial (blue line) and transverse (red line) forces acting upon a witness electron versus *z*, at r = +26.5μm from the central axis in a witness bunch channel. The witness bunch would be placed at z=3500 μm.

The transverse electric field, mostly from the Coulomb field of the drive bunch charge, is also quite high. Fig. 3.C. 5 shows a map of this field, at the same time as Fig. 3.C.3. The maximum value of this field is 880 MeV/m (of course, the transverse force and the transverse

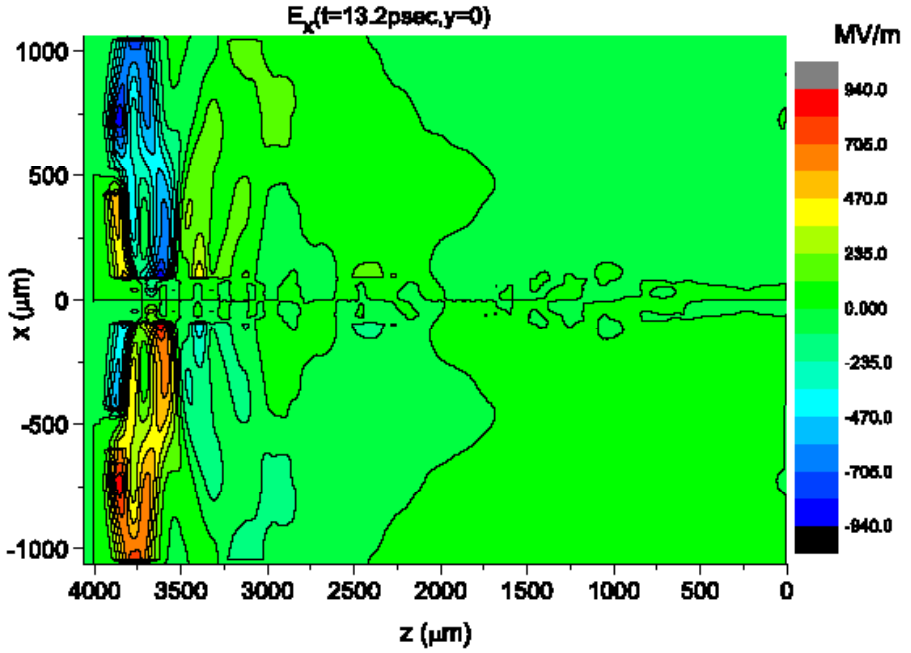

Fig. 13. Map of the transverse component of electric field along the structure for time t = 13.2 psec. The annular drive bunch has moved to the far left side of the map.

electric field are not the same). Fortunately, these fields appear to be within the capability of dielectrics such as alumina to withstand without breakdown [11], in part because of the very short time that they occur at a given surface element.

Table II is computed for a dielectric having ε = 5.7 (as for diamond). However, there is no reason that the dielectric constant of the outer cylinder and the inner cylinder must be the same. For example, diamond might be a good choice for the outer dielectric cylinder because it can transfer heat rapidly to the metallic jacket. The heat would originate at the inner cylinder, which might be alumina. Alumina would be easier to fabricate as a long tube, and it can reach temperature ~ 1700C if necessary. We will explore heating issues in the next section: these become important for high repetition rate operation. Fig. 14 shows the axial electric fields on the centers of the witness bunch channel and the drive bunch channel after an elapsed time of 13.2psec. This permits a calculation of the transformer ratio for this design, namely T ~ 6:1. We note here that the behavior of these fields is nearly homogeneous in radius.

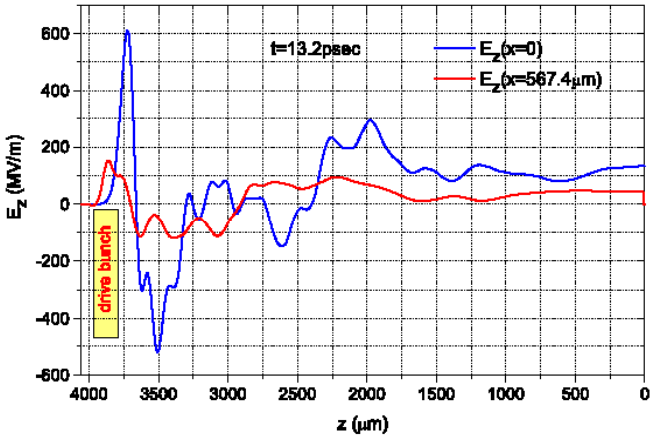

Fig. 14. Axial wakefields of the drive bunch (red) and witness bunch (blue) at the centers of their respective channels.

We have also studied a six-zone structure, having three dielectric shells and three vacuum channels (Table III) for the purpose of demonstrating that the transformer ratio can be enhanced. The inner vacuum channel contains the witness bunch, the outer one contains the drive bunch, and the middle one is empty. This structure can provide a larger transformer ratio (~ 14:1) via a stepwise increase of the longitudinal field that can occur at each dielectric shell. The radial dependence of the longitudinal electric fields of the several modes is shown in Fig. 15, and the behavior of the transformer ratio is shown in Fig. 16. The peak composite E_z field is slightly higher than found for the original 4-zone structure having comparable dimensions.

External radius of outer coaxial cylinder r_6	1431.5 μm
Inner radius of outer coaxial waveguide r_5	1418.5 μm
External radius of middle coaxial cylinder r_4	460.5 μm
Inner radius of middle coaxial waveguide r_3	447.5 μm
External radius of inner coaxial cylinder r_2	89.5 μm
Accl. channel radius (inner radius of inner coaxial cylinder) r_1	50.0 μm
Relative dielectric constant ε	5.7
Bunch axial RMS dimension $2\sigma_z$ (Gaussian charge distributition)	69.28 μm
Full bunch length (=2 cutoff length of bunch)	173.2 μm
Outer drive bunch radius (Box charge distribution)	718.5 μm
Inner drive bunch radius	418.5 μm
Bunch energy	5 GeV
Bunch charge	6 nC
Number of bunches	1

Table III. Parameters of a six-zone THz CxDWA structure. **Fix border.**

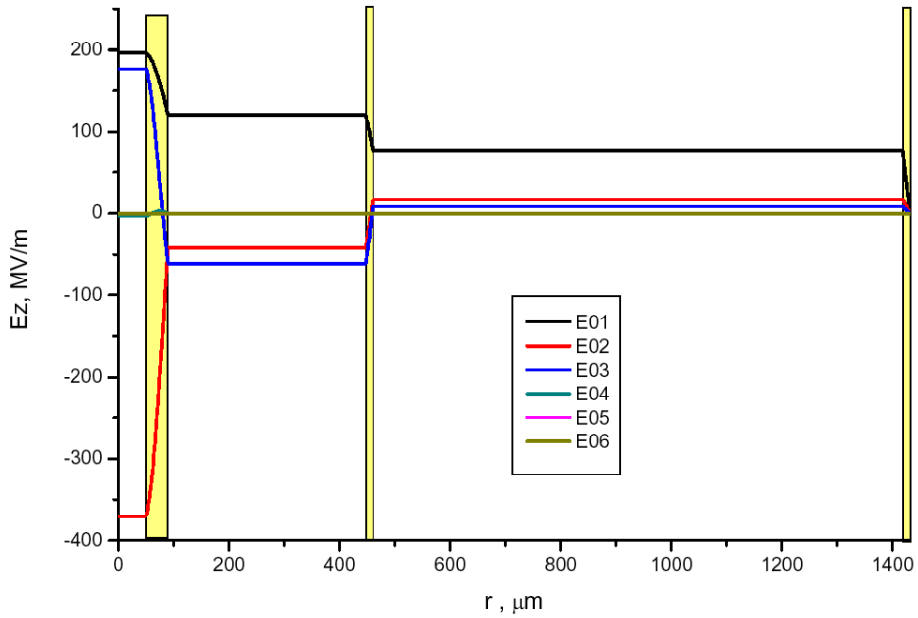

Fig. 15. Stepwise increase in the radial dependence of E_z for several modes.

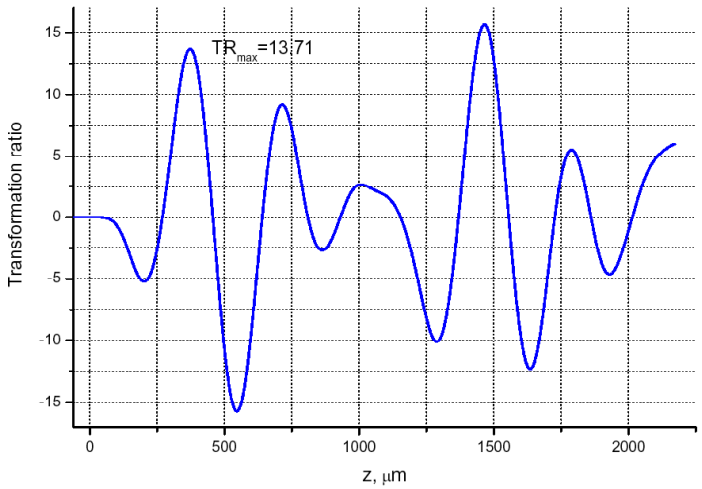

Fig. 16. Transformer ratio behavior of the composite longitudinal electric field dependence in the witness channel of the structure of Table III.

Id. Studies of Specific Problems Relating to the THz CDWA Design

The Phase I list of topics for study included specific items concerning the THz device. The first one we undertake has to do with the stability of a 6-nC, 5-GeV drive bunch. This study gives some indication of the length a modular element can be without undue beam interception , and provides some guidance about what further research must be done. The problem we immediately faced was one of computing capacity. In Section Ic, the computations were carried out for (an adequate) distance of travel, namely 4mm (since then extended to 10mm) which was the limit of our computing capacity. The reason for this is that the dielectric structures are thin, and thus require a fine mesh. However, to study bunch propagation over 1 m, a likely choice for the length of an accelerating module, a better system is needed. As it turned out, a computer briefly became available to us that could handle this problem: the machine was slower than ours, but it had eight processors, >100GB of memory, and a Windows XB 64 bit system (the 64bit OS makes use of the large memory); it ran over one week and generated a movie of the bunch motion in our THz structure which extended to 1m. We do not show the movie here, but instead present still frames of the bunch when it has traveled approximately 50 cm (1.65nsec) along the structure described by Table II. The full bunch length duration is 0.58 psec and the still frames contain particles in a 0.02 psec slice. We present three frames (Fig. 17) showing respectively the front end of the drive bunch (top frame), the middle of the drive bunch (middle frame), and the tail of the drive bunch (bottom frame). From these it is found that the head of the drive bunch expands slowly as the drive bunch moves, the middle remains approximately its original size, and the tail section of the drive bunch contracts in radius. Most of the particles lose energy as the bunch moves, but the bunch head remains at nearly the input energy, as expected. There are no particle losses in 0.5m travel, and less than 20% are lost in 1m.

What causes the distortion of the annular drive bunch? Fig. 18 shows the transverse forces surrounding a radial section of the annular drive bunch after it has moved only 3.4 mm. If we examine the radial forces acting on the edge of this drive bunch, we find the front lateral boundaries of the bunch should undergo defocusing while the rear parts should undergo focusing. These forces at the edge of the drive bunch are ~ +/-15MeV/m: acting alone, these

forces would cause a radial expansion or contraction of the bunch transverse profile by only a small fraction of a millimeter in 50 cm of travel, as the code would have it. Further study of the drive bunch as it is emitted from the cathode used in the PIC code reveals a strong transverse force at the edges of the cathode that imprints the disturbances shown in Fig. 18. Thus it may be that the head-to-tail distortion we have obtained from this simulation is an artifact of the computational model. (In reality, the source of the bunch would be many meters removed from the CDWA structure.) More work must be done to understand this problem and modify the code so that it will provide a more realistic way of simulating the injection of the drive bunch into our structure, for example by excluding the zone of the cathode from emission where there are large fringing forces. But, even under these adverse initial conditions, the PIC bunch appears to move along the structure in a nearly- stable way.

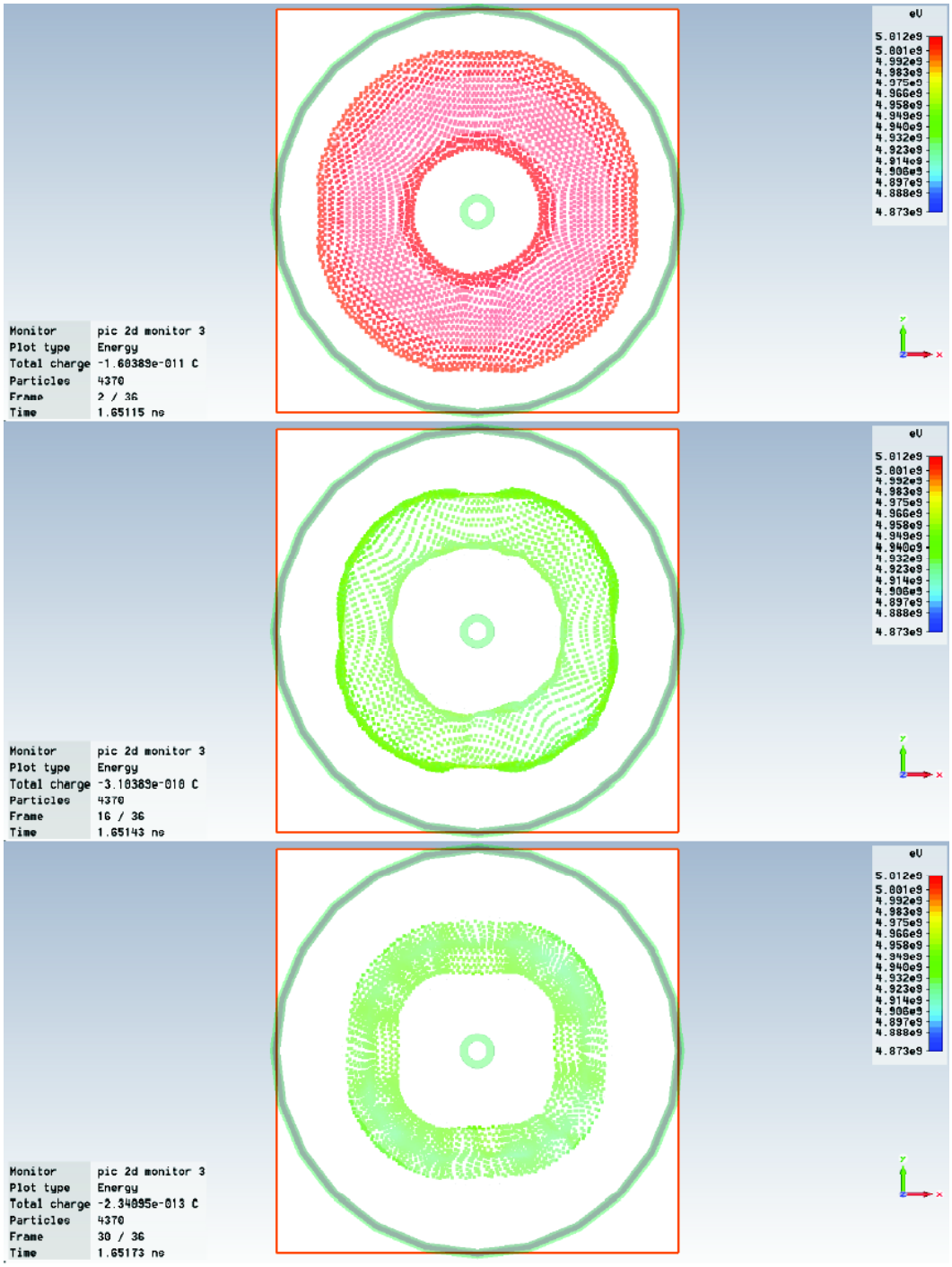

Fig. 17. Transverse distribution of simulated drive bunch particles, approximately 50 cm beyond launch point. Top: bunch head; Middle: bunch midsection; Bottom: bunch tail. Slices of the bunch 0.02 psec wide are shown. The inner and outer cylinders of dielectric are indicated in dark green.

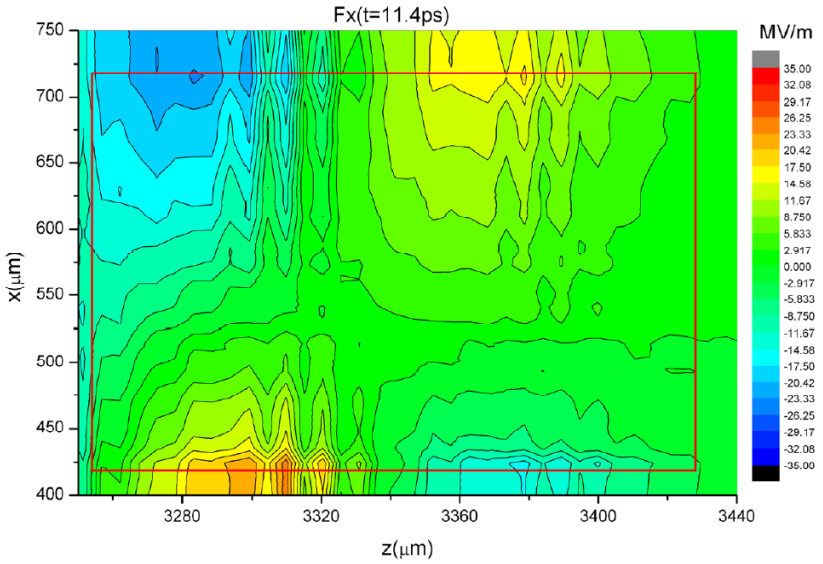

Fig. 18. The area surrounding the annular THz drive bunch (boundary outlined as the red box) showing the transverse forces in the y=0 plane after the bunch head has moved 3.43mm. The polarity of the transverse force reverses from head to tail of the bunch.

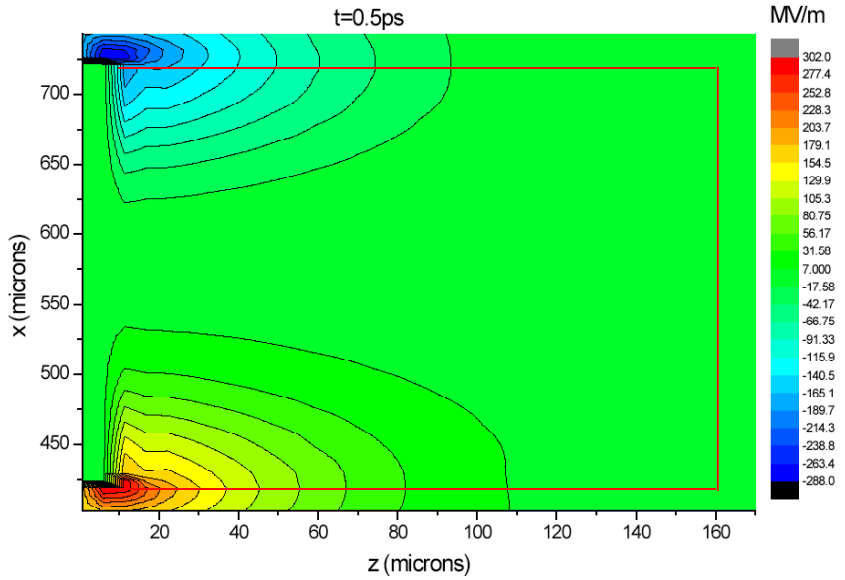

Fig. 19. The drive bunch as it is emitted from the cathode (far left), showing the large transverse forces that originate at the edges of the cathode in the simulation. Bunch moves from left to right. The cathode projects outward 10μm into the CDWA structure. Notice the color/force scale is much different in this figure than the preceding one.

Regarding support of the inner dielectric cylinder we can report the following. A thin (~250μm) aluminum foil can support the cylinder, it will not cause significant energy loss or scatter (low Z) for a 5 GeV drive bunch, and it will provide a boundary condition for

vanishing tangential electric field such as used in the simulations. It does not, however, provide for adjustment, unless it is configured into three separate and adjustable "vanes" of metal. A potentially more useful material is carbon nanotube, which can be made into a fabric; it is a good electrical conductor and can be thinner (25μm) than the aluminum foil, thereby reducing energy loss and scatter. As a fabric it would cover the entire cross section of the accelerator tube, or, as separate filaments, it can be used as a strong, flexible wire (thereby allowing adequate pumping). The wire might be formed into a loop encircling the inner dielectric tube; this would allow it to be shortened or lengthened by a servomechanism to adjust the alignment of the concentric alumina dielectric element with respect to the outer shell or wall. This is a very promising new material, but it should be evaluated carefully by experienced personnel for this application and its value may only become evident after a detailed study devoted to that purpose. While we can identify it as a potential solution to the complex problem of adjustable alignment of the inner cylinder component, we have not had the manpower to study this beyond exploring some of the technical literature and a few conversations with workers in that field. If further work on the CDWA continues to demonstrate promise as an advanced accelerator concept, then the matter of a suspension technique using carbon nanotube technology should be pursued by a team having experience in this field. We shall begin this in the Phase II project.

One area not on our list of Phase I tasks that we explored was the matter of energy loss in the copper conducting wall jacket, and in the dielectric inner cylinder. These obviously become important when repetitive-pulse operation is necessary (as it would be for a collider). We can compute the Ohmic losses in the copper using the tangential component of magnetic field adjacent to the conductor. The code gives us the magnetic field from the passing drive bunch, and from that we can compute the inward Poynting flux into the finite-resistivity conductor. The magnetic field pulse is shown in Fig. 20.

For copper with vacuum magnetic permeability μ_0, the surface dissipation per unit area is (MKSA) $dP(\omega)/dA = (\mu_0\omega\delta/2)\,|H_\theta^2|$, where H_θ is the magnetic vector parallel to the copper surface. Taking the conductivity σ of copper as 5.8×10^7 MKSA, the skin depth $\delta = [2/\mu_0\omega\sigma]^{1/2}$ is ~ 0.1 micron at 0.9 THz, much less than the thickness of a real wall. (However, this small skin depth may not be appropriate for the surface, which could have micron-scale scratches and imperfections that enhance its area.) Also, the pulse of magnetic field has a spectrum of frequencies, and thus there must be an integration of $dP(\omega)/dA$ over this spectrum because the skin depth and power loss depend on frequency. The power spectrum at the surface is shown in Fig. 3.D.6. The computed power that is dissipated in the copper surface from the passing drive bunch is found by integrating $R_s(f)|\,H_\theta(f)\,|^2$ where $R_s = [\pi f\mu_0/\sigma]^{1/2}$, using Parseval's theorem. The spectral peak at ~ 0.8 THz is mostly the wakefield power, while the lower-frequency peak ~ 0.2 THz is the empty-tube effect without the dielectric. The latter accounts for substantial losses. Computing the average power from an example of 5×10^4 drive bunches per second, (14 MW witness beam power, 0.2 nC/bunch) we find the thermal input to the copper wall is 8.5 W/cm^2. Over the length of a module, this would be a tiny fraction of the input bunch power, and a magnitude that should be easily dissipated externally.

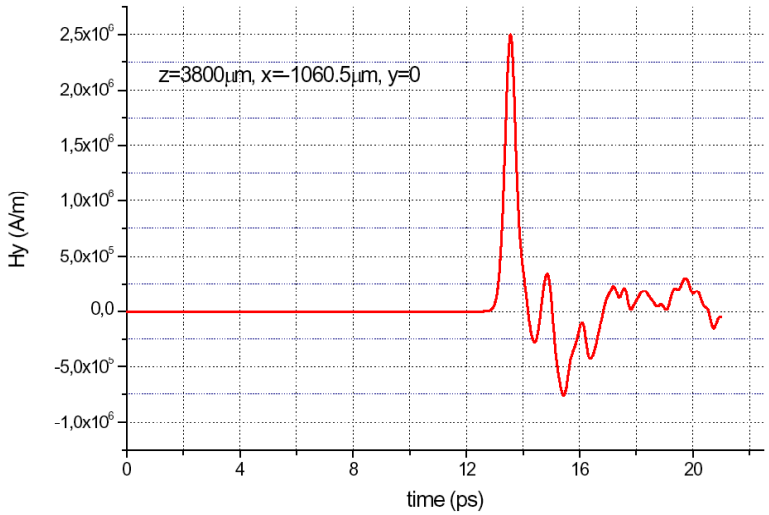

Fig. 20. Magnetic field pulse tangential to the copper surface set up by the psec passage of a 5GeV, 6nC drive bunch charge (radius of inner copper cylinder wall = 1.06mm). Field is observed at z = 3800µm, y = 0, x = -1060.5µm (just outside surface).

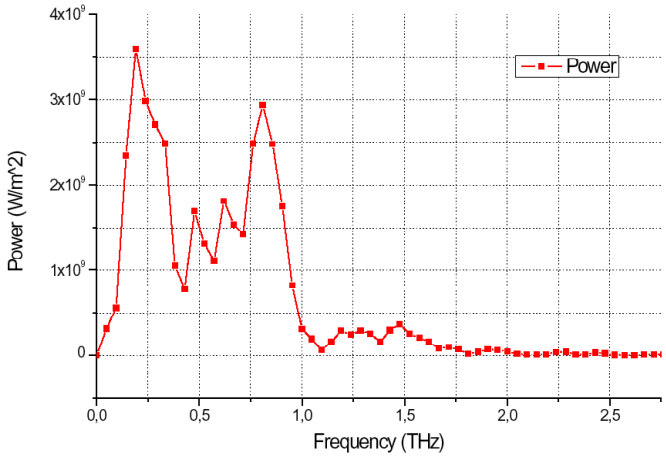

Fig. 21. Pulse power intensity spectrum from the passage of the drive bunch at the surface of the copper wall, at the location given in Fig. 20.

As far as dissipation in the dielectric is concerned, the central dielectric element is the most critical, because it is thermally isolated from its surroundings, and thus must cool by radiative transfer. The outer shell is thin, and diamond has a large thermal conductivity and is located adjacent to the copper vacuum wall, hence the outer dielectric wall temperature is determined by the copper jacket and its heat sink. As a single 6-nC 5- GeV drive bunch moves along the accelerator, it excites a short traveling section of intense fields in the dielectric, forming a radiation pulse ~ 10^{-12} sec in duration (300 microns long), with an internal electric field ~300 MeV/m when averaged over radius and different interfering modes. Next we compute the wave attenuation factor by the dielectric components, each having a loss tangent 10^{-4} and a total filling factor of 0.03. From this we obtain, after accounting for the specific heat of the material and the short pulse length, a temperature rise of 10^{-4} ^{o}C per drive bunch in the dielectric; thus, a total rise ~ 5^{o} C from 5×10^{4} drive bunches in one second (one second is probably less than the radiative cooling time constant of the central alumina tube). Fortunately, the peak operating temperature of alumina is 1700 °C, but high pulse repetition rate introduces the complication of appreciable dielectric heating in the

module. (The repetition rate depends on the demands of the collider and the witness bunch charge that must be used; the latter could be as high as 0.2nC.

We have also studied a simple scheme about how annular drive bunches might be injected into a new section following a preceding module where the drive bunch energy has become too low due to accumulated drag losses. We propose a simple length of space that the injected bunch must traverse, in which a 1-T magnetic field transverse to its motion is imposed. The length of this vacuum inter-modular space is taken to be 0.5 m. Electrons in the small, short annular 5GeV drive bunch will have a radius of curvature ~ 17 m, which should cause a deflection ~ 8 mm in the half-meter travel distance: this is more than adequate clearance between the injected bunch and the accelerator beam-line. In this magnetic field, the witness bunch (>30GeV) will suffer much less deflection, and the spent drive bunch will suffer much more deflection than the injected bunch. We are interested in what complications the centripetal drift and the space charge field might cause. For computational purposes, the moving annular bunch is enclosed in a cylindrical metal tube having radius 3 cm. Table IV gives the parameters of this run. In Fig. 21 we see the transverse profile of a central section of the short THz bunch at z = 65.5cm, it having been deflected by 1.4 cm. The bunch motion at this distance shows the bunch has no serious change in profile (minor changes in energy are shown in color). There was no important change in axial charge distribution. From this, we conclude that this simple scheme of injecting an annular bunch into the accelerator beam-line should be successful.

Finally, a word regarding alignment issues for the THz structure. Although the drive bunch energy is much higher than for the experiment to be run at AWA, the module is longer (~ 1m maximum). Thus, we expect the alignment tolerances to be tighter. In order to estimate the requirement, lacking computational power as described earlier, we scaled up the deflecting force to see a deflection of the witness bunch at a travel distance of ~5 mm. We used 5 GeV for the energy of the witness and drive bunches, increased the drive bunch charge to 600 nC, and chose a drive bunch displacement of 50 μm off the axis of symmetry. The deflecting force was found to be linear in these quantities. First we determined that the centered drive bunch would cause no deflection, and then found that the 50 μm off-centered drive bunch would cause a witness bunch deflection of 6.3μm in 5 mm travel. If the drive bunch actually contains 6 nC and is displaced 5 μm, the witness bunch should suffer 1/1000 of that displacement. Then we can then scale the travel length for 1 m (deflection scales as $[\text{distance}]^2$) and witness bunch energy (deflection scales as $1/\gamma$) to 25 GeV (much less than the typical energy of a witness bunch in a collider). Such a witness electron then would deflect only 50 μm in traveling 1 m.

Radius metal cylinder waveguide R_e	30mm
Length of cylinder waveguide	1000mm
Bunch axial RMS dimension σ_z (Gaussian charge distributition)	0.04mm
Full bunch length (=2 cutoff length of bunch)	0.2mm
Outer drive bunch radius (Box charge distributition)	0.7mm
Inner drive bunch radius	0.4mm
Drive bunch energy	5 GeV
Drive bunch charge	6 nC
Cathode length	5mm

Table IV. Simulation parameters for the 5GeV 6nC annular drive bunch moving across a 1-T magnetic field.

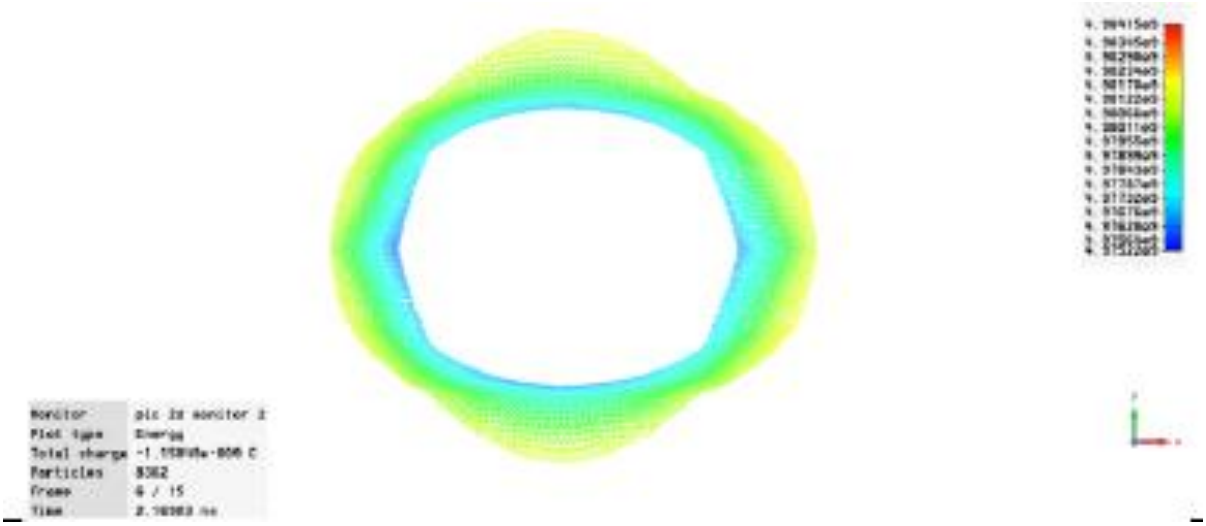

Fig. 22. Annular bunch, center section, having moved ~0.65m across the 1-T transverse field in a 3-cm radius metal pipe.

Thus, a 5 μm alignment tolerance for the annular drive bunch appears to be a reasonable goal. Is this achievable? The recent successful operation of the 1.5A° FEL at SLAC required 5 μm alignment tolerances of its undulators over a distance of 112 m: so we are not asking for the impossible.

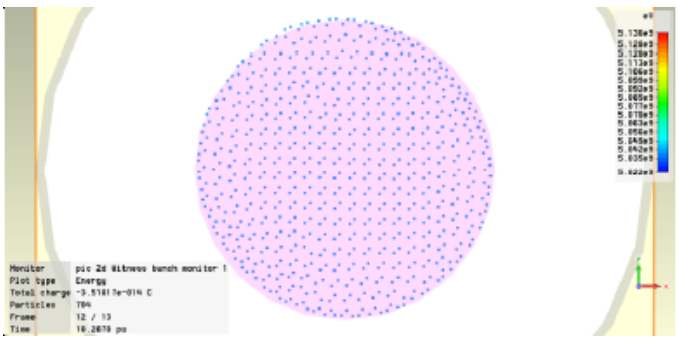

Fig. 23a. Test case for perfect alignment: 600 nC hypothetical drive bunch, showing a section of the 50 μm diameter 5 GeV witness bunch after it has moved 18 psec through its 100 μm diameter witness channel (outline, gray ring) in our CDWA structure.

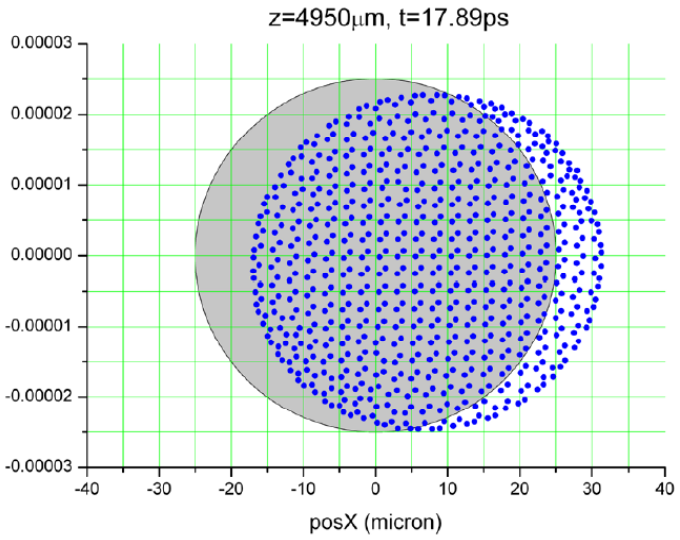

Fig. 23b. Same as above, but now the drive bunch is displaced 50 μm from the axis of symmetry, causing the witness bunch here to be deflected 6.3μm.

References

[1] "Coaxial Two-Channel High Gradient Dielectric Wakefield Accelerator", G.V. Sotnikov, T.C. Marshall, and J.L. Hirshfield, *Phys. Rev. ST--AB*, **12**, 061302, (2009).

[2] "Two-Channel Rectangular Dielectric Wakefield Accelerator Structure Experiment", G.V. Sotnikov, T.C. Marshall, S.V. Shchelkunov, A. Didenko, and J.L Hirshfield, p. 415, *Advanced Accelerator Concepts Workshop, AIP Conference Proceedings* **1086**, C.B. Schroder, W. Leemans and E. Esarey, editors (2008); and: "A Symmetric Terahertz Dielectric-Lined Rectangular Structure for High Gradient Acceleration", T.C. Marshall, G.V. Sotnikov, S.V. Shchelkunov, and J.L. Hirshfield, p, 421 *Advanced Accelerator Concepts Workshop* (2008), *ibid*.

[3] I.N. Onischenko, D. Yu. Sidorenko, G.V. Sotnikov, Phys. Rev. E65, 066501 (2002).

[4] A. Sessler and G. Westenskow, "Two-Beam Accelerators," in *Handbook of Accelerator Physics and Engineering*, A. W. Chao and M. Tigner, eds.(World Sci, NJ, 2002), pp. 46-48.

[5] J. P. Delahaye, "The Compact Linear Collider (CLIC) Study," CERN Particle Physics Seminar, http://clic-study.web.cern.ch/CLIC-Study/Presentations/20050421.pdf

[6] E. Chojnacki, W. Gai, P. Schoessow, and J. Simpson, in *Proc. Of IEEE 1991 Particle Accelerator Conference* (APS Beams Physics); (IEEE, 1991), vol.4, pp. 2557-2559.

[7] M.E. Conde, W. Gai, R. Konecny, J. Power, P. Schoessow, and P. Zouer, in *Advanced Accelerator Concepts: Eighth Workshop*, edited by W. Lawson, C. Bellamy, and D. F. Brosius, AIP Conf. Proc. **472**, (AIP, NY, 1998), pp. 626-634.

[8] M. Bieler et al. (1988),
http://accelconf.web.cern.ch/AccelConf/e88/PDF/EPAC1988_0967.PDF
also, F-J. Decker et al,
http://accelconf.web.cern.ch/AccelConf/e88/PDF/EPAC1988_0613.PDF

[9] Wanming Liu and Wei Gai, Phys. Rev. ST Accel and Beams **12**, 051301 (2009).

[10] *"A Fast Kicker Using a Rectangular Dielectric Wakefield Accelerator Structure"*, J.L. Hirshfield, G.V. Sotnikov, T.C. Marshall, and S.V. Shchelkunov, Particle Accelerator Conference 2009 Proceedings, paper FR2RAC03.

[11] M. C. Thompson, H. Badakov, A. M. Cook et.al., *Phys. Rev. Lett.* **100**, 214801 (2008).

[12] The numerical simulations in this project used the following software: CST Studio Suite 2009, which includes CST Design Studio, CST Microwave Studio, and CST Particle Studio (PIC).

[13] G, V. Sotnikov, I.N. Onischenko, and T.C. Marshall, "3D Analysis of Wakefield Excitation
in a Dielectric Loaded Rectangular Resonator", p. 888, Advanced Accelerator Concepts, M. Conde and C. Eyberger eds., AIP Conference Proceedings **877** (2006); see also additional articles on pp. 851 and 866.

II. PHASE II RESULTS AND PUBLICATIONS

Archival publications that resulted from research carried out with support under this grant include the following.

1. S. V. Shchelkunov, G. V. Sotnikov, T. C. Marshall, and J. L. Hirshfield, "A high gradient THz coaxial dielectric wakefield accelerator", AIP Conf. Proc. 1507, 945 (2013)

2. S.V. Shchelkunov, T.C. Marshall, G. Sotnikov, J.L Hirshfield, and M.A. LaPointe, "High-Gradient THZ-scale Two-channel Coaxial Dielectric -lined Wakefield Accelerator", Procs of IPAC2012, New Orleans, LA, USA, ISBN 978-3-95450-115-1, pp. 2747-2749 (2012)

3. G. V. Sotnikov and T. C. Marshall, "Improved ramped bunch train to increase the transformer ratio of a two-channel multimode dielectric wakefield accelerator", Phys. Rev. ST Accel. Beams 14, 031302 (2011)

4. T. C. Marshall, G. V. Sotnikov, and J. L. Hirshfield, "A THz Two-Channel Dielectric Wakefield Structure for High Gradient Acceleration", AIP Conf. Proc. 1299, pp. 336-341 (2010)

5. G. V. Sotnikov, T. C. Marshall, J. L. Hirshfield, and S. V. Shchelkunov, "Accelerated Bunch Stability in a Coaxial Dielectric Wakefield Structure When its Symmetry is Broken ", AIP Conf. Proc. 1299, 342 (2010)

6. G. V. Sotnikov, T. C. Marshall, and J. L. Hirshfield, "Coaxial two-channel high-gradient dielectric wakefield accelerator", Phys. Rev. ST-AB, V. 12, 061302 (2009)

Copies of these publications are appended here, providing a complete record of results obtained under this grant.

A THz Coaxial Two-Channel Dielectric Wakefield Structure for High Gradient Acceleration

T.C. Marshall[a,b], G.V. Sotnikov[b,c], and J.L. Hirshfield[b,d]

[a]*Columbia University, New York, NY USA;* [b]*Omega-P, Inc., New Haven, CT USA;*
[c]*NSC Kharkov Institute of Physics and Technology, Kharkov, Ukraine;* [d]*Yale University, New Haven, CT USA*

Abstract. A coaxial two-channel dielectric wakefield structure is examined for use as a high gradient accelerator. A THz design, having radius ~1mm, is shown to provide GeV- level acceleration gradient, high transformer ratio, and stable accelerated bunch motion when excited by a stable-moving 5-GeV 6-nC annular drive bunch.

Keywords: wakefield acceleration, coaxial two-channel dielectric waveguide structure, collider.
PACS: 41.75.Jv, 41.75.Lx, 41.75Ht, 96.50.Pw

INTRODUCTION

A new concept [1], a coaxial dielectric wakefield accelerator structure (CDWA), has been proposed that uses two hollow concentric dielectric tubes with vacuum channels for drive and accelerated bunches; the outer dielectric tube is enclosed by a metallic jacket (Fig. 1). In [1] an analytic theory was developed and a number of examples were studied using a PIC code. An annular drive bunch is to be decelerated in the wider outer channel by setting up Cherenkov wakefields, and a "witness" or "test" bunch is to be accelerated in the narrower diameter inner channel. This arrangement yields a transformer ratio $T >>1$, while the circular symmetry can provide a high acceleration gradient (> 1 GeV/m) and a focusing force on the test bunch. The latter appears as a consequence of the "quenching wave", a significant field component that is set up by the entry of the drive bunch into the structure. The quenching wave moves more slowly than the drive bunch.

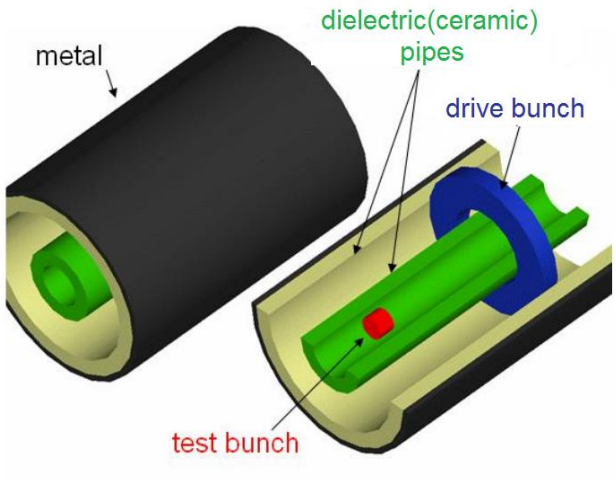

FIGURE 1. Schematic of the CDWA structure, showing a single annular drive bunch followed by an accelerated test bunch that moves along the axis.

A structure concept with circular symmetry is an improvement upon the rectangular two-channel dielectric wakefield accelerator [2], currently under test [3] at the Argonne Wakefield Accelerator facility, because zeroth-order transverse deflecting forces on the test bunch do not arise. The nested inner dielectric cylinder requires support: we suggest that this can be provided by a series of spaced carbon nanotube filaments attached to an aligning servomechanism. In this paper we shall summarize our findings about this structure and provide a

simple example of how it might operate as a collider; in a companion paper [4] is presented studies of alignment and stability issues.

DESIGN AND NUMERICAL RESULTS

A design study has been carried out for a sub-THz coaxial DWA that could have relevance to a future collider application. The purpose of this work is to determine if this technology can provide a path towards a TeV machine, and identify where advantages and potential problems occur. Table I provides a list of parameters that we have chosen; note the radius of the structure is ~1 mm. The radii and thicknesses of the dielectric cylinders determine the wakefield period and size of the on-axis wakefield longitudinal gradient that would accelerate to higher energy a lower charge, co-moving, delayed witness bunch. The analytic theory finds that two modes are excited strongly. The amplitude of the composite wakefield along the axis is shown in Figure 2. Important wakefield modes, which

TABLE I. Parameters of the THz CDWA design example (diamond dielectric).

Design mode	~912 GHz
Boundary condition	Electric + open output end
Surrounding space	Vacuum
Outer radius of copper waveguide	1160.5 μm
Inner radius of copper waveguide	1060.5 μm
Conductivity of the copper, σ	$5.8 \cdot 10^7$ S/m
External radius of outer coaxial cylinder R_e	1060.5 μm
Inner radius of outer coaxial waveguide R_i	1047.5 μm
Accl. channel radius (inner radius of inner coaxial cylinder) a	50.0 μm
External radius of inner coaxial cylinder b	89.5 μm
Real part of relative dielectric constant ε'	5.7
Tangent delta of dielectric losses at frequency 170 GHz	0.00013
Bunch axial RMS dimension $2\sigma_z$ (Gaussian charge distributition)	69.28 μm
Full bunch length (cutoff)	173.2 μm
Outer drive bunch radius (box charge distribution)	718.5 μm
Inner drive bunch radius	418.5 μm
Drive bunch energy, charge	5 GeV, 6nC
Witness bunch energy	5 GeV
Witness bunch charge	0.01 nC
Number of bunches	1

have wavelengths ~ 400 μm, are excited to different amplitudes by the passage of a single 6 nC, 5 GeV annular drive bunch, such as might be provided by a conventional efficient rf linac accelerator. The composite wakefield accelerating force at the location where the witness bunch should be positioned behind the drive bunch is 580 MeV/m. The analytic theory assumes an infinitely long structure, thus the wakefields repeat periodically behind the drive bunch. The transverse force computed from the analytic theory is found to be in quadrature with the axial force, so the transverse force on an electron located slightly off the axis of symmetry at the peak of the axial force is zero. However, this is not born out by the PIC calculation, which includes the important effect of the more realistic boundary condition where the drive bunch enters the structure.

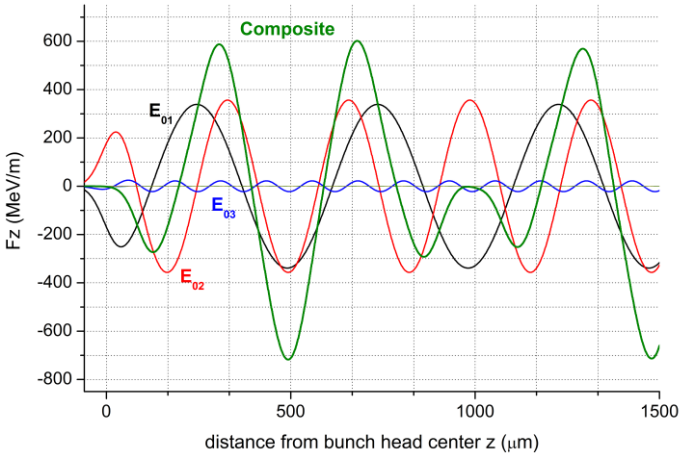

FIGURE 2. Axial profiles, calculated from analytical theory, of the longitudinal individual and composite forces of the $E_{0,m}$ modes acting on a test electron along the center of the accelerating channel. The drive bunch moves from right to left and its center (maximum charge) is located at $z = 0$. These calculations do not include the quenching wave.

Figure 3 shows a map of the longitudinal electric field set up by the wakefield obtained from a PIC simulation; the quenching wave (group velocity is less than c and the particle velocity) that is caused by the input boundary interferes with the otherwise orderly oscillation of the wakefield behind the drive bunch, for $z <$ 3300μm. Between the drive bunch and the quenching wave front is a region where the conventional wakefield oscillations occur. A plot of the accelerating force on the axis and the radial force near the axis is shown in Fig. 4, where a peak accelerating force of 520 MeV/m is found. This force is slightly lower than that predicted by analytic theory because of the extra waves that must appear as the drive bunch enters the structure at $z = 0$. Figure 4 shows the radial force acting on a witness electron located slightly off the axis of symmetry that has a focusing sense at

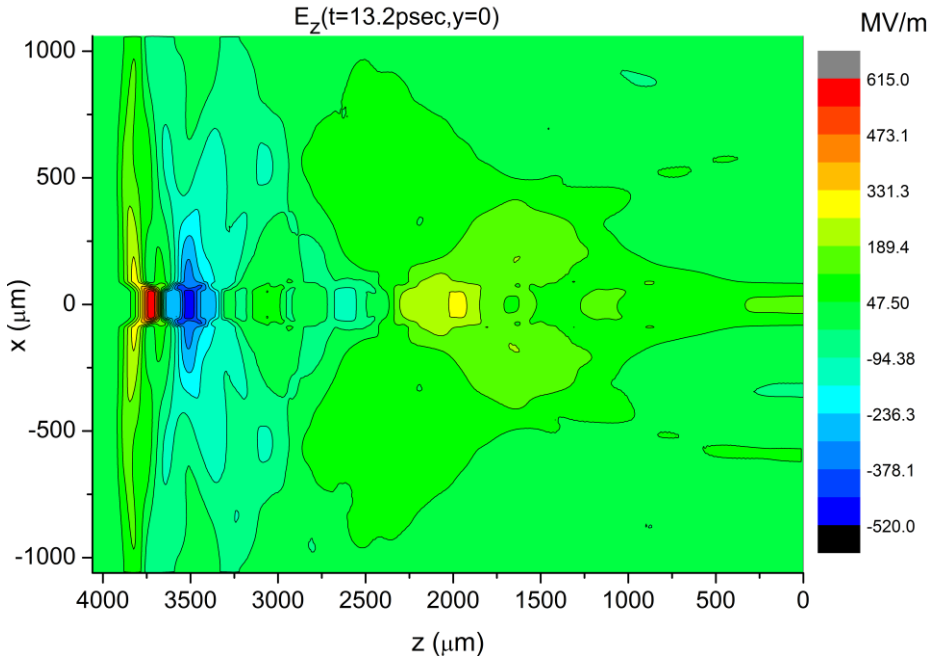

FIGURE 3. Map of the axial electric component of wakefield when the drive bunch has moved 13.2 psec and is found at $z =$ 3.88 mm from the entrance ($z = 0$). The witness bunch would be located at the central blue zone of high E_z field, $z =$ 3500 μm.

the location of the peak longitudinal force where the witness bunch should be located; this focusing pulse of force has been found to follow the test bunch along the structure in this design and others. From analytic theory, we have also found that the radial profile of the longitudinal force is nearly flat (Fig. 5), which favors uniform acceleration of a finite width bunch. Slightly different designs reveal a longitudinal gradient as high as 1.4 GeV/m; thus an average gradient for a structure assembled of many modules spaced apart might exceed 500 MeV/m.

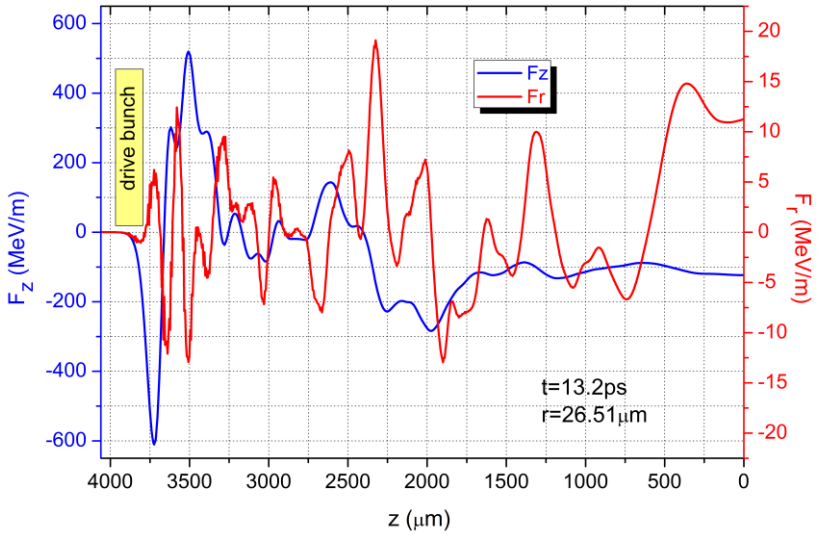

FIGURE 4. Axial (blue line) and transverse (red line) forces acting upon a witness electron at z = 3500 μm, located at r = +26.5 μm from the central axis in the witness bunch channel.

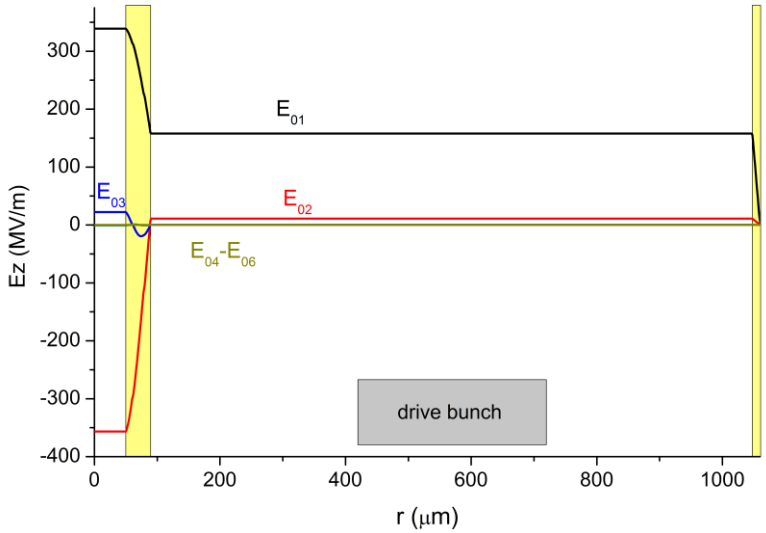

FIGURE 5. Transverse profiles E_z(r) for the first six TM-modes, with E_{02} being the operating mode. Location of the two dielectric shells is highlighted in yellow, and location and width of the 5-GeV drive bunch is shown in gray. Notice the large ratio of field amplitudes between the two channels.

A six-zone structure that contains an additional thin-walled dielectric cylinder and an additional empty anulus has been found to cause an increase of the transformer ratio from 6:1 to ~ 14:1 in single bunch operation. On the other hand, the use of a short train of drive bunches having ramped charge [5] and different spacing has been found to increase the transformer ratio and efficiency in a collinear wakefield accelerator experiment. Our recent paper reports that a train of four annular drive bunches has good stability against small lateral displacements [1] which might otherwise cause a beam breakup instability in a multibunch collinear structure; this technique for enhancing transformer ratio has been investigated for use in the coaxial configuration. An train of differently charged and differently spaced drive bunches has been found to increase the transformer ratio by as much as a factor of 6.

We have studied stability of the drive bunch as it moves along the structure, starting from a position of symmetry. A lengthy computer run was necessary, and Fig. 6 shows three axial slices of the annular drive bunch after it has traveled 50 cm along the structure. The sections are respectively the head, central zone, and tail of the Gaussian-distributed charge in the bunch. There appears to be some modification of the bunch structure, causing the head to expand and the tail to contract; however, no instability appears and few particles appear to be lost if the motion continues as far as 1 m.

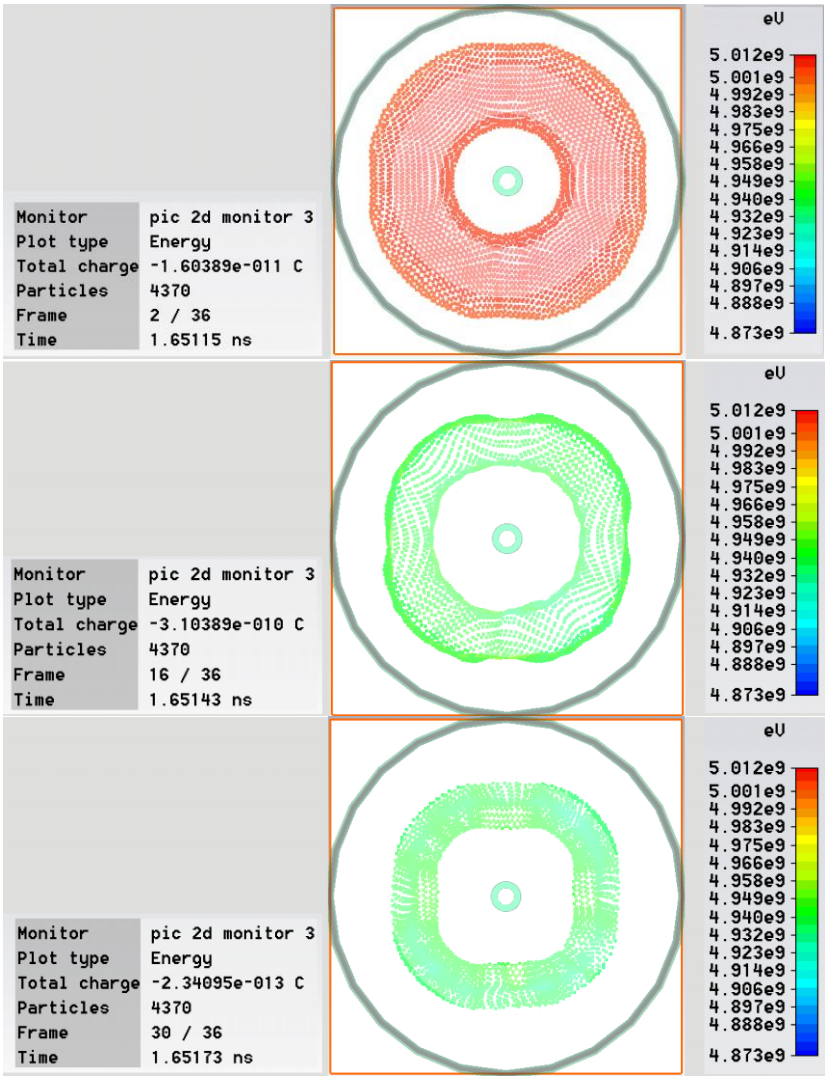

FIGURE 6. Transverse distribution of simulated drive bunch particles, approximately 50 cm beyond entry point. Top: bunch head; Middle: bunch midsection; Bottom: bunch tail. Slices of the bunch 0.02 psec wide are shown. The inner and outer cylinders of dielectric are indicated in dark green. Colors indicate energy of particles (scale right).

COLLIDER EXAMPLE

The above study of the stability of the 6 nC, 5 GeV annular drive bunch finds that the motion is stable to 50 cm and beyond; thus we might contemplate a collider made up of ~1 m modules separated by small gaps to allow pumping and beam focusing. These modules would be grouped into a "section", through which a single drive bunch is passed, loses most of its energy, and then is deflected from the beam-line by a 1-T zone of transverse magnetic field; a new drive bunch is then deflected into the beam-line to power the next section, etc. Taking the average gradient to be 500 MeV/m, leads to need for a 3km length to accelerate the witness bunch to 1.5 TeV. For a transformer ratio of 6:1, the number of sections is then $N = 1500\ \text{GeV}/(6 \times 5\ \text{GeV}) = 50$; the energy gain in each section is 30 GeV and the length of each section is 60 m. If the repetition rate of the accelerator is 50 kHz (witness bunches per second), the power input to this branch of the collider is 75 MW. The next issue is how large should be the charge of the witness bunch? A study of the effect of witness bunch charge upon the gradient is given in Figure 7 (loading). Two points along the bunch are studied: a leading point in the bunch head, and one at the center of the bunch. The witness bunch is positioned so that its center is at the peak of the accelerating wakefield waveform, so the head of the bunch experiences reduced gradient; however the head suffers very little loading because there is very little charge ahead of it. The center of the witness bunch suffers a much larger loading effect; thus, we choose for it a charge = 0.1 nC which appears to avoid excessive loading. The witness bunch current is then 5 μA, the witness beam power is 7.5 MW, and the efficiency of power conversion is 10%. This "efficiency" can no doubt be improved upon by further design studies.

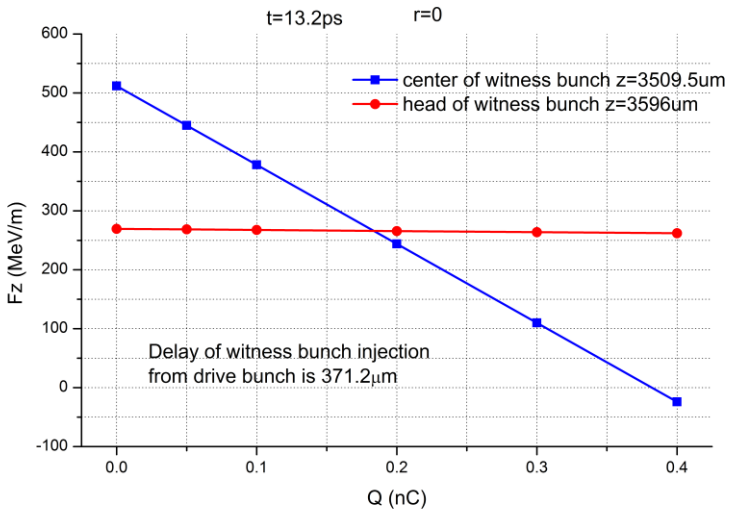

FIGURE 7. Loading of witness bunch charge on the acceleration gradient (see parameters, Table I).

Ohmic power loss into the accelerator conducting wall is found to be ~10 W/cm^2, and a temperature rise ~ 5^o C in one second due to losses in the inner dielectric cylinder is to be anticipated at the 50 kHz rate of operation.

ACKNOWLEDGMENT

This research was supported by the U.S. Department of Energy, Office of High Energy Physics.

REFERENCES

1. G.V. Sotnikov, T.C. Marshall, and J.L. Hirshfield, *Phys. Rev. ST--AB*, **12**, 061302, (2009)
2. G.V. Sotnikov, T.C. Marshall, S.V. Shchelkunov, A. Didenko, and J.L Hirshfield, "Two-Channel Rectangular Dielectric Wakefield Accelerator Structure Experiment", *Advanced Accelerator Concepts, 13th Workshop*, edited by C.B. Schroder, W. Leemans and E. Esarey, AIP Conference Proceedings **1086**, , p. 415 (2008)
3. S.V. Shchelkunov, et al., "Two Channel Dielectric-Lined Rectangular High Transformer Ratio Structure and Acceleration Experiment", these proceedings
4. G.V. Sotnikov, T.C. Marshall, J.L. Hirshfield, and S.V. Shchelkunov, "Accelerated bunch stability in a coaxial dielectric wakefield structure when its symmetry is broken", these proceedings.
5. C. Jing, A. Kanareykin, J. Power, M. Conde, Z. Yusof, and W. Gai, "Observation of Enhanced Transformer Ratio in Collinear Wakefield Acceleration", *Advanced Accelerator Concepts, 12th Workshop*, edited by M. Conde and C. Eyberger, AIP Conference Proceedings **877**, p. 511 (2006)

A High Gradient THz Coaxial Dielectric Wakefield Accelerator

S.V. Shchelkunov[a], G.V Sotnikov[b,c], T.C. Marshall[c,d], and J.L. Hirshfield[a,c]

[a]Yale University, New Haven, *CT*; *USA*
[b]*NSC Kharkov Institute of Physics and Technology, Kharkov, Ukraine*
[c]*Omega-P, Inc., New Haven CT, USA*
[d]*Columbia University, NY*; *USA*

Abstract. We have designed a mm-scale THz Coaxial Dielectric Wakefield Accelerator structure to produce acceleration gradients approaching 0.35 GeV/m per each nC of drive charge when excited by an annular-like bunch, which we propose to build and test at FACET/SLAC. The details of design and experimental plans are presented.

Keywords: dielectric wakefield accelerator, THz radiation, high gradient, high transformer ratio.
PACS: 41.75.Lx, 41.75.Ht, 41.60.Bq

INTRODUCTION

A new scheme [1] for a dielectric wakefield accelerator has been proposed that uses two hollow concentric dielectric tubes with vacuum channels for drive and accelerated bunches. Such a two-channel coaxial dielectric accelerator (CDWA) can be a promising candidate for a future TeV [2] collider. The scheme of the CDWA structure consists of two coaxial dielectric tubes, enclosed one inside the other, with two vacuum channels for the annular drive bunch and an accelerated witness bunch. In addition to providing a high acceleration gradient ~ 1GeV/m for mm-scale structures, the two-channel structure has a larger transformer ratio than the single-channel DWA, the transverse forces acting upon the bunch to be accelerated are focusing, and the annular drive bunch has been shown to move an appreciable distance without undergoing distortion or deflection [2]. An experiment is proposed for conduct at FACET (SLAC) to test a mm-scale THz CDWA using their "point-like" drive bunch. While it might appear initially that only an annular bunch could be used to set up the desired wakefields in this structure, we can show that the point drive bunch will establish the fields we wish to study; furthermore, we shall show how we may obtain information from this study whereby the data can be compared with theoretical simulations obtained with the CST STUDIO code. Experience with this THz structure, together with information obtained from a cm-scale GHz structure now under study at the Argonne Wakefield Accelerator facility (ANL), will provide the necessary stimulus for further possible development of this type of DWA structure for collider applications.

DESIGN OVERVIEW

The basic configuration for this type of DWFA is shown in Fig.1. One or a few annular drive bunches can be used to produce the wakefields. When several drive bunches are used, the ratio of drive bunch charges and the distances between bunches should be adjusted to constitute a ramp bunch train with constructive wake fields [3].

The structure and related parameters are presented in Table I; it is instructive to also show in Table II the parameters of the cm-scale coaxial structure that is being tested at AWA/Argonne. Both structures are to be driven by a single drive bunch; the THz structure will be excited by the ~3-nC 23-GeV bunch available at FACET, and the GHz structure is to be excited by a 14-MeV AWA near-annular bunch with charge up to 50 nC.

There are several modes excited in each structure; the design mode for the THz structure is E_{04} at 0.472 THz, while the design mode for the GHz version is E_{02} at 18.8 GHz. The test bunch should lag the drive bunch by ~700 microns to experience acceleration in the THz structure, and by ~17 mm in the GHz structure. Figs. 2-3 present some drawings and photos of these structures.

*Work supported by DoE, Office of High Energy Physics
#sergey.shchelkunov@gmail.com

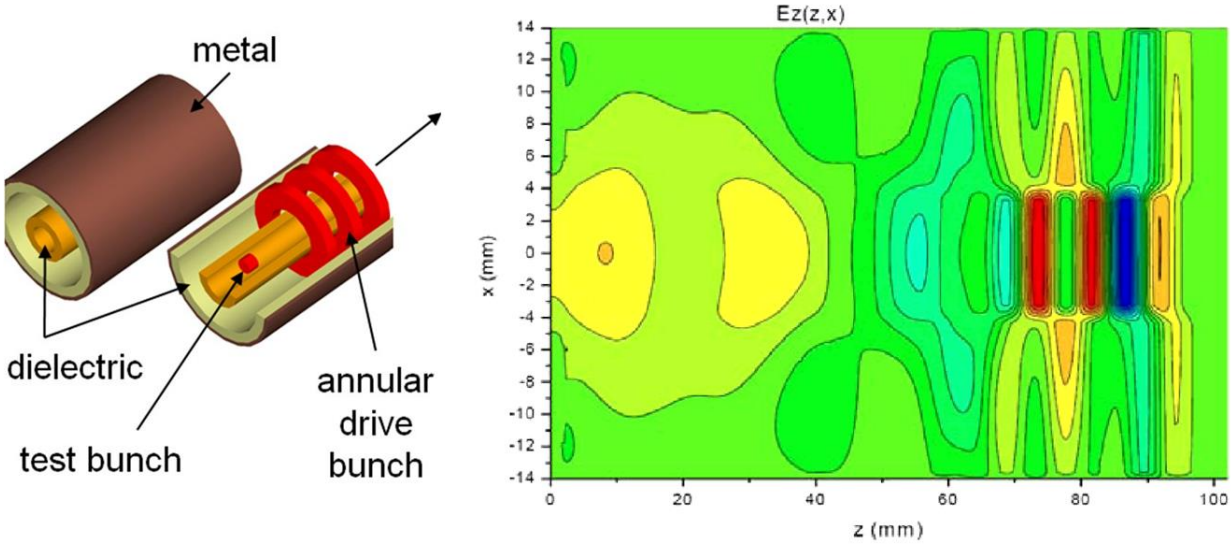

FIGURE 2. Basic configuration for coaxial type of DWFA (left), and an example of the fields one might find in such a structure (a so-called field map is shown that presents E_z in the *z*-*x* plane after the bunch has moved 92 mm).

TABLE I. THz (mm-scale) coaxial structure parameters.

parameter	**value**
OD of outer dielectric tube (mm)	2.0
ID of outer dielectric tube (mm)	1.0
OD of inner dielectric tube (microns)	360
ID of inner dielectric tube (microns)	100-150
Length (mm)	21
Dielectric constant (quartz)	3.75
Acceleration Gradient (MV/m/nC)	317-220
Transformer Ratio (1 drive bunch)	4.7:1 – 3.3:1

TABLE II. GHz (cm-scale) coaxial structure parameters.

parameter	**value**
OD of outer dielectric tube (mm)	30.16
ID of outer dielectric tube (mm)	27
OD of inner dielectric tube (mm)	8
ID of inner dielectric tube (mm)	4.8
Length (mm)	100
Dielectric constant (Al_2O_3)	9.8
Acceleration Gradient (MV/m/nC)	0.4
Transformer Ratio (1 drive bunch)	6.5:1

The most challenging aspect of micro-fabrication of the THz-scale structure is to support the inner ceramic pipe, while having it centered with the outer pipe. We achieved this by using three pins at either end of the structure as shown in Fig. 2 (at right). The pins are made out of the same ceramic material as the inner pipe, and are secured by micrometer screws. One can use a digital microscope (with the output on a computer screen) to observe the position of the inner pipe when performing its alignment. Three sectors are formed between the pins in the outer channel; this is a suitable arrangement since it is expected ultimately to have a point-like electron bunch [see the following sections] that has transverse dimensions that will fit into a single sector.

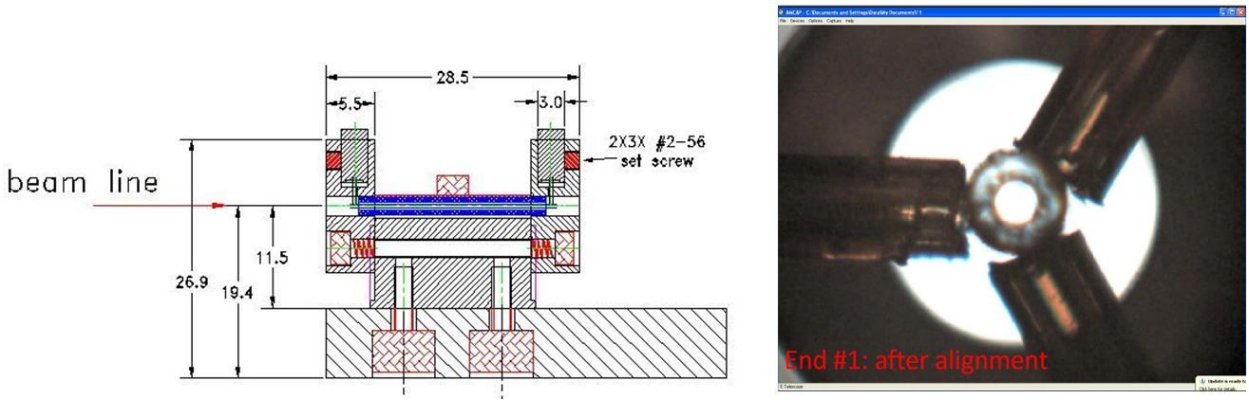

FIGURE 2. (left) Cross-section view of the THz structure to be tested at FACET (dielectric tubes are in blue), and a digital photo showing that the inner ceramic tube is supported by 3 alignment pins, and is centered [see explanations in the text].

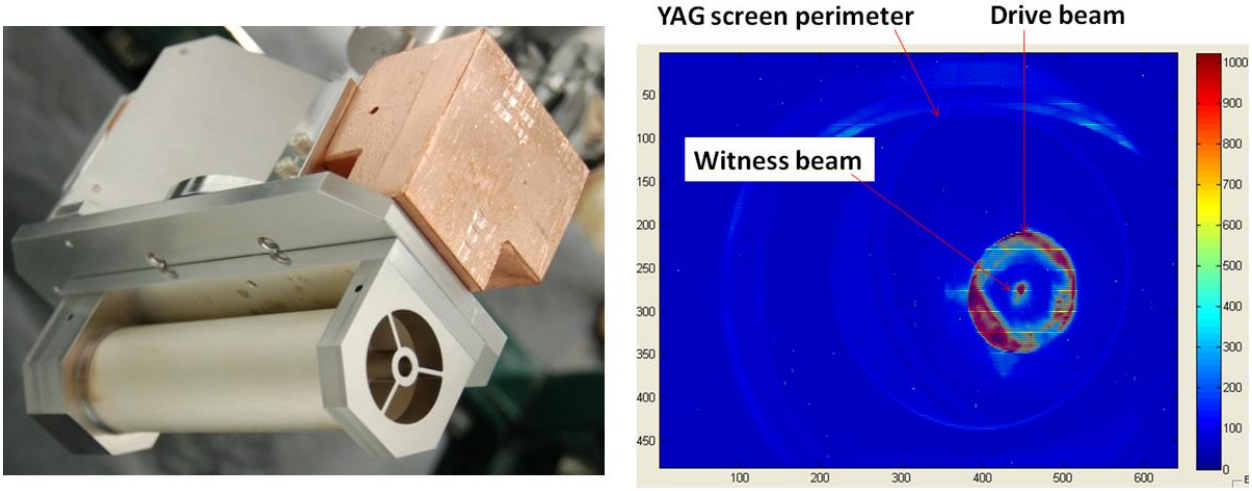

FIGURE 3. (left) Photo of the GHz structure being tested at AWA/Argonne, and a frame-grabber snapshot of the annular drive bunch beam at AWA (screen calibrated in pixels) together with a centered, delayed witness bunch. Further efforts are underway to form a more uniform ring distribution for the drive bunch. The ring shown has 20 nC of total charge.

PLANNED EXPERIMENTS

The experiment with the THz-structure at FACET will use a point-like beam to probe the structure. We will show below that this allows us to obtain information sufficient to draw conclusions about the structure's behaviour when it would be excited by an annular bunch.

The experiment at AWA/Argonne uses a ring-like bunch. Fig.3 (right) shows results of our first attempt to produce such a bunch.

In the initial stage of the experiments at FACET, the plan is to direct the electron bunch to either the outer, annular channel or the inner channel, and to compare the amount of THz radiation produced (see Fig 4). The amount of radiation yields the ratio of drag forces acting on the drive bunch when it goes through each channel, and is computed to be ~ 5.3 for the case of the 100 μm central channel and ~4.0 for the case of the 150 μm central channel. As of now, a 2cm-long module has been manufactured, shipped to FACET, and awaits installation on the beam-line.

In the second stage of the FACET experiment, the plan is to determine the fields produced by a point-like bunch in the inner channel (Fig. 5) by measuring the energy change of the drive bunch itself, which should yield the deceleration gradient. Together with information obtained at the first stage, this will allow us to infer the transformer ratio and the acceleration gradient that would occur in this structure when it is driven by an annular-like beam as described in [1,3,4].

The experiment at AWA will use a test bunch to probe the fields; if this test bunch is situated ~56 ps behind the drive bunch, it should undergo peak acceleration. The probing technique and measurement procedures will be the same as used before when investigating the rectangular two-channel GHz-scale DWFA [5].

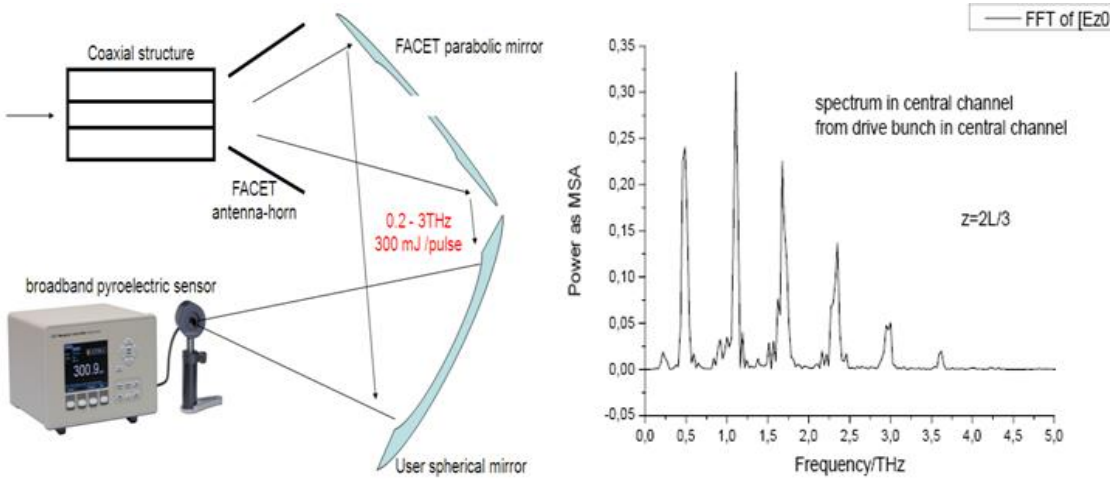

FIGURE 4. At FACET, the plan is to direct the e-beam to either the outer, annular channel, or inner channel and compare the amount of THz radiation produced (the right-hand side shows an example of spectrum expected when the e-beam goes through the inner channel).

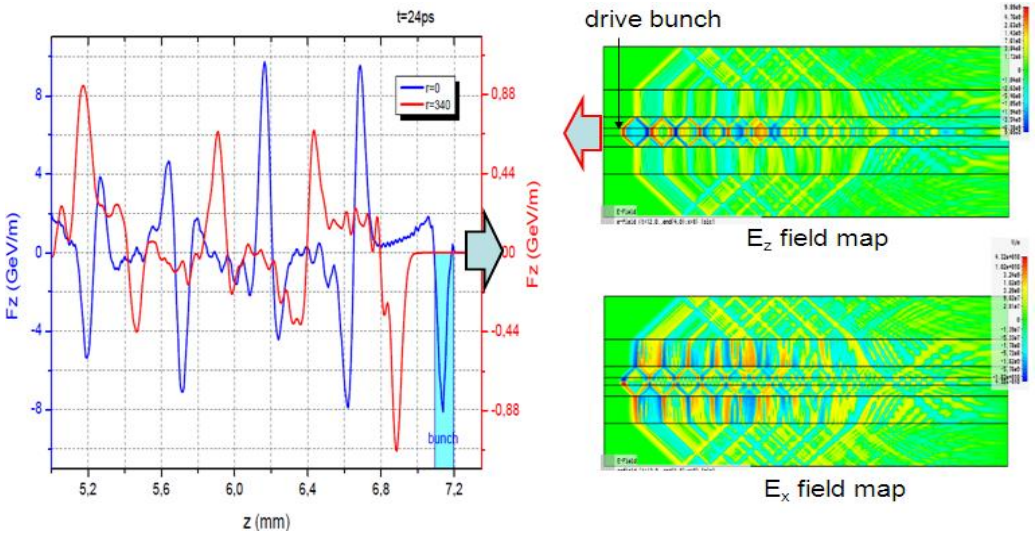

FIGURE 5. Prediction of the fields produced by a bunch propagating in the inner channel (FACET experiment). The drive bunch propagates in the direction shown by the arrows. On the left-hand side, the blue curve presents the composite F_z force along the axis of the structure (in the inner, tube-like channel), and the red curve presents the composite F_z in the annular channel, as setup by a 3nC point-like drive bunch moving along the axis of the structure (in the inner channel). At the first acceleration peak, the composite force delivers an acceleration of ~9 GV/m.

A RAMPED BUNCH TRAIN CONCEPT

A ramped bunch train (RBT) technique was proposed some time ago to allow nearly the same energy loss for all drive bunches in a train, and thus to generate a high transformer ratio TR. By now, there a few publications on the subject, among them that by Kanareykin and co-authors where an experiment is described demonstrating the technique for a single channel device [6]. We have investigated the RBT for the coaxial configuration [3]. Presently, the technique is being considered for a cm-scale device (an experiment that can be done at AWA/Argonne); but the feasibility for THz-scale coaxial structures might be investigated too, if and when suitable, multiple, annular-like bunches become available.

Basically, the recipe is to (a) take the first bunch with the charge Q_1, compute TR_1 and the location of the first trailing acceleration peak; (b) place the second bunch at that location, and select its charge to be $Q_2 = Q_1 \times (1+ TR_1)$, and (c) repeat this algorithm stepwise; that is, for a bunch train with n-1 bunches, one should find TR_{n-1}, find the closest acceleration peak, and place there the n^{th} bunch having its charge $Q_n = Q_1 \times (1 + TR_{n-1})$. The placement and charge of each bunch in the train are thereby determined with the assistance of a numerical computation that determines the resulting wakefield at each step. This will optimize the energy loss of the train of drive bunches.

Further details can be found in [3] and in references therein.

ACKNOWLEDGMENTS

This research was supported by US DoE.

REFERENCES

1. G.V. Sotnikov, T.C. Marshall, and J.L. Hirshfield, *Phys. Rev. ST--AB*, **12**, 061302, (2009)
2. T.C. Marshall, G.V. Sotnikov, and J.L. Hirshfield, *AAC: Fourteenth Workshop*, edited by S. Gold and G. Nusinovich, AIP Conf. Proc. 1299, 336 (2010).
3. G. V. Sotnikov and T. C. Marshall, Phys. Rev. ST Accel. Beams **14**, 031302 (2011)
4. G. V. Sotnikov, et al., WEPPP004, IPAC 2012 proceedings (to be published)
5. S. V. Shchelkunov, et al., Phys. Rev. ST Accel. Beams **15**, 031301 (2012)
6. C. Jing, et al., Phys. Rev. ST Accel. Beams **14**, 021302 (2011)

Dielectric Structures for Two-Beam Accelerators, with Parameters Ranging from GHz to THz

S.V. Shchelkunov[1], J.L. Hirshfield[1,2], M.A.LaPointe[1], T.C. Marshall[2], G. Sotnikov[3], Wei Gai[4], M. Conde[4], J. Power[4], D. Mihalcea[4]

[1]Yale University, New Haven, CT 06511, USA, sergey.shchelkunov@gmail.com
[2]Omega-P, Inc, New Haven, CT 06510, USA
[3]NSC Kharkov Institute of Physics and Technology, 61108 Kharkov, Ukraine;
[4]Argonne National Laboratory, Argonne, IL, 60439,USA

Dielectric-lined structures are appealing candidates for a future collider or other accelerators because they offer simplicity and cost-effectiveness, withstand high fields, and can be configured to provide direct energy transfer from the drive bunch train to accelerated bunches without intermediate coupling elements (waveguides, input/output couplers, etc). Promising versions are those that have two distinct adjacent channels – one for the drive bunch train and the other for the accelerated bunches – because these versions can exhibit both high transformer ratio and appreciable gradients, while not requiring sophisticated means to profile the drive bunches or the drive bunch trains to obtain desired performance [1, 2, 3].

An overview of recent work (at Yale University and Argonne National Lab., USA) on two-channel rectangular and coaxial dielectric lined structures [Fig.1] is presented covering numerous topics such as a recently conducted proof-of-principle experiment. We shall also describe theoretical investigations of cm-scale (GHz) and mm-scale (THz) structures that are excited by a ramped bunch train, together with an extensive study of bunch stability issues. The described work is supported by US Department of Energy, Office of High Energy Physics.

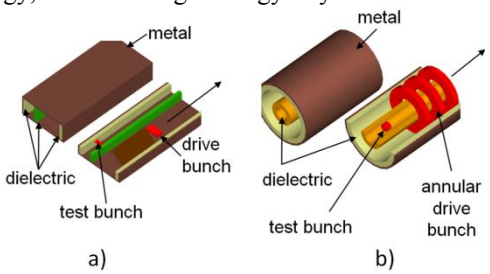

Fig. 1. Examples of two-channel rectangular (a), and coaxial (b) dielectric-lined structures. Note that the number of drive bunches may be greater than one

A recently conducted proof-of-principle experiment with a rectangular 10-cm long two-channel module is the first experiment to test the 2-channel DWA concept. The experimental objective was to design, build, and test a 2-channel dielectric wakefield structure and compare results with theory model predictions via observations of the test bunch energy acceleration and transverse kick. The experiment was carried out at the AWA beam-line (Argonne National Lab). The structure is designed to have a maximum transformer ratio (TR) of ~12.5:1. It is excited by a single drive bunch, and operates mainly in the LSM_{31} mode (~ 30 GHz). The time-delayed test bunch is produced off-axis on the same photocathode where the drive bunch is produced. The dielectric liner is cordierite (dielectric constant ~ 4.76). Details of the experimental setup are described in [4]. One notes that the 10-15 nC drive bunch was typically off the channel center by 2-3 mm [Fig.2]. However, this did not prevent obtaining data to confirm the theory.

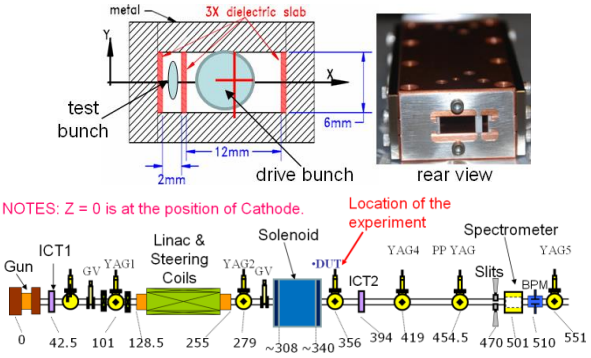

Fig. 2. (Top, left) Cross-section of the apparatus (dielectric slab thicknesses, from left to right, are 1.26, 2.03 and 1.06 mm); and (bottom) its position in the AWA beam line

Data were collected for different delays between the drive bunch and the test bunch, including measurements of the energy gain or loss received by test electrons, and the horizontal kick they received. The latter is processed to obtain the value of the horizontal deflecting force responsible for bunch deflection [5]. Space limitations prevent us from presenting here the results for more than one value of test bunch delay.

With a delay of ~11 mm or ~37 ps [Fig.3], a jitter of 50-60 keV, and an energy slit error of 77 keV required recalibration of the data. The resulting inferred energy loss was up to 65 keV, while the energy gain was in the range 65 – 150 keV; the average energy change was ~50 keV. The horizontal kick that led to the typical shifts presented in Fig.3 ranged from -2.45 to -5.2 mrad, averaging -3.9 mrad. When the aforementioned values are scaled to a 50 nC drive bunch charge, excellent agreement is found between theory and the measurements [Fig. 4]. To have loss, the accelerating force F_z (re-computed for a 50 nC drive bunch) must be up to -2.85 MeV/m; to

have the observed gains, F_z must be between 2.85 and 6.7 MeV/m; to have the obseved x-kicks, the horizontal deflecting force F_x (re-computed for a 50 nC drive bunch) must range between -1.72 and -3.6 MeV/m, and be on average -2.8 MeV/m. All these values (pointed at by the arrows) can be found on the $F_z(z)$ and $F_x(z)$ theoretical curves just where the test bunch was located.

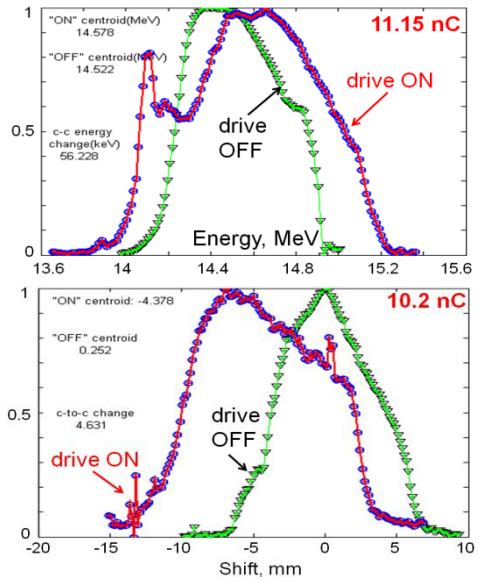

Fig. 3. Typical energy distributions, and bunch horizontal distributions (observed in 80-85% of shots) when the delay was ~11mm; distributions are normalized to unity

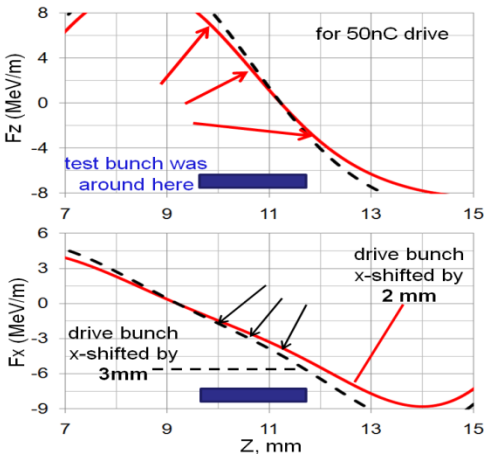

Fig. 4. Theoretical simulations of F_z and F_x as obtained by use of CST Microwave Studio for the test channel

In summary, the theory model predictions are well confirmed by the experimental data. Considering Fig.4, one may note that moving a narrower bunch to a delay of 9 mm would allow both high acceleration and low deflection. However in general, deflection in a rectangular configuration is an intrinsic feature. An exceedingly far better choice for accelerator applications is a coaxial geometry, where inherent symmetry implies no undesirable deflection [3].

The planned near-term proof-of-principle experiment with a coaxial structure will be installed and operated at AWA-Argonne in 2011-2012. The structure uses two alumina (dielectric constant ~9.8) 100 mm long pipes. The outer pipe has OD 30.16 mm, and ID 27 mm; the inner pipe has OD 8 mm, and ID 4.8 mm. The structure is to be driven by a single 14 MeV annular bunch having charge up to 50 nC. The structure is to be mainly excited in the TM_{02}-mode. This module is predicted to exhibit TR 6.2:1, and acceleration gradient 18 MV/m. The experimental objectives are the same as they were for the rectangular module.

Another experiment that may be conducted in collaboration with AWA-Argonne after the planned upgrades [6] is to test the so-called ramped bunch train (RBT) concept [7]. In [8], a cm-scale example of this was described for coaxial geometry, and a recipe was obtained to enhance TR up to ~17:1 following only four drive bunches. Most importantly, the proposed scheme ensures that all the drive bunches undergo the same deceleration.

Coaxial mm-scale structures are promising candidates as acceleration modules for a future multi-TeV collider because they should provide high transformer ratio and large accelerating gradient, should have transverse forces acting on the accelerated bunch that are focusing, and can be designed to have weak drive bunch instabilities that permit utilizing the drive trains over long distances [3, 9]. In [10], an example is given for a mm-scale coaxial module that would operate in the TM_{02}-mode at ~912 GHz, and when driven by one 6 nC bunch would exhibit ~520 MV/m accelerating gradient in a ~100 micron-diameter inner channel. [The outer channel has OD ~1 mm]. The RBT concept is under further study, and drive and test bunch stability issues are being investigated as well [9, 10].

References

1. *Changbiao Wang, et al.,* Rectangular Dielectric-loaded Structures for Achieving High Acceleration Gradients // AIP Conf. Proc. 877, pp. 910-917 (2006).

2. *Wanming Liu and Wei Gai,* Wakefield generation by a relativistic ring beam in a coaxial two-channel dielectric loaded structure // Phys. Rev. ST-AB, V. 12, 051301 (2009) and references therein.

3. *G. V. Sotnikov, T. C. Marshall, and J. L. Hirshfield*, Coaxial two-channel high-gradient dielectric wakefield accelerator // Phys. Rev. ST-AB, V. 12, 061302 (2009) and references therein.

4. *S. V. Shchelkunov, et al.,* Status of Dielectric-Lined Two-Channel Rectangular High Transformer Ratio Accelerator Structure Experiment // Procs of 2011 Particle Accelerator Conf., MOP107, link: http://www.c-ad.bnl.gov/pac2011/proceedings/papers/mop107.pdf and refs. therein.

5. *J.L. Hirshfield, et al.,* A Fast Kicker Using a Rectangular Dielectric Wakefield Accelerator Structure // Particle Accelerator Conference 2009 Procs, paper FR2RAC03, link: http://trshare.triumf.ca/~pac09proc/Proceedings_091005 papers/fr2rac03.pdf and references therein.

6. *M.E. Conde, et al.,* Upgrade of the Argonne Wakefield Accelerator Facility (AWA) and Commissioning of a new RF Gun for Drive Beam Generation // Procs of 2011 Particle Accelerator Conf., MOP008, link: http://www.c-ad.bnl.gov/pac2011/proceedings/papers/mop008.pdf.

7. *C. Jing, et al.,* Increasing the transformer ratio at the Argonne wakefield accelerator // Phys. Rev. ST-AB, V. 14, 021302 (2011) and references therein.

8. *G.V. Sotnikov and T.C. Marshall,* Improved ramped bunch train to increase the transformer ratio of a two-channel multimode dielectric wakefield accelerator // Phys. Rev. ST Accel. Beams, V. 14, 031302 (2011).

9. *G.V. Sotnikov, et al.,* Accelerated Bunch Stability in a Coaxial Dielectric Structure When its Symmetry is Broken // AIP Conf. Proc. 1299, pp. 342-347 (2010).

10. *T. C. Marshall, G. V. Sotnikov, and J. L. Hirshfield,* A THz Two-Channel Dielectric Wakefield Structure for High Gradient Acceleration // AIP Conf. Proc. 1299, pp. 336-341 (2010).

HIGH-GRADIENT THZ-SCALE TWO-CHANNEL COAXIAL DIELECTRIC-LINED WAKE FIELD ACCELERATOR*

S.V. Shchelkunov[1], T.C. Marshall[2], G. Sotnikov[3], J.L. Hirshfield[1,2], M.A. LaPointe[1]
[1]Yale University, New Haven, CT, 06520, USA; [2]Omega-P, Inc, New Haven, CT 06511, USA;
[3]NSC Kharkov Institute of Physics and Technology, 61108, Kharkov, Ukraine

Abstract

A mm-scale THz coaxial dielectric-lined two-beam wakefield accelerator concept is currently under study by Yale University Beam Physics Lab and collaborators. Performance of this structure is based on use of annular drive bunches. The structure has the attractive feature that the drive and accelerated bunches both have good focusing and stability properties, and also exhibits a large transformer ratio. We have had recent successful experiments at AWA/Argonne National Lab with a cm-scale GHz rectangular dielectric-lined two-beam accelerator module, and plan further activity there with a cm-scale GHz coaxial structure. The research reported here has two objectives. The first is to design a structure to produce acceleration gradients on a scale of 0.35 GeV/m per each nC of annular drive charge. The second goal is to build and test the structure at FACET/SLAC. At FACET the structure can be excited only with the available pencil-like drive bunch, but a reciprocity principle allows one to infer some of the properties that would be seen if the excitation were to be by an annular drive bunch. This presentation shows our latest findings, discusses related issues, and discusses our plans for experiments.

Introduction

In [1], a new scheme for a two-beam dielectric wakefield accelerator was proposed that uses two hollow concentric dielectric tubes with vacuum channels for drive and accelerated bunches. This two-channel coaxial dielectric accelerator (CDWA) appears to be a promising candidate for a future TeV-scale collider [2].

The CDWA structure consists of two coaxial dielectric tubes enclosed one inside the other, thereby forming two vacuum channels, the outer for the annular drive bunches and the inner for accelerated witness bunches. It could provide a high acceleration gradient, in the GeV/m range for mm-scale structures, while demonstrating a larger transformer ratio (TR) than would a single-channel structure. The transverse forces acting upon the accelerated bunch can be focusing, while the annular drive bunch has been shown to move an appreciable distance without undergoing distortion or deflection [2].

An experiment is now underway at FACET (SLAC) to test a mm-scale THz CDWA using their point-like drive bunch. It might appear that only an annular bunch could be used to set up the desired wakefields in this structure. However it can be shown that the point drive bunch will establish the fields one wishes to study; furthermore, it will be shown how one may obtain information from this study whereby the data can be compared with theoretical simulations obtained with the CST STUDIO code.

Experience with this THz structure, together with information obtained from a larger GHz structure now under study at the Argonne Wakefield Accelerator facility (ANL), could provide the necessary stimulus for further development of this type of DWA structure for a collider-type accelerator.

Design Overview

The basic configuration for this type of DWFA is shown in Fig.1.

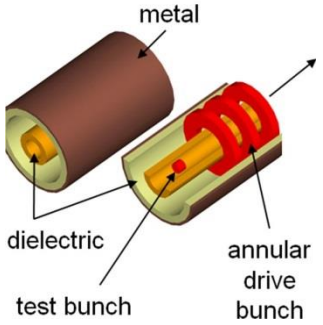

Figure 1. Coaxial CDWA schematic.

One or a few annular drive bunches can be used to produce the wakefield. When several drive bunches are used, the ratio of drive bunch charges and the distances between bunches should be adjusted to constitute a ramp bunch train with constructive wake fields [3].

The structure and related parameters are presented in Table I; it is instructive to also show in Table II the parameters of the cm-scale coaxial structure that is being tested at AWA/Argonne. Both structures are to be driven by a single drive bunch; the THz structure will be excited by the ~3-nC 23-GeV bunch available at FACET, and the GHz structure is to be excited by a 14-MeV AWA annular bunch with charge up to 50 nC.

There are several modes excited in each structure; the design mode for the THz structure is E_{04} at 472 THz, while the design mode for the GHz version is E_{02} at 18.8 GHz. The test bunch should lag the drive bunch by ~700 microns to experience acceleration in the THz structure, and by ~17 mm in the GHz structure. Figs. 2-3 present some drawings/photos of these structures.

Table I: THz (mm-scale) coaxial structure parameters

OD of outer dielectric tube (mm)	2.0
ID of outer dielectric tube (mm)	1.0
OD of inner dielectric tube (microns)	360
ID of inner dielectric tube (microns)	100-150
Length (mm)	21
Dielectric constant (quartz)	3.75
Acceleration Gradient (MV/m/nC)	310-138
Transformer Ratio (1 drive bunch)	8:1 - 7:1

Table II: GHz (cm-scale) coaxial structure parameters

OD of outer dielectric tube (mm)	30.15
ID of outer dielectric tube (mm)	27
OD of inner dielectric tube (mm)	8
ID of inner dielectric tube (mm)	4.8
Length (mm)	100
Dielectric constant (Al_2O_3)	9.8
Acceleration Gradient (MV/m/nC)	0.4
Transformer Ratio (1 drive bunch)	6.5:1

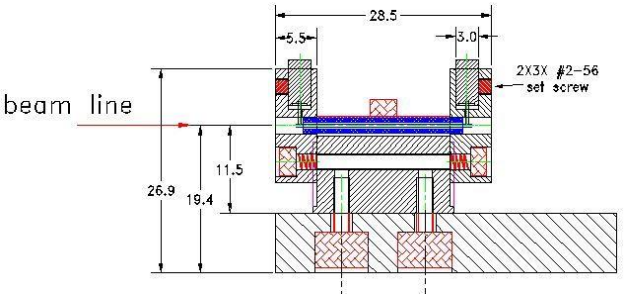

Figure 2. Cross-section view of the THz structure to be tested at FACET (dielectric tubes are in blue)

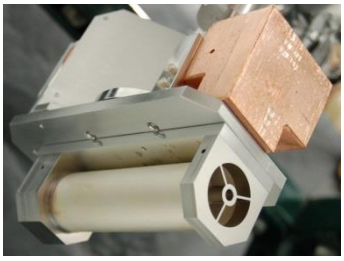

Figure 3. Photo of the GHz structure being tested at AWA/Argonne.

Planned Experiments

The experiment with the THz-structure at FACET will use a point-like beam to probe the structure. We will show later that this allows us to obtain information sufficient to draw conclusions about the structure's behaviour when excited by an annular bunch.

The experiment at AWA/Argonne uses a ring-like bunch. Fig.4 shows results of our first attempt to produce such a bunch.

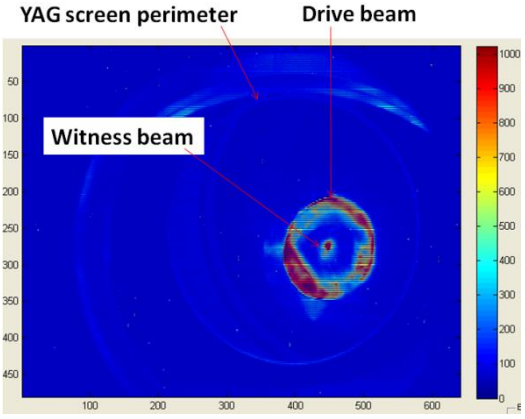

Figure 4. Frame-grabber snapshot of the annular-like beam at AWA (screen calibrated in pixels). Further efforts are under way to form a more uniform ring distribution. The ring shown has 20 nC of total charge.

In the initial stage of the experiments at FACET, the plan is to direct the e-beam to either the outer, annular channel or the inner channel, and to compare the amount of THz radiation produced (see Fig 5). The amount of

*Work supported by DoE, Office of High Energy Physics
#sergey.shchelkunov@gmail.com

radiation yields the ratio of drag forces acting on the drive bunch when it goes through each channel. This ratio is computed to be ~ 3.8.

In the second stage of the FACET experiment, the plan is to map the fields produced by a point-like bunch in the inner channel by measuring the energy changes of the drive bunch itself, to yield the deceleration gradient. Together with information obtained at the first stage, this will allow us to infer the transformer ratio and the acceleration gradient that would occur in this structure when it is driven by an annular-like beam as described in [1,3 and 4].

The experiment at AWA will use a test bunch to probe the fields; if this test bunch is situated ~56 ps behind the drive bunch, it should undergo acceleration. The probing technique and measurement procedures will be the same as used before when investigating the rectangular two-channel GHz-scale DWFA [5].

References

[1] G.V. Sotnikov, T.C. Marshall, and J.L. Hirshfield, *Phys. Rev. ST--AB*, **12**, 061302, (2009)

[2] T.C. Marshall, G.V. Sotnikov, and J.L. Hirshfield, *AAC: Fourteenth Workshop*, edited by S. Gold and G. Nusinovich, AIP Conf. Proc. 1299, 336 (2010)

[3] G. V. Sotnikov and T. C. Marshall, Phys. Rev. ST Accel. Beams 14, 031302 (2011)

[4] G. V. Sotnikov, et al., WEPPP004, these proceedings

[5] S. V. Shchelkunov, et al., Phys. Rev. ST Accel. Beams 15, 031301 (2012)

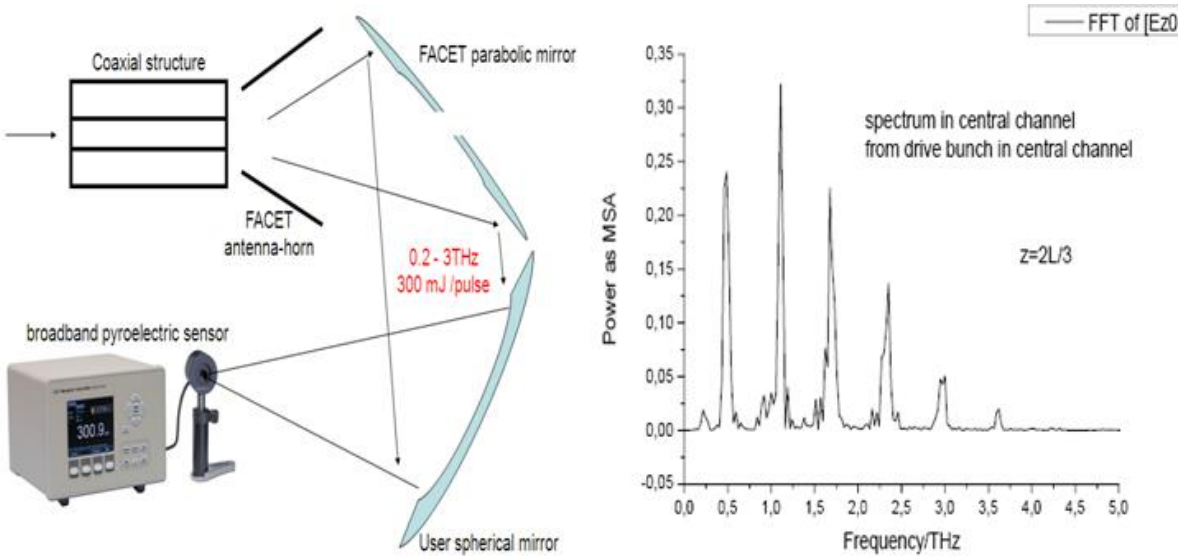

Figure 5. At FACET, the plan is to direct the e-beam to either the outer, annular channel, or inner channel and compare the amount of THz radiation produced (the right-hand side shows an example of spectrum expected when the e-beam goes through the inner channel)

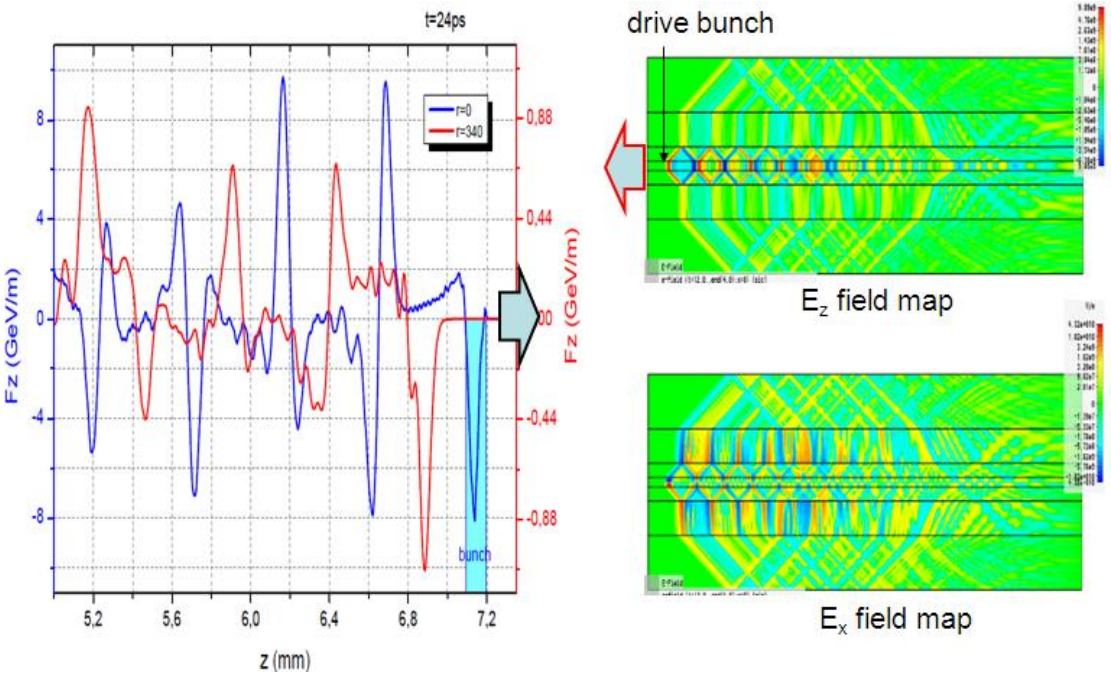

Figure 6. Prediction of the fields produced by a bunch propagating in the inner channel (FACET experiment). The drive bunch propagates in the direction shown by the arrows. On the left-hand side, the blue curve presents the composite F_z force along the axis of the structure (in the inner, tube-like channel), and the red curve presents the composite F_z in the annular channel as setup by a 3nC point-like drive bunch moving along the axis of the structure (in the inner channel).

Coaxial two-channel high-gradient dielectric wakefield accelerator

G. V. Sotnikov,[1,2,*] T. C. Marshall,[3,2,†] and J. L. Hirshfield[4,2,‡]

[1]*NSC Kharkov Institute of Physics and Technology, 1 Akademicheskaya St., Kharkov 61108, Ukraine*
[2]*Omega-P, Inc., 199 Whitney Avenue, New Haven, Connecticut 06511, USA*
[3]*Columbia University, New York City, New York 10027, USA*
[4]*Yale University, New Haven, Connecticut 06520, USA*

(Received 27 March 2009; published 22 June 2009)

A new scheme for a dielectric wakefield accelerator is proposed that employs a cylindrical multizone dielectric structure configured as two concentric dielectric tubes with outer and inner vacuum channels for drive and accelerated bunches. Analytical and numerical studies have been carried out for such coaxial dielectric-loaded structures (CDS) for high-gradient acceleration. An analytical theory of wakefield excitation by particle bunches in a multizone CDS has been formulated. Numerical calculations are presented for an example of a CDS using dielectric tubes with dielectric permittivity 5.7, having external diameters of 2.121 and 0.179 mm with inner diameters of 2.095 and 0.1 mm. An annular 5 GeV, 6 nC electron bunch with rms length of 0.035 mm energizes a wakefield on the structure axis having an accelerating gradient of ~600 MeV/m with a transformer ratio ~8:1. The period of the accelerating field is ~0.33 mm. If the width of the drive bunch channel is decreased, it is possible to obtain an accelerating gradient of >1 GeV/m while keeping the transformer ratio approximately the same. Full numerical simulations using a particle-in-cell code have confirmed results of the linear theory and furthermore have shown the important influence of the quenching wave that restricts the region of the wakefield to within several periods following the drive bunch. Numerical simulations for another example have shown nearly stable transport of drive and accelerated bunches through the CDS, using a short train of drive bunches.

DOI: 10.1103/PhysRevSTAB.12.061302 PACS numbers: 41.75.Jv, 41.75.Lx, 41.75.Ht, 96.50.Pw

I. INTRODUCTION

In this paper we describe a coaxial cylindrical two-channel dielectric wakefield traveling-wave accelerator (DWFA) that is energized by a drive bunch having an annular cross section. This configuration can have a number of unique attributes, including (a) a transformer ratio T, defined as the peak accelerating field that can be applied to a test particle divided by the average decelerating field experienced by the drive bunch, which can be considerably greater than the value of about 2 that is typical for a collinear DWFA; (b) design flexibility in the tradeoff between high T and high acceleration gradient G; (c) fabrication of the accelerator structure which can be comparatively simple and precise; (d) continuous energy coupling from drive to test bunch in the central accelerator channel without need for transfer structures; (e) single-bunch operation with high values of G that should minimize disruptions due to long-range wakefields; (f) inherent transverse focusing forces for particles in the accelerated bunch; and (g) nearly stable motion of the annular drive bunch.

It will be shown below that a mm-scale version of this class of structures can be designed with $T \gg 1$ that can be capable of developing accelerating wakefields $G >$ 1 GeV/m when excited by a single drive bunch with charge of a few nC. This is naturally of great significance because of the high magnitude of G. But it is also significant because it is achieved with only a single drive bunch. Several years ago, a theory was published predicting that exceptionally high accelerating fields could be achieved in a collinear dielectric-loaded structure by superimposing wakefields from successive bunches in a periodic train, so long as the bunch frequency matched the frequency of the dominant luminous wakefield mode [1,2]. Since then, that theory has been shown to be incomplete, since quenching fields that originate at the input boundary of the structure can interfere with the longer-range components of the wakefields, destroying their periodicity and greatly diminishing their magnitude [3,4]. Quenching fields are not included in the theory presented in Ref. [1]. Thus, we are now led to conclude that multibunch drive schemes with more than a few bunches are probably ineffective, and that single-bunch operation for a DWFA appears to be the most promising choice for achieving accelerating gradients of 100's of MeV/m. Accordingly, the coaxial DWFA structure described here is being studied and developed with a long-range view towards its possible application in a future high-gradient, multi-TeV electron-positron collider operating in a single-bunch mode. Nevertheless, an example of multibunch wakefield excitation is presented where interference from quenching waves is not overwhelming. The limited conditions under which this can occur will be discussed.

*sotnikov@kipt.kharkov.ua
†tcm2@columbia.edu
‡jay.hirshfield@yale.edu

In conventional linear accelerators, the rf power used to accelerate the beam is derived from high-power rf amplifiers. To achieve multi-TeV energies, high accelerating gradients are necessary to limit the lengths of the two linacs, but the number of amplifiers needed could become excessive. Thus, alternative two-beam schemes have been proposed [5] wherein rf power is extracted from a low-energy, high current drive beam which is decelerated in power extraction and transfer structures. This power is then fed into the structures of the main linac, and used to accelerate the high-energy, low-current main beam. The most active two-beam project now under study is the Compact Linear Collider (CLIC) concept at CERN [6], where an rf frequency of 12 GHz has been chosen for the fields in the acceleration channel, in the expectation of sustaining a working gradient of 100 MeV/m in a metallic structure with highly infrequent breakdowns.

In contrast to CLIC, the rf generation mechanism for the structure proposed here is by creation of wakefields (Cherenkov radiation) induced by passage of a charge bunch along a dielectric-lined drive channel. This radiation couples continuously into a parallel acceleration channel, without need for auxiliary coupling elements. A diagram for the cross section of the simplest coaxial structure in this class is shown in Fig. 1. The path of the drive bunch moving in the outer annular channel in Fig. 1 is separated from that of the accelerated bunch that moves in the central channel. A rectangular two-channel DWFA is now under construction for tests at the Argonne National Laboratory (ANL)—the Argonne Wakefield Accelerator (AWA) facility. In another configuration, parallel cylindrical dielectric channels were used with a step-up coupling element between channels [7]; a prototype of that design was tested at the ANL-AWA facility [8].

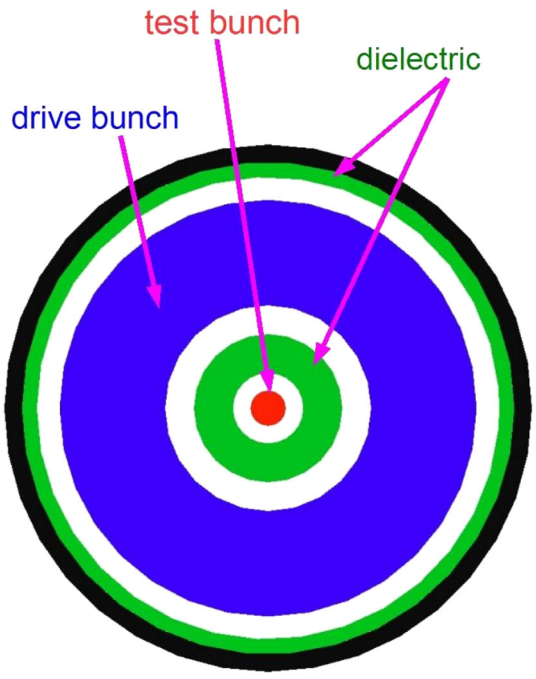

FIG. 1. (Color) Cross section of a coaxial DWFA. Dielectric tubes are green, drive bunch is blue; test bunch is red, and black outer shell is metal.

The two-channel coaxial wakefield accelerator structure that will be investigated below is one version within a class of multilayered dielectric-loaded accelerating structures in which the central region and one of the concentric layers are vacuum channels [9–11]. Use of multilayered concentric dielectrics in a collinear acceleration scheme allows concentration of the excited wakefields in the central vacuum channel for particle acceleration. As a consequence, it is possible to reduce the high-frequency losses on metal walls of a surrounding waveguide [9,11], or to discard the surrounding waveguide altogether as in the design of the optical Bragg accelerator [10].

It is expected that a high acceleration field ($\sim$ 1–2 GeV/m) can be sustained in traveling-wave dielectric structures without breakdown because the dielectric is exposed to intense fields for only short times, according to supporting experimental evidence [12]. The breakdown limit of a wakefield structure is not determined by the slow filling time of a resonant cavity by electromagnetic energy, but rather by the much shorter time of the passing field pulses set up by the short bunches which generate the wakefield. The vacuum-based wakefield structure is geometrically rigid and therefore could be a precisely reproducible element in a staged system. Also, the structure is capable of accurate microfabrication, an important consideration when staging a large number of mm-scale modules that must be identical. The two-channel wakefield accelerator is already a step forward in improving the performance and versatility of wakefield accelerators by avoiding the requirement of collinearity between the drive bunch train and the accelerated bunch which occurs in a single-channel DWFA device. The continuous coaxial dielectric configuration preserves the symmetry of the structure, which might result in fewer beam transport difficulties and provide a less complicated way to inject power into the accelerated bunch line than does the point-to-point power injection via transfer couplers as is required with conventional accelerator structures [7]. Finally, operation in a single-bunch mode should avoid beam disruptions that can arise due to long-range wakes acting on following bunches. These exceptional advantages for this accelerator structure seem to justify continued analysis, leading to design of a proof-of-principle experiment. This paper is intended as a step towards that goal.

II. DISPERSION EQUATION AND EIGENMODES

The coaxial two-channel dielectric wakefield accelerating structure analyzed analytically and numerically in the following sections is a particular case of a general multizone dielectric structure. One of the basic analytical methods for finding wakefields excited by charged particle

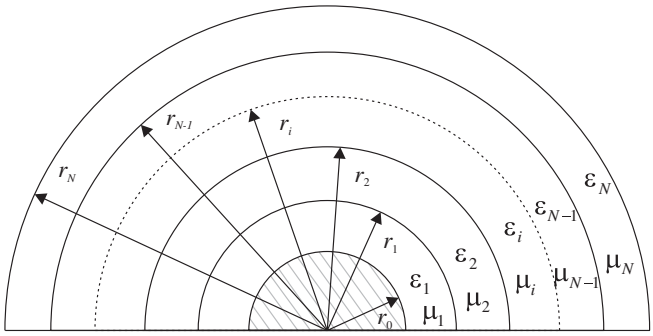

FIG. 2. Cross section of an N-zone dielectric-lined coaxial waveguide structure. The innermost vacuum zone of radius r_o is for transport of the accelerated beam.

bunches in such structures is decomposition into eigenmodes, where the eigenfrequency and wave number for each mode correspond to a phase velocity equal to the drive bunch axial velocity. In this section we will derive the general dispersion equation of a multizone dielectric structure. The equations we obtain will be valid for any number of axisymmetric dielectric layers, each having its own scalar value of dielectric permittivity.

The sketch of a generalized multizone dielectric structure is shown in Fig. 2. The external radius of the first layer is r_1, and its internal radius is r_0. In general, the structure is composed of a simply connected zone (for the case $r_0 = 0$), and several doubly connected zones. The external layer of the structure ($r_{N-1} < r \le r_N$) can be bounded by free space or by a conducting metal pipe. Zones in which the drive bunch and the accelerated test particle reside are vacuum, wherein $\mu = \varepsilon = 1$.

For deriving a compact form of the dispersion equation for a multizone dielectric structure, a matrix approach with use of corresponding transition matrices has proven effective. Recently this method has been applied for rectangular multizone dielectric structures [1]. The essence of this approach consists in knowing electromagnetic fields at one boundary of a zone, from which it is possible to find fields at the other boundary of the same zone, and then carrying this forward to include all zones [13]. We apply the method developed in Ref. [1] to obtain the dispersion equation of an axially symmetrical multizone cylindrical dielectric structure.

As trial solutions of Maxwell equations for components of the electromagnetic fields in each layer of the dielectric structure, we take the following:

$$\begin{aligned} E_z^{(i)} &= e_z^{(i)}(r)\exp[j(k_z z - \omega t)] \\ E_r^{(i)} &= j e_r^{(i)}(r)\exp[j(k_z z - \omega t)] \\ H_\varphi^{(i)} &= h_\varphi^{(i)}(r)\exp[j(k_z z - \omega t)], \end{aligned} \tag{1}$$

where k_z and ω are the longitudinal wave number and frequency of a wave and i is the zone number ($1 \le i \le N$). The absence of other components is valid when the source function (drive beam) is axisymmetric. The functions describing the transverse structure of the fields in the absence of external sources are obtained:

$$e_r^{(i)} = \frac{k_z}{k^2\varepsilon_i\mu_i - k_z^2}\frac{\partial e_z^{(i)}}{\partial r}, \qquad h_\varphi^{(i)} = \frac{k\varepsilon_i}{k_z}e_r^{(i)}. \tag{2}$$

Taking into account Eqs. (1) and (2), the solutions of the Maxwell equations for the ith layer of a multizone dielectric structure have the form

$$\begin{aligned} e_z^{(i)} &= A^{(i)}J_0(\kappa_i r) + B^{(i)}Y_0(\kappa_i r), \\ e_r^{(i)} &= -A^{(i)}\frac{k_z}{\kappa_i}J_1(\kappa_i r) - B^{(i)}\frac{k_z}{\kappa_i}Y_1(\kappa_i r), \end{aligned} \tag{3}$$

where $\kappa_i^2 = k^2\varepsilon_i\mu_i - k_z^2$, J_n, and Y_n are Bessel functions and Weber functions of the nth order with $n = 0, 1$; and $A^{(i)}$ and $B^{(i)}$ are arbitrary constants which are defined from the boundary conditions. The boundary conditions comprise continuity of the longitudinal electric field $e_z^{(i)}$ and the transverse component of the displacement vector $\varepsilon_i e_r^{(i)}$. Taking this into account, the expressions can be rewritten in the matrix representation,

$$\begin{pmatrix} \frac{\varepsilon_i}{\kappa_i^2}\frac{\partial e_z^{(i)}(r)}{\partial r} \\ e_z^{(i)}(r) \end{pmatrix} = M_i(r)\begin{pmatrix} A^{(i)} \\ B^{(i)} \end{pmatrix}, \tag{4}$$

where

$$M_i(r) = \begin{pmatrix} -\frac{\varepsilon_i}{\kappa_i}J_1(\kappa_i r) & -\frac{\varepsilon_i}{\kappa_i}Y_1(\kappa_i r) \\ J_0(\kappa_i r) & Y_0(\kappa_i r) \end{pmatrix}. \tag{5}$$

Thus, boundary conditions at $r = r_i$ can be represented by

$$M_i(r_i)\begin{pmatrix} A^{(i)} \\ B^{(i)} \end{pmatrix} = M_{i+1}(r_i)\begin{pmatrix} A^{(i+1)} \\ B^{(i+1)} \end{pmatrix}, \qquad 1 < i < N-1. \tag{6}$$

Applying boundary conditions sequentially at boundaries $r = r_n$, $n = i+1, i+2, \ldots, N-1$, we can express arbitrary constants $A^{(i)}$ and $B^{(i)}$ through constants $A^{(N)}$ and $B^{(N)}$ thusly:

$$\begin{aligned} \begin{pmatrix} A^{(i)} \\ B^{(i)} \end{pmatrix} &= M_i^{-1}(r_i)S^{(i+1)}S^{(i+2)}\cdots S^{(N-2)}M_{N-1}(r_{N-2}) \\ &\quad \times \begin{pmatrix} A^{(N-1)} \\ B^{(N-1)} \end{pmatrix}, \end{aligned} \tag{7}$$

where the transition matrices $S^{(i)}(r_i)$ are defined as follows:

$$S^{(i)} = M_i(r_{i-1})M_i^{-1}(r_i) = \begin{pmatrix} S_{11}^{(i)}(r_{i-1}, r_i) & S_{12}^{(i)}(r_{i-1}, r_i) \\ S_{21}^{(i)}(r_{i-1}, r_i) & S_{22}^{(i)}(r_{i-1}, r_i) \end{pmatrix}, \tag{8}$$

with

$$
\begin{aligned}
S_{11}^{(i)}(r_{i-1}, r_i) &= \frac{\pi}{2}\kappa_i r_i[J_1(\kappa_i r_{i-1})Y_0(\kappa_i r_i) \\
&\quad - Y_1(\kappa_i r_{i-1})J_0(\kappa_i r_i)], \\
S_{12}^{(i)}(r_{i-1}, r_i) &= \frac{\pi}{2}\varepsilon_i r_i[J_1(\kappa_i r_{i-1})Y_1(\kappa_i r_i) \\
&\quad - Y_1(\kappa_i r_{i-1})J_1(\kappa_i r_i)], \\
S_{21}^{(i)}(r_{i-1}, r_i) &= -\frac{\pi}{2} r_i \frac{\kappa_i^2}{\varepsilon_i}[J_0(\kappa_i r_{i-1})Y_0(\kappa_i r_i) \\
&\quad - Y_0(\kappa_i r_{i-1})J_0(\kappa_i r_i)], \\
S_{22}^{(i)}(r_{i-1}, r_i) &= -\frac{\pi}{2}\kappa_i r_i[J_0(\kappa_i r_{i-1})Y_1(\kappa_i r_i) \\
&\quad - Y_0(\kappa_i r_{i-1})J_1(\kappa_i r_i)].
\end{aligned} \tag{9}
$$

In Eq. (7), the constants $A^{(N-1)}$ and $B^{(N-1)}$ are connected with the constants $A^{(N)}$ and $B^{(N)}$ in the outer layer of the dielectric structure by a relation similar to Eq. (6). But the constants $A^{(N)}$ and $B^{(N)}$ are not independent, and are connected by an additional condition, taking into account the outer border. Setting to zero the longitudinal electric field component at the outer conducting boundary surrounding the dielectric structure can be such a condition. The Sommerfeld radiation condition for the dielectric structure bounded by free space can be another possible condition. Not concretizing this condition before consideration of a specific dielectric structure, we will write down the boundary condition at $r = r_{N-1}$ as

$$
M_{N-1}(r_{N-1})\begin{pmatrix} A^{(N-1)} \\ B^{(N-1)} \end{pmatrix} = \begin{pmatrix} 1 \\ Z_N \end{pmatrix} A^{(N)}, \tag{10}
$$

where the value Z_N represents a surface impedance (to within a factor) and is given by

$$
Z_N = \frac{e_z^{(N)}(r_{N-1})}{\frac{\varepsilon_N}{\kappa_N^2}\frac{\partial e_z^{(N)}(r_{N-1})}{\partial r}}. \tag{11}
$$

Expressing constants $A^{(N-1)}$ and $B^{(N-1)}$ from Eq. (10) and substituting them into Eq. (7), we obtain

$$
\begin{pmatrix} A^{(i)} \\ B^{(i)} \end{pmatrix} = M_i^{-1}(r_i)S^{(i+1)}S^{(i+2)}\cdots S^{(N-1)}\begin{pmatrix} 1 \\ Z_N \end{pmatrix} A^{(N)}, \quad 1 < i < N-1. \tag{12}
$$

At the boundary of the 1st and 2nd zones we write down a condition from Eq. (10), namely,

$$
M_2(r_1)\begin{pmatrix} A^{(2)} \\ B^{(2)} \end{pmatrix} = \begin{pmatrix} 1 \\ Z_1 \end{pmatrix} A^{(1)}, \tag{13}
$$

where

$$
Z_1 = \frac{e_z^{(1)}(r_1)}{\frac{\varepsilon_1}{\kappa_1^2}\frac{\partial e_z^{(1)}(r_1)}{\partial r}}. \tag{14}
$$

Expressing constants $A^{(2)}$ and $B^{(2)}$ from Eq. (12) (with $i = 2$), we substitute them into Eq. (13). After multiplication of the resulting matrix equation on the left by the row $(-Z_1, 1)$ we come to the final dispersion equation:

$$
(-Z_1, \quad 1)\left(\prod_{n=2}^{N-1\geq 2} S^{(n)}\right)\begin{pmatrix} 1 \\ Z_N \end{pmatrix} = 0. \tag{15}
$$

The dispersion equation (15) is valid for $N \geq 3$. But it can be generalized for a two-layer dielectric structure by interposing a layer with coincident radii (see Ref. [1]). Such an operation is similar to the condition that the product of transition matrices $S^{(i)}$ in Eq. (15) is equal to the unit matrix. The equation remains valid for a single-zone structure (when the external boundary is a conducting wall) if we furthermore set $Z_2 = 0$. In this manner, the equation is valid for any number of layers of a multizone dielectric structure.

We now provide examples for the expressions Z_1 and Z_N for specific configurations of a multizone dielectric waveguide. If the dielectric waveguide has a sequence of concentric layers surrounded by a conducting pipe, then

$$
\begin{aligned}
Z_N &= \frac{\kappa_N}{\varepsilon_N} \\
&\quad \cdot \frac{J_0(\kappa_N r_{N-1})Y_0(\kappa_N r_N) - Y_0(\kappa_N r_{N-1})J_0(\kappa_N r_N)}{-J_1(\kappa_N r_{N-1})Y_0(\kappa_N r_N) + Y_1(\kappa_N r_{N-1})J_0(\kappa_N r_N)}.
\end{aligned} \tag{16}
$$

If the dielectric structure is open to free space ($r_N \to \infty$, $\varepsilon_N = 1$), then the value Z_N is described by

$$
Z_N = p_N \frac{K_0(p_N r_{N-1})}{K_1(p_N r_{N-1})}, \tag{17}
$$

where $p_N = \sqrt{k_z^2 - k^2}$, and K_0 and K_1 are the Macdonald functions of zero and first order.

If the first zone is a cylindrical ($r_0 = 0$) vacuum channel then the impedance Z_1 at its outer surface $r = r_1$ is given by

$$
Z_1 = -p_1 \frac{I_0(p_1 r_1)}{I_1(p_1 r_1)}, \tag{18}
$$

where $p_1 = \sqrt{k_z^2 - k^2}$, and I_0 and I_1 are the modified Bessel functions of a zero and first order.

Solutions of the dispersion equation (15) for fixed longitudinal wave number k_z give eigenfrequencies $\omega = \omega_m(k_z)$, and at fixed frequency ω give eigen-wavenumbers $k_z = k_m(\omega)$. However, in the case of the excitation of a dielectric waveguide by a moving charge, the frequencies and wave numbers are connected by an equiphase condition $\omega_m = k_m v_0$ (where v_0 is the velocity of the charge). Subject to this proviso the dispersion equation (15) gives frequencies and wave numbers for eigenmodes that comprise Cherenkov (wakefield) radiation in

dielectric structures that must move synchronously with the drive charges. Having found from Eq. (4) with the use of Eq. (12) the quantities $e_z^{(i)}$ and $e_r^{(i)}$, and having replaced in the derived expressions the frequency ω and the wave vector k_z by their eigenvalues, we obtain the following expressions for the electric field intensities of the eigenwaves inside the ith layer ($1 < i < N$):

$$e_z^{(i)} = [S_{21}^{(i)}(r, r_i), S_{22}^{(i)}(r, r_i)]\Lambda_m^{(i)}, \tag{19}$$

$$e_r^{(i)}(r) = \frac{k_m}{\varepsilon^{(i)}}[S_{11}^{(i)}(r, r_i), S_{12}^{(i)}(r, r_i)]\Lambda_m^{(i)}. \tag{20}$$

For determination of fields in the first zone we shall use Eq. (13). After simple transformations we find

$$\begin{aligned} e_z^{(1)}(r) &= \varphi_z^{(1)}(r) \cdot (1, 0)\Lambda_m^{(1)}, \\ e_r^{(1)}(r) &= \varphi_r^{(1)}(r) \cdot (1, 0)\Lambda_m^{(1)}. \end{aligned} \tag{21}$$

In expressions (19)–(21) the quantity $\Lambda_m^{(i)}$ is defined as follows:

$$\Lambda_m^{(i)} = A^{(N)} \begin{cases} \left(\prod_{n=i+1}^{N-1 \geq 2} S^{(n)}\right) \begin{pmatrix} 1 \\ Z_N \end{pmatrix}, & 1 \leq i < N-1 \\ \begin{pmatrix} 1 \\ Z_N \end{pmatrix}, & i = N-1. \end{cases} \tag{22}$$

Functions $\varphi_z^{(1)}(r)$ and $\varphi_r^{(1)}(r)$ which define the radial dependence of fields in the first zone are normalized so as to satisfy Eq. (13), as follows:

$$\varphi_z^{(1)}(r = r_1) = Z_1, \qquad \varphi_r^{(1)}(r = r_1) = 1. \tag{23}$$

Considering boundary conditions and Eq. (10), we write down fields in the remaining Nth layer of the structure in the form

$$e_z^{(N)}(r) = \varphi_z^{(N)}(r)A^{(N)}, \qquad e_r^{(N)}(r) = \varphi_r^{(N)}(r)A^{(N)}, \tag{24}$$

where the functions $\varphi_z^{(N)}(r)$ and, $\varphi_r^{(N)}(r)$ satisfy the conditions

$$\varphi_z^{(N)}(r = r_{N-1}) = Z_N, \qquad \varphi_r^{(N)}(r = r_{N-1}) = 1. \tag{25}$$

We present as examples the expressions for functions $\varphi_{r,z}^{(1,N)}$ of some typical configurations. If the first zone is a vacuum cylindrical channel, then

$$\varphi_z^{(1)} = -p_1 \frac{I_0(p_1 r)}{I_1(p_1 r_1)}, \qquad \varphi_r^{(1)} = \frac{I_1(p_1 r)}{I_1(p_1 r_1)}. \tag{26}$$

If the cylindrical multizone dielectric structure is surrounded by a metal sheath, then the radial structure of fields in the last zone with index N is described by expressions

$$\varphi_z^{(N)} = \frac{\kappa_N}{\varepsilon_N} \cdot \frac{J_0(\kappa_N r)Y_0(\kappa_N r_N) - Y_0(\kappa_N r)J_0(\kappa_N r_N)}{-J_1(\kappa_N r_{N-1})Y_0(\kappa_N r_N) + Y_1(\kappa_N r_{N-1})J_0(\kappa_N r_N)}, \tag{27}$$

$$\varphi_r^{(N)} = \frac{J_1(\kappa_N r)Y_0(\kappa_N r_N) - Y_1(\kappa_N r)J_0(\kappa_N r_N)}{J_1(\kappa_N r_{N-1})Y_0(\kappa_N r_N) - Y_1(\kappa_N r_{N-1})J_0(\kappa_N r_N)}. \tag{28}$$

Finally, if the dielectric structure is surrounded by free space,

$$\varphi_z^{(N)} = p_N \frac{K_0(p_N r)}{K_1(p_N r_{N-1})}, \qquad \varphi_r^{(N)} = \frac{K_1(p_N r)}{K_1(p_N r_{N-1})}. \tag{29}$$

III. WAKEFIELD OF A THIN ANNULAR BUNCH

Next we find the fields (Green's function) that are excited in a multizone coaxial dielectric structure by a charged particle bunch having the shape of an infinitesimally thin ring. The density of particles of such a bunch is described by the expression

$$\rho = \frac{Q}{2\pi r}\delta(r - r_b)\delta(z - z_0 - v_0 t), \tag{30}$$

where r_b is the radius of the annular bunch, z_0 is its position at the moment of time $t = 0$, $\delta(x)$ is the Dirac delta function, v_0 is the bunch velocity along z, and Q is charge of a bunch.

Neglecting entry and exit boundary effects, we can consider that the excited electromagnetic fields are defined only by this external source. Therefore, the dependence of fields upon time and longitudinal coordinates is defined only by the combined variable $\xi = v_0 t - z$. Then, from Maxwell equations we obtain the following inhomogeneous differential equation for determining the longitudinal electric field:

$$\frac{1}{r}\frac{\partial}{\partial r}\left[\frac{\varepsilon r}{1 - \beta_0^2 \varepsilon \mu}\frac{\partial E_z^G}{\partial r}\right] + \varepsilon \frac{\partial^2 E_z^G}{\partial \xi^2} = -4\pi \frac{\partial \rho}{\partial \xi}. \tag{31}$$

Here $\beta_0 = v_0/c$ and the dielectric permittivity depends on radius, $\varepsilon = \varepsilon(r)$, $\mu = \mu(r)$, i.e., the equation is true for any axisymmetric radially nonuniform dielectric structure. In the case we study here, $\varepsilon = \varepsilon_i$, $\mu = 1$ when $r_{i-1} \leq r < r_i$.

A Fourier transformation with respect to the variable ξ is then carried out, namely,

$$(E_z^k, \rho^k) = \frac{1}{2\pi}\int_{-\infty}^{\infty} d\xi (E_z^G \rho) \exp[ik_z \xi], \tag{32}$$

from which we obtain the equation for finding the Fourier amplitudes of the longitudinal electric field:

$$\frac{1}{r}\frac{\partial}{\partial r}\left[\frac{\varepsilon r}{1-\beta_0^2\varepsilon\mu}\frac{\partial E_z^k}{\partial r}\right]-\varepsilon k_z^2 E_z^k = 4\pi i k_z \rho^k, \quad (33)$$

where

$$\rho^k = \frac{Q}{4\pi^2 r}\delta(r-r_b)\exp[-ik_z z_0]. \quad (34)$$

We will find the solution of Eq. (33) by decomposition into waves, i.e.,

$$E_z^k = \sum_m a_m e_{zm}(r). \quad (35)$$

Having substituted Eq. (35) into the left side of Eq. (33) and having multiplied both sides of the equation by the complex conjugate eigenfunction $e_{zn}^*(r)$, and having integrated both sides of the equation over the cross section of a multilayered dielectric structure, we obtain for the decomposition coefficients a_m the expression

$$a_m = -\frac{ik_z}{k_z^2-k_m^2}\frac{Q}{\pi r_{N-1}^2}\frac{e_{zm}^*(r_b)}{\|e_{zm}\|^2}\exp[-ik_z z_0]. \quad (36)$$

In deriving Eq. (36) we made use of the orthogonality condition

$$\frac{1}{r_{N-1}^2}\int_{r_0}^{r_N} dr\cdot r\varepsilon(r)e_{zm}(r)e_{zn}^*(r) = \|e_{zm}\|^2\delta_{mn}, \quad (37)$$

and that the eigenfunction $e_{zm}(r)$ satisfies the equation:

$$\frac{1}{r}\frac{\partial}{\partial r}\left[\frac{\varepsilon r}{1-\beta_0^2\varepsilon\mu}\frac{\partial e_{zm}(r)}{\partial r}\right]-\varepsilon k_m^2 e_{zm}(r) = 0, \quad (38)$$

where δ_{mn} is the Kronecker symbol, and $\|e_{zm}\|^2$ is the normalizing factor of the eigenfunction $e_{zm}(r)$.

The orthogonality relation Eq. (37) is similar to that found in [2], and applies for eigenwaves with equal phase velocities (appropriate for Cherenkov excitation) in a multilayered dielectric structure. But, it was derived in [2] a cumbersome way starting with the overlap integral for transverse components of electric and magnetic fields in a particular dielectric layer. By way of transformation of this integral and summation of overlap integrals of all layers, it was reduced to the orthogonality relation for axial components of electric and a magnetic fields. The general notation of the relation Eq. (38), valid in any layer, with use of nonuniform dielectric permittivity and magnetic permeability allows one to obtain at once, and in a simpler way, the orthogonality relation for the axial component of electric and magnetic fields. Thus, we write the equation similar to Eq. (38) for a complex conjugate function $e_{zn}^*(r)$, multiply it by $e_{zm}(r)$, and subtract it from the equation (38) multiplied by $e_{zn}^*(r)$. After integration of the obtained expression by parts we arrive at an orthogonality condition. It is necessary to make use of the following boundary conditions: for the last zone $e_{zm}(r=r_N)=0$; for the first zone $e_{zm}(r=r_0)=0$, if $r_0\neq 0$, or $e_{rm}(r=r_0)=0$, if $r_0=0$.

Substituting Eq. (36) into Eq. (35) and executing the inverse Fourier transform, we obtain the final expression for the longitudinal component of the electric field for the annular bunch:

$$E_z^G(r,\xi) = -\frac{2Q}{r_{N-1}^2}\sum_m \frac{e_{zm}(r)e_{zm}^*(r_b)}{\|e_{zm}\|^2}\Psi_{zm}(\xi+z_0), \quad (39)$$

where

$$\Psi_{zm}(\xi) = \begin{cases}\cos(k_m\xi)\theta(\xi), & k_m^2>0\\ X_{\|m}(\xi), & k_m^2<0\end{cases}, \quad (40)$$

$$X_{\|m}(\xi) = \tfrac{1}{2}[e^{-|k_m|\xi}\theta(\xi) - e^{|k_m|\xi}\theta(-\xi)], \quad (41)$$

$\theta(\xi)$ is the Heaviside step function. The function $X_{\|m}(\xi)$ describes the axial profile of longitudinal (nonradiating) electric field in the case of purely imaginary solutions of the dispersion equation that corresponds to the (self) Coulomb field of a charge, present with or without Cherenkov radiation.

After deriving the expression for the longitudinal field $E_z^G(r,\xi)$, the other components of the electromagnetic field are obtained from the Maxwell equations, as follows:

$$E_r^G(r,\xi) = \frac{2Q}{r_{N-1}^2}\sum_m \frac{e_{rm}(r)e_{zm}^*(r_b)}{\|e_{zm}\|^2}\Psi_{\perp m}(\xi+z_0), \quad (42)$$

$$H_\varphi^G(r,\xi) = \beta_0 E_r^G(r,\xi), \quad (43)$$

where

$$\Psi_{\perp m}(\xi) = \begin{cases}\sin(k_m\xi)\theta(\xi), & k_m^2>0\\ X_{\perp m}(\xi), & k_m^2<0\end{cases} \quad (44)$$

$$X_{\perp m}(\xi) = \frac{1}{2i}[e^{-|k_m|\xi}\theta(\xi) + e^{|k_m|\xi}\theta(-\xi)]. \quad (45)$$

The wakefield energized by finite-size annular bunches is obtained by summation of the fields from infinitesimally thin ring bunches. Let the charge distribution in a bunch be described by the separable function $\rho_b(r_b,z_0) = \rho_\|(z_0)\rho_\perp(r_b)$. Then,

$$(E_r, E_z, H_\varphi) = \iint_{V_b} dz_0 dr_b r_b (E_r^G, E_z^G, H_\varphi^G)\rho_b(r_b,z_0), \quad (46)$$

with

$$\int dz_0\rho_\|(z_0) = 1, \qquad \int dr_b r_b \rho_\perp(r_b) = 1. \quad (47)$$

Thus, for a finite-size bunch we can write down the field components in the following form:

$$E_z(r,\xi) = -\frac{2Q}{r_{N-1}^2}\sum_m \frac{R_m}{\|e_{zm}\|^2}\cdot e_{zm}(r)Z_{\|m}(\xi), \quad (48)$$

$$E_r(r,\xi) = \frac{2Q}{r_{N-1}^2}\sum_m \frac{R_m}{\|e_{zm}\|^2}\cdot e_{rm}(r)Z_{\perp m}(\xi),$$
$$H_\varphi(r,\xi) = \beta_0 E_r(r,\xi), \tag{49}$$

where

$$Z_{\|,\perp m}(\xi) = \int dz_0 \rho_\|(z_0)\Psi_{\|,\perp m}(\xi + z_0), \tag{50}$$

$$R_m = \int dr_b \cdot r_b \rho_\perp(r_b) e^*_{zm}(r_b). \tag{51}$$

For excitation of the dielectric structure by a sequence of N_b collinear bunches with a Gaussian distribution of charge in each bunch, one has

$$\rho_\|(z_0) = \frac{1}{\sqrt{2\pi}\sigma_z}\sum_{n=1}^{N_b}\exp\left[-\frac{[z_0 + (n-1)L_m]^2}{2\sigma_z^2}\right], \tag{52}$$

$$\rho_\perp(r_b) = \frac{1}{\sigma_r^2}\exp\left[-\frac{(r_b - r_c)^2}{2\sigma_r^2}\right] \tag{53}$$

for functions $Z_{\|,\perp m}$ and R_m we find

$$Z_{\|m}(\xi) = \sum_{n=1}^{N_b} C_m \cos(k_m\xi_n) + S_m \sin(k_m\xi_n), \qquad k_m^2 > 0 \tag{54}$$

$$Z_{\|m}(\xi) = \sum_{n=1}^{N_b} C_m^h e^{-|k_m|\xi_n} - S_m^h e^{|k_m|\xi_n}, \qquad k_m^2 < 0 \tag{55}$$

$$Z_{\perp m}(\xi) = \sum_{n=1}^{N_b} C_m \sin(k_m\xi_n) - S_m \cos(k_m\xi_n), \qquad k_m^2 > 0 \tag{56}$$

$$Z_{\perp m}(\xi) = -i\sum_{n=1}^{N_b} C_m^h e^{-|k_m|\xi_n} + S_m^h e^{|k_m|\xi_n}, \qquad k_m^2 < 0 \tag{57}$$

$$R_m = \frac{1}{\sigma_r^2}\int_{r_{l-1}}^{r_l} dr_b r_b \cdot e^*_{zm}(r_b)\exp\left[-\frac{(r_b - r_c)^2}{2\sigma_r^2}\right], \tag{58}$$

where

$$C_m = \frac{1}{\sqrt{2\pi}}\int_{-\infty}^{\xi_n/\sigma_z} dx \cos(k_m\sigma_z x)e^{-x^2/2},$$
$$S_m = \frac{1}{\sqrt{2\pi}}\int_{-\infty}^{\xi_n/\sigma_z} dx \sin(k_m\sigma_z x)e^{-x^2/2}, \tag{59}$$

$$C_m^h = \frac{1}{2\sqrt{2\pi}}\int_{-\infty}^{\xi_n/\sigma_z} dx \exp[|k_m|\sigma_z x - x^2/2], \tag{60}$$

$$S_m^h = \frac{1}{2\sqrt{2\pi}}\int_{\xi_n/\sigma_z}^{\infty} dx \exp[-|k_m|\sigma_z x - x^2/2], \tag{61}$$

$\xi_n = \xi - (n-1)L_m$, L_m is the space bunch-repetition interval, σ_z and σ_r are the longitudinal and transverse rms bunch dimensions, r_c is the bunch center radius, and l is the zone number in which these drive bunches travel.

For the numerical study which is described below, we shall use bunches having a rectangular transverse density profile $\rho_\perp(r_b)$. Such a profile is often used in a full numerical simulation by a particle-in-cell (PIC) code. In this case the quantity R_m should be calculated according to the expression

$$R_m = \frac{2}{(r_{b2}^2 - r_{b1}^2)k_m^*}[r_{b2}e^*_{rm}(r_{b2}) - r_{b1}e^*_{rm}(r_{b1})], \tag{62}$$

where r_{b2} and r_{b1} are the outer and inner bunch radii.

Radiation power loss for a finite-size bunch can be obtained by integration of the expression for radiation losses of each particle of the bunch integrated over the volume occupied by the bunch, i.e. $P_{\rm rad} = -\int_{V_b}\rho v_0 E_z dV$. $P_{\rm rad}$ is equal to the work of retarding forces acting on particles from the fields excited by the bunch itself:

$$P_{\rm rad} = \sum_{m,k_m^2>0} P_m = \frac{2Q^2 v_0}{r_{N-1}^2}\sum_{m,k_m^2>0}\frac{|R_m|^2}{\|e_{zm}\|^2}\cdot\Phi_m, \tag{63}$$

where

$$\Phi_m = \int_{-L_b/2}^{L_b/2} d\xi \rho_\|(\xi)Z_{\|m}(\xi). \tag{64}$$

In the case of the longitudinal distribution of density of a bunch according to Gauss's law in Eq. (63), the limits of integration $-L_b/2$ and $L_b/2$ should be replaced by $-\infty$ and ∞.

Equation (63) for energy losses allows one to define the average braking force or drag acting on an elementary charge q within a bunch:

$$F_{\rm drag} = \frac{2qQ}{r_{N-1}^2}\sum_{m,k_m^2>0}\frac{|R_m|^2}{\|e_{zm}\|^2}\cdot\Phi_m. \tag{65}$$

Using the definition for the transformer ratio T given in the Introduction, we find, from Eqs. (48) and (65),

$$T(r = r_{\rm ac},\xi) = -\frac{\sum_m R_m Z_{\|m}(\xi)e_{zm}(r = r_{\rm ac})/\|e_{zm}\|^2}{\sum_{m,k_m^2>0}|R_m|^2\Phi_m/\|e_{zm}\|^2}. \tag{66}$$

In Eq. (66), the sign on an elementary charge of an accelerated test particle is taken to coincide with the sign of the charges of the drive bunch, and $r_{\rm ac}$ is the radial position of a test particle.

IV. NUMERICAL RESULTS

Using the analytical expressions for wakefields derived in the previous sections, numerical calculations relevant to specific coaxial dielectric accelerating structures have been carried out. These are described and discussed here. The simplest multizone coaxial structure is a four-zone structure having vacuum channels for the drive and witness bunches and two dielectric shells. A schematic of this structure is shown in Fig. 1.

To have much practical relevance, an accelerating module should show promise for efficient high-energy gain of accelerated particles, so that many (but not too many) such modules can be arranged to achieve electron or positron acceleration into the TeV energy range. We take for numerical calculations an annular drive bunch with charge (6 nC) and energy (5 GeV) similar to the SLAC bunch [12]. We ask what test bunch energy could be achieved by using a sequence of 1-m long DWFA modules, each with an effective acceleration gradient $G = 500$ MeV/m and a transformer ratio $T \sim 10$. Taking a drive bunch energy loss of 50 MeV per module would allow traversal of nearly 100 modules by the drive bunch before energy exhaustion, with an overall energy gain of about 50 GeV by the test bunch. After 10 similar groups of structures each fed by 5 GeV drive bunches (1000 modules altogether) in a total length $\sim$1 km, the test beam energy would ideally be 0.5 TeV. The challenge is to devise a module with $G = 500$ MeV/m and $T \sim 10$. As shall be shown, this challenge could be met in the single-bunch mode using a mm-scale coaxial DWFA structure.

To obtain such high accelerating gradients it is necessary to use ultrahigh-frequency structures having a small cross section. At a given frequency of a wakefield mode, the necessary cross-section dimensions of the dielectric layers are determined from the dispersion equation (15), together with Eqs. (16) and (18). It is necessary to observe that the frequency and wave vector are connected by the Cherenkov resonance condition $\omega_m = k_m v_0$. In Table I the dimensions of the dielectric shells calculated for an operating frequency of 912 GHz are listed. The symmetric E_{02} mode is chosen, for which the longitudinal field intensity has a different sign in the drive bunch channel and the accelerating channel. We use the following simplifying method to optimize the dimensions of the dielectric layers, similar to that used to find the necessary cross-section sizes of a rectangular two-channel [15] and a symmetric three-channel [16] dielectric structure. Suppose that, at the radius of the vanishing of longitudinal electric field in a dielectric shell, we place a metal cylindrical surface; this will not change the structure of the E_{02}-mode fields. Thus, we can split our four-zone structure into a two-zone one (an interior dielectric waveguide with its internal vacuum channel) and a three-zone one (a coaxial metal waveguide with dielectric layers on the internal and external conductors). Having found the necessary zone dimensions, we can perform the reverse procedure, i.e., assemble the required four-zone structure from these two-zone and three-zone structures. In order to obtain a high transformer ratio, it is necessary that the radial thickness of the drive bunch channel be considerably larger than the radius of the accelerating channel.

The thicknesses of the dielectric shells, and the cross-section sizes of the vacuum channels are shown in Table I; these coincide with the thickness of dielectric plates and width of vacuum channels in a symmetric terahertz dielectric rectangular accelerating structure, recently investigated by us [16]. The latter provided a working frequency of 1.003 THz. Two synchronously moving bunches with energy of 5 GeV and a charge of 3 nC each developed accelerating gradients $G \sim 350$ MeV/m in that structure. For the computation results described below for the coaxial device, the same drive bunch parameters are chosen except that a single annular drive bunch having total charge of 6 nC is used.

In Fig. 3, radial profiles of the longitudinal electric field amplitudes of the dominant E_{0m} modes of the wakefield are shown. The radial dependence of E_z is uniform inside the vacuum spaces and steps up in the dielectric layers. The ratio of the field amplitude in the accelerating channel to the field amplitude in the drive bunch channel for the E_{02} mode is equal to 32.5. For phase synchronism with a 5 GeV drive bunch, the frequencies of the first six modes in

TABLE I. Parameters for a two-channel coaxial dielectric wakefield accelerator module.

Frequency of the E_{02} design mode	912.459 GHz
External radius of outer coaxial dielectric shell r_4	1060.5 μm
Inner radius of outer coaxial dielectric shell r_3	1047.5 μm
External radius of inner coaxial dielectric shell r_2	89.5 μm
Accelerating channel radius (inner radius of inner coaxial dielectric shell) r_1	50.0 μm
Relative dielectric constant of dielectric shells ε	5.7
rms bunch length σ_z (Gaussian charge distribution)	34.64 μm
Outer drive bunch radius (box charge distribution) r_{b2}	718.5 μm
Inner drive bunch radius r_{b1}	418.5 μm
Bunch energy	5 GeV
Bunch charge	6 nC

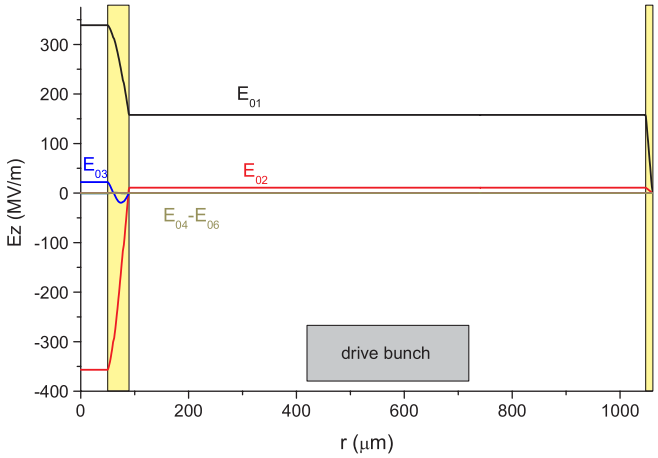

FIG. 3. (Color) Transverse profiles $E_z(r)$ for the first six TM modes, with the E_{02} operating mode. Locations of the two dielectric shells is highlighted in yellow, and location and width of the 5-GeV drive bunch is shown in gray.

ascending order are 611.252 GHz (E_{01}), 912.459 GHz (E_{02}), 2417.845 GHz (E_{03}), 4018.595 GHz (E_{04}), 5393.728 GHz (E_{05}), and 5665.204 GHz (E_{06}). Only the first three of these modes have appreciable field strength in the accelerating channel; the amplitudes of the E_{01} and the E_{02} modes at the structure axis are $\sim$350 MV/m.

In Fig. 4 the axial profiles of the composite longitudinal force along the axis of the accelerating channel are shown. The maximum [17] of the accelerating gradient G of 587.6 MeV/m is located at about 306 μm behind the drive bunch center. The transformer ratio at this maximum, according to Eq. (66), is 7.74. Although this value of transformer ratio is high, it is significantly less than the transformer ratio calculated using only the E_{02} mode (see Fig. 3). The reason is the strong coupling of the E_{01} and the E_{02} modes, which are approximately equal in absolute

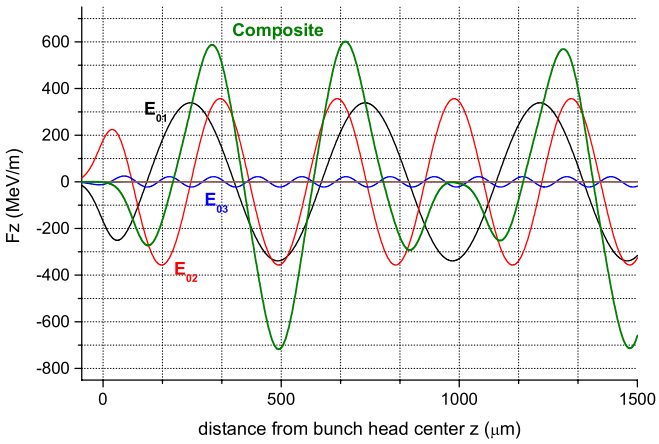

FIG. 4. (Color) Axial profiles of the longitudinal composite force and components of the force of the E_{0m} modes acting on a test electron along center of accelerating channel. The drive bunch moves from right to left and its center is located at $z = 0$.

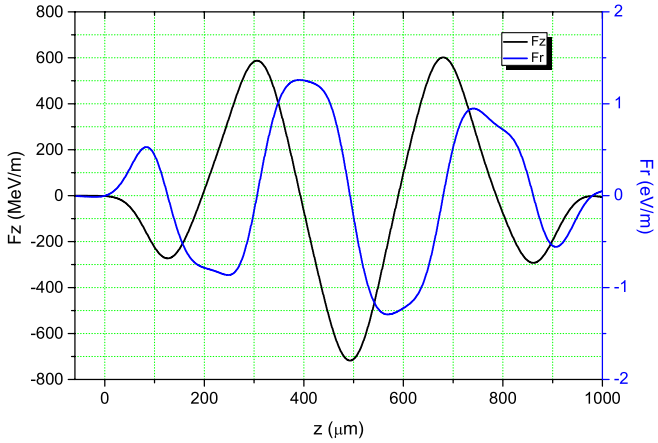

FIG. 5. (Color) Axial profiles of the composite transverse force (blue line) and composite longitudinal force (black line) acting on a test electron at the distance of 25 μm from center of the accelerating channel. The drive bunch moves from right to left and its center is located at $z = 0$. Parameters of the structure and drive bunch are given in the Table I.

value but opposite in sign in the witness channel. By carrying out computations using different dimensions of the coaxial dielectric-loaded structures (CDS), we find that it is impossible to suppress the E_{01} mode appreciably and, thereby increase the transformer ratio.

The axial profile of the transverse force acting on a test electron, moving at a distance 25 μm from the axis of the accelerating channel, is shown in Fig. 5. The transverse force at the maximum of the accelerating field is equal to zero. If the center of a test bunch is placed at the maximum of this accelerating field, the transverse force will be focusing for the bunch head and defocusing for the bunch tail and that will lead to slight pinching of the bunch. As follows from Fig. 5, it is desirable to place a witness bunch a little ahead of the maximum of the accelerating field. Although there is some loss in acceleration, the radial force there is focusing and thus there is better transverse stability of the witness bunch. But even if we place a witness bunch at exactly the maximum of the accelerating field, the radial forces there are not dangerous for accelerating modules having a small length, since they are insignificant in absolute value. For example, if we take the accelerating module to have a length 1 m (see above), a test electron, located 34.6 μm behind the maximum of the accelerating field (same rms length as the drive bunch) and at distance 25 μm from an axis, will deflect only 0.85 μm in the transverse direction.

The simplified procedure to choose the dimensions of coaxial dielectric structure described above is preliminary as it uses only one operating mode of the excited field (in our example, the E_{02}). However, the reference structure is excited not only by the operating mode which is an eigenmode for the partial structures into which we have split the reference structure, but also other modes. The composite

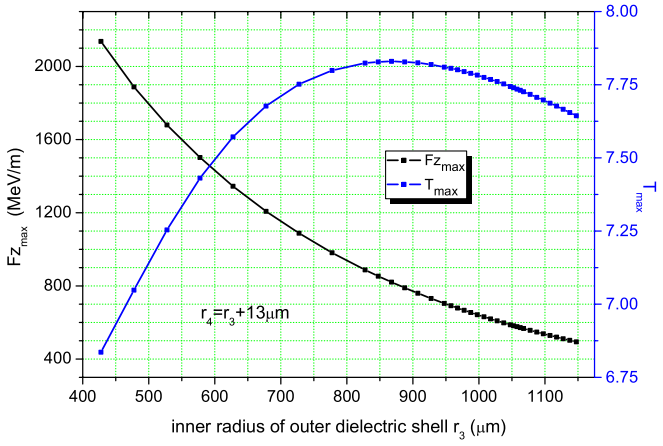

FIG. 6. (Color) The value of the composite longitudinal electric field at the first axial maximum and corresponding transformer ratio versus the dimension of the drive channel. The thickness of the outer dielectric shell is fixed and equal 13 μm. The other parameters are the same as those in Table I.

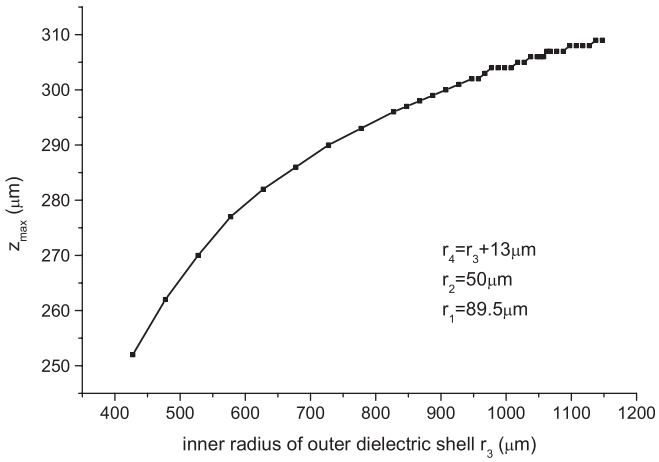

FIG. 7. The location (from drive bunch center) of the first maximum of the accelerating field versus the width of the drive channel. The thickness of the outer dielectric shell is fixed and equal to 13 μm. The other parameters are as in Table I.

field is a complex superposition of all excited modes and, therefore, to obtain the best characteristics of this accelerating structure it is necessary to optimize its parameters. Such optimization and finding characteristics of the structure depends on the dimensions of vacuum channels and dielectric layers, as discussed below.

The dependence of the accelerating gradient on the width of the drive channel is presented in Fig. 6. With decreasing drive channel width the maximum of the accelerating gradient grows approximately in inverse proportion to the square of the external radius of the channel. The transformer ratio changes little for considerable change of width of the channel. The transformer ratio varies gradually from 6.83 to 7.83 as the width of the vacuum channel changes from 338 to 1048 μm. The coaxial wakefield accelerating structure differs from the rectangular accelerating structure [15,16] where the transformer ratio strongly depends on width of drive channel. We also note that the transverse forces operating at the accelerated test bunch increase with decreasing drive channel width approximately in the same proportion as the accelerating field.

While decreasing the drive channel width, the longitudinal distance to the first maximum from the center of a drive bunch shortens (see Fig. 7). This shortening is not large and, as follows from Fig. 8, it is connected with the decrease of wavelength of the first two radial harmonics of the field.

From Figs. 6–8, one can propose an accelerating structure for which the inner and external radii of the outer dielectric shell are $r_3 = 777.5$ μm and $r_4 = 790.5$ μm, and the inner and outer radii of the inner dielectric shell are $r_1 = 50$ μm and $r_2 = 89.5$ μm. With these dimensions it is possible to obtain an accelerating field $\sim$1 GeV/m at a distance of 293 μm behind the center of the drive bunch. However, for technical reasons it might be desirable to use thicker dielectric tubes as they are more sturdy and are simpler to manufacture and mount.

In Fig. 9, we show the dependence of the accelerating field and transformer ratio at the first axial maximum upon the external radius of the inner dielectric tube r_2. Upon increasing, the increase in r_2 from its original size to 110 μm, there is an abrupt decrease of the accelerating gradient to 775 MeV/m. A further increase in the thickness of the dielectric tube causes an increase in the accelerating gradient, and for $r_2 = 150$ μm it is 888.5 MeV/m. Though such an acceleration gradient is less than optimum, it is high enough to recommend a structure with a thick inner tube as a possible candidate for a prototype of the wakefield accelerator. An increase in the outer radius of the inner shell causes the location of the first maximum of a

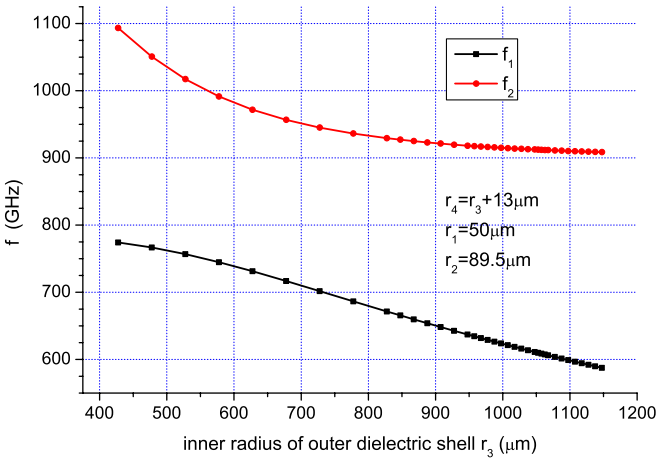

FIG. 8. (Color) Dependence of the first two frequencies of excited modes upon the width of the drive channel. The thickness of the outer dielectric shell is fixed and equal to 13 μm. The other parameters are as in Table I.

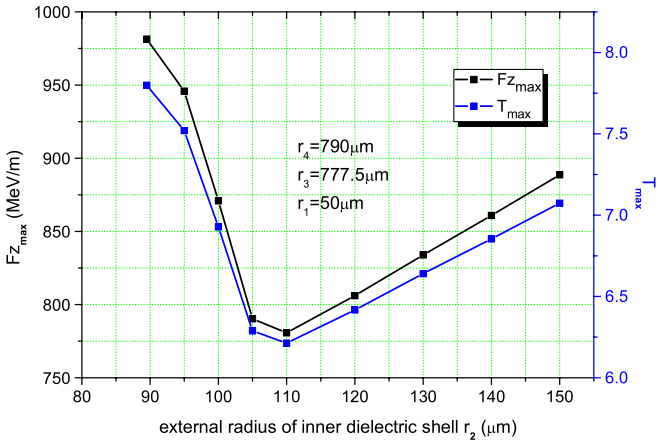

FIG. 9. (Color) The value of the composite longitudinal electric field at the first axial maximum and corresponding transformer ratio versus the external radius of the inner dielectric shell. The radii of the outer dielectric shell are $r_3 = 777.5$ μm and $r_4 = 790.5$ μm. The rest of the parameters are the same as in Table I.

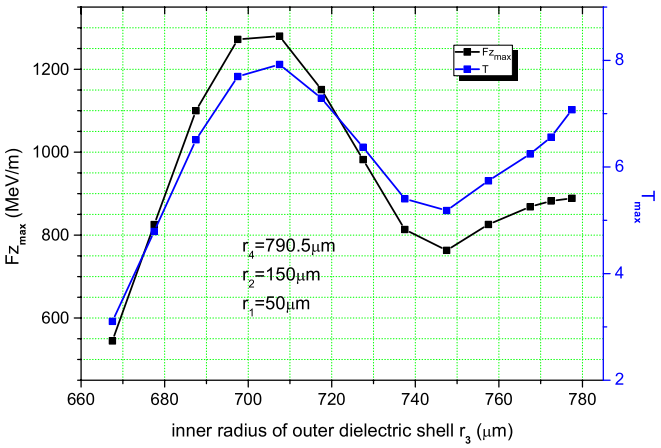

FIG. 11. (Color) The value of the composite longitudinal electric field at the first axial maximum and corresponding transformer ratio versus the inner radius of the outer dielectric shell. The radii of the inner dielectric shell are 50 and 150 μm. The external radius of the outer dielectric shell is 790 μm. The other parameters are the same as those in Table I.

field to change nonmonotonically (see Fig. 10). This is caused by the complex interference of some of the radial modes that form the composite field.

Having fixed the position and a thickness of the inner dielectric cylinder, we can investigate the dependence of the accelerating field on the thickness of the outer dielectric shell. Let the radii of the inner shell be taken as 50 and 150 μm. In Figs. 11 and 12, dependencies of the first maximum of accelerating field and its axial location and transformer ratio, upon the inner radius of the outer dielectric shell r_3, are given. Dependence of the accelerating field on the thickness of the outer dielectric shell has two local maxima. The first is near the initial shell thickness of 13 μm ($r_3 = 777.5$ μm) and the second is when shell thickness is approximately 83 μm ($r_3 = 707.5$ μm). The amplitude of the field at the second maximum exceeds the amplitude at the first maximum and is equal 1.28 GeV/m, located at a distance of 689 μm from the center of the drive bunch. The transformer ratio at the second maximum is 7.92. The dependence of the transformer ratio qualitatively follows the dependence of the accelerating field maximum behavior. The axial distance from the center of the drive bunch to the field maximum increases on the average when we increase the thickness of the outer dielectric shell.

When increasing the thicknesses of the dielectric shells, the number of modes giving an important contribution to the composite field increases. As an example, in Fig. 13 are shown the radial profiles of E_{0m} mode amplitudes of lon-

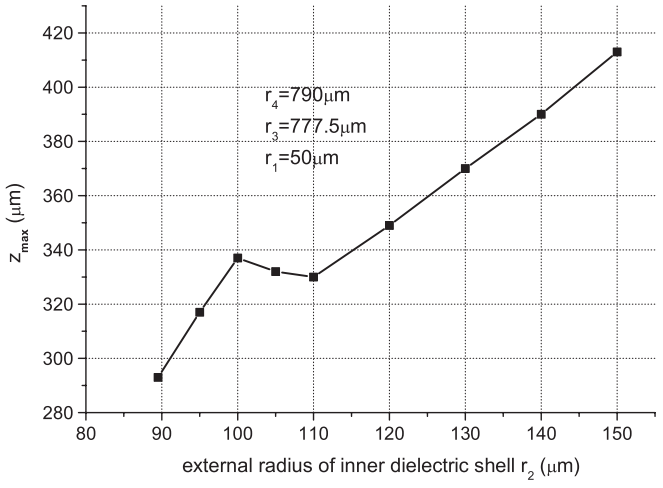

FIG. 10. The location (from drive bunch center) of the first maximum of the accelerating field versus width of the drive channel. The parameters are the same as those in Fig. 9

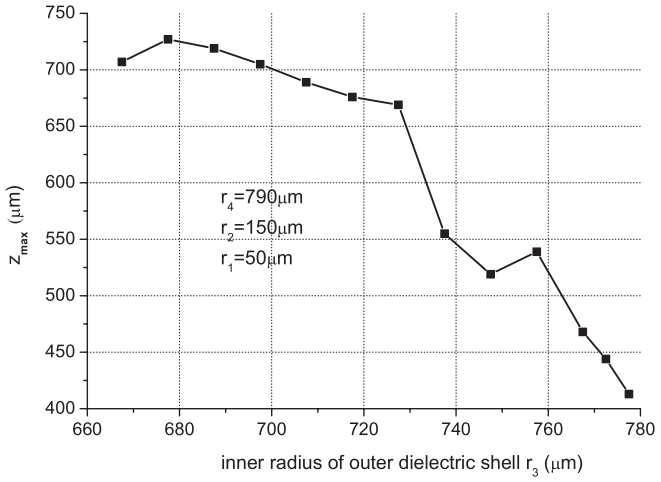

FIG. 12. The location (from drive bunch center) of the first maximum of the accelerating field versus the thickness of the inner radius of the outer dielectric shell. The parameters are the same as those in Fig. 11.

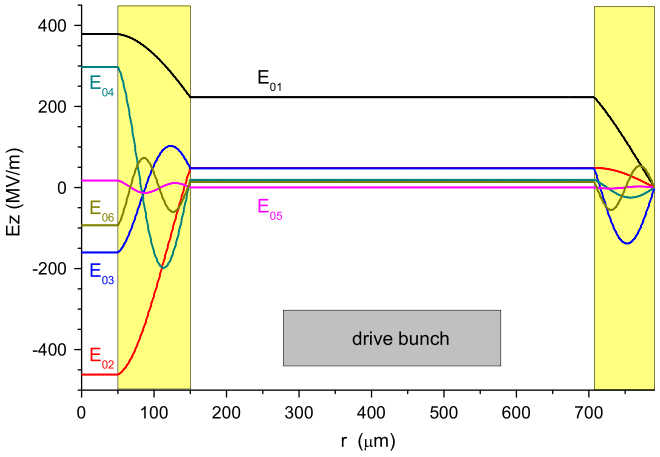

FIG. 13. (Color) Transverse profiles $E_z(r)$ for the first six TM modes. Radii of the inner dielectric shell are 50 and 150 μm, radii of the outer dielectric shell are 707.5 and 790.5 μm. Locations of the two dielectric shells are highlighted in yellow, and location and width of the 5-GeV drive bunch is shown in gray.

gitudinal electric field, and, in Fig. 14, axial profiles of the composite longitudinal force and its components which act upon a test electron at the axis of the accelerating channel in a coaxial dielectric waveguide having radii of $r_1 = 50$ μm, $r_2 = 150$ μm, $r_3 = 707.5$ μm, and $r_4 = 790.5$ μm. Six modes give significant contributions to the composite field excited by the electron bunch. Comparing Figs. 13 and 14 with similar, but considerably smaller, thicknesses of dielectric shells (Figs. 3 and 4) allows one to come to the conclusion that the increase in the thicknesses of the dielectric shells leads to enrichment of the spectrum of excited modes. As one might expect, as the frequencies of excited modes decrease, the longitudinal

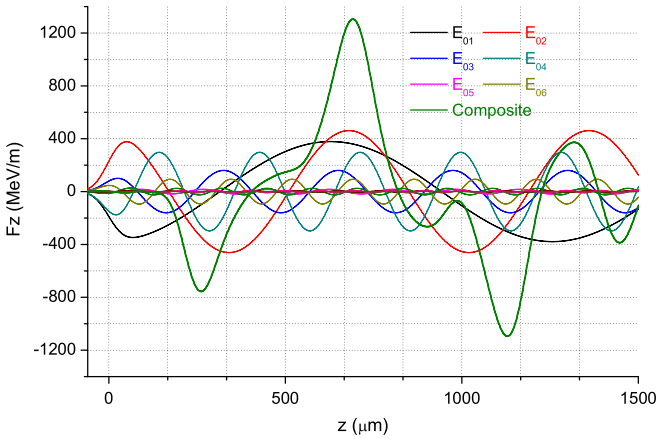

FIG. 14. (Color) Axial profiles of the longitudinal composite force and components of the force of the E_{0m} modes acting on a test electron along the center of the accelerating channel. The drive bunch moves from right to left and its center is located at $z = 0$. The dimensions of the dielectric shell and parameters of the drive bunch are the same as those in Fig. 13.

distance from the center of a drive bunch to the first maximum increases. The frequencies of the first six resonant waves in Figs. 13 and 14 in ascending order are 238.491 GHz (E_{01}), 440.861 GHz (E_{02}), 922.488 GHz (E_{03}), 1052.853 GHz (E_{04}), 1677.309 GHz (E_{05}), and 1733.222 GHz (E_{06}).

V. PIC SIMULATIONS

In this section we show results from numerical simulations of excitation by an annular electron bunch of a coaxial dielectric structure, for which analytical studies were carried out in the previous sections. For this simulation we used the PIC solver of the CST PARTICLE STUDIO code of the CST STUDIO SUITE. A ring cathode with internal and external radii specified in Table I was placed at the input end of the structure as an electron source for the drive bunch. Its length has been chosen to be 10 μm, and the cathode surface is a perfect electric conductor (PEC). As for the emission model, a Gaussian emission longitudinal profile with a fixed electron energy of 5 GeV and bunch charge of 6 nC has been chosen. The rms length of the drive bunch was taken to be the same as for the analytical investigations in the previous section, i.e. 34.64 μm, and the cutoff length of the bunch has been chosen to be 2.5 rms lengths of the bunch, i.e., it is equal to 86.6 μm. For boundary conditions we take the vanishing of the tangential component of electric field at all boundary surfaces, except for the output end of the structure where we applied an open boundary condition. For the best matching with free space, a vacuum gap of 50 μm was added onto the dielectric structure.

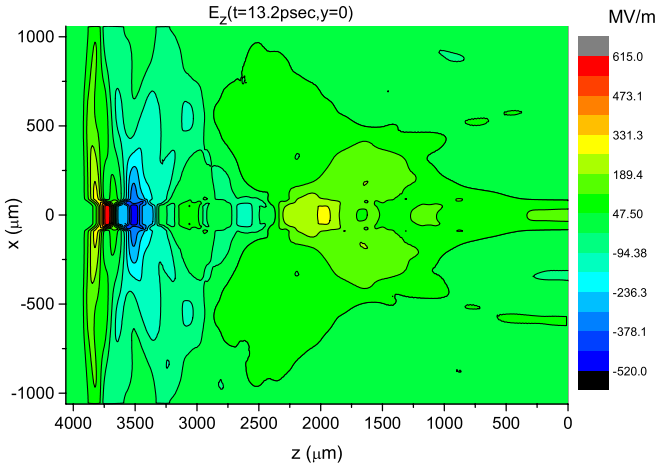

FIG. 15. (Color) Map of the axial wakefield in the coaxial DWFA. The origin of the Cartesian coordinate system is at the axis ($x = 0$, $y = 0$), at the input end ($z = 0$) of the structure. The annular bunch drives these fields, and its center is located on the far left from the entrance into DWFA at the $z = 3880$ μm. The wakefield pattern moves with the drive bunch, towards the left, and it has been followed here for $t = 13.2$ psec.

In Fig. 15, the image/contour plot of axial electric field in the x-z plane ($y = 0$) of the coaxial structure for time $t = 13.2$ psec is shown. The bunch head is approximately at a distance of 3967 μm from the entrance to the structure. One can see the Cherenkov cones of the radiation at the forward front of wakefields in the inner dielectric tube. The wakefield in the accelerating channel at short distances from the drive bunch is very strong. With increasing distance behind the drive bunch the field energized in the structure becomes more and more irregular. This irregular character of the wakefield is caused by interference between Cherenkov radiation, the quenching wave, and transition radiation [4]. The quenching wave interferes with the field of the Cherenkov wakefield radiation behind the wave group velocity front of the Cherenkov radiation. When we use thin dielectric shells, the group velocity is close to the bunch velocity and therefore the excited field has considerable amplitude only for small distances behind the drive bunch. This conclusion is confirmed by results of the numerical computations presented in Figs. 15 and 16. Behind the drive bunch there is only one strongly pronounced maximum of the accelerating field. The accelerated bunch would be positioned at the center of the intense blue stripe at $z = 3500$ μm.

Sections of the image/contour plot of the electric field are presented in Fig. 16 where one-dimensional profiles of electric field along the centers of the accelerating and the drive channels are presented. The accelerating field has a maximum of 520 MV/m, located at $z = 3500$ μm, i.e., in longitudinal direction it is displaced 380 μm from the center of the drive bunch. The position and the value of the first maximum of the accelerating field show good agreement between the analytical results of the previous section and the results of the particle-in-cell simulation. However, as Figs. 15 and 16 show, the validity of the analytical results presented in the previous section is approximately limited here to a region extending from the drive bunch to the first maximum of the accelerating field. As the longitudinal electric field in the transverse section of the drive bunch is nearly homogeneous, from the data of Fig. 16 it is possible to calculate a transformer ratio $T \sim 6$.

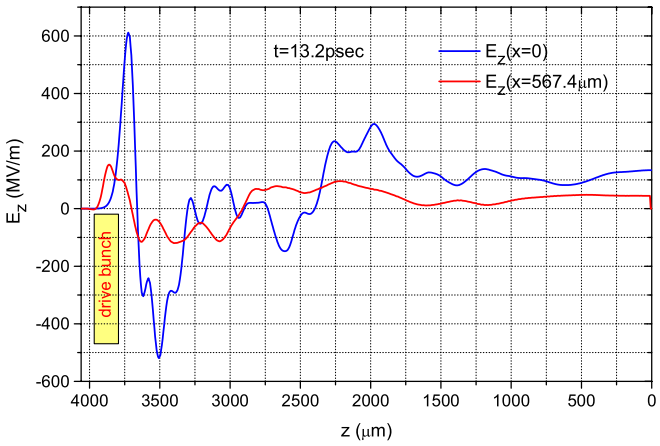

FIG. 16. (Color) Axial wakefields at the centers of drive (red line) and accelerating channels (blue line) of the coaxial DWFA for time $t = 13.2$ psec when the drive bunch center is located at $z = 3880$ μm from the entrance from the structure ($z = 0$).

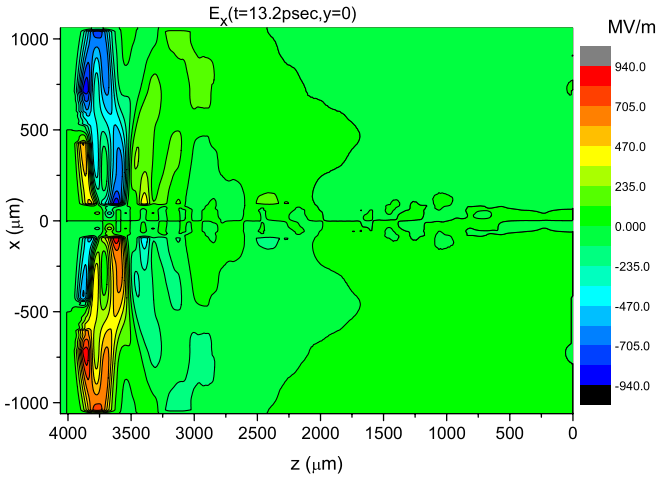

FIG. 17. (Color) Map of the transverse component of electric field along the structure for time $t = 13.2$ psec. The annular drive bunch is at the left side of the map.

The image/contour plot of the transverse electric field is shown in Fig. 17; in the transverse direction this field vanishes at the structure axis and inside the drive bunch, but it has a maximum at the bunch surface (from the space charge field) and at the inner surfaces of the dielectric shells. The maximum of the transverse field intensity is $\sim$880 MV/m.

One important feature found by the PIC simulation is that in the vicinity of the accelerating field maximum the transverse force is focusing (see Fig. 18): the transverse force is negative while the displacement from the axis is

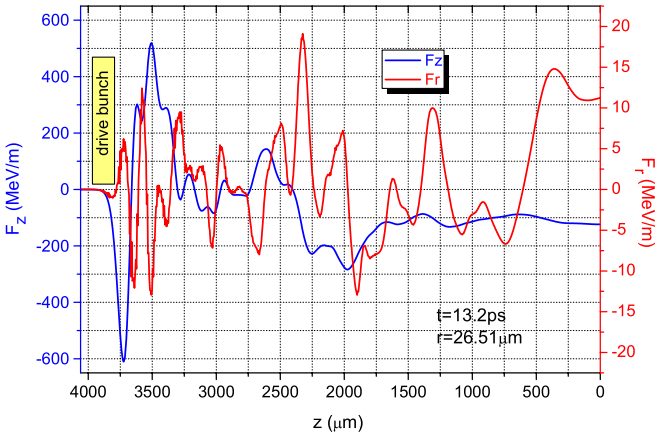

FIG. 18. (Color) Axial (blue line) and transverse (red line) forces acting upon electron versus z, at $r = 26.51$ μm from the central axis in a witness bunch channel. The witness bunch would be placed at $z = 3500$ μm.

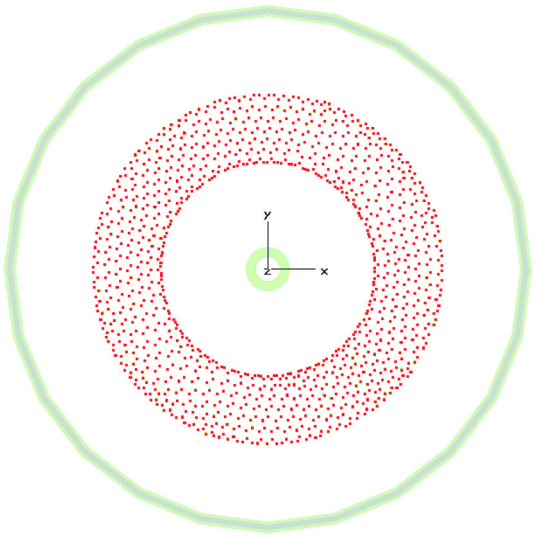

FIG. 19. (Color) The front view of drive bunch electrons after 13.2 psec of the travel (bunch head is located at 3.967 mm from the structure input). Different colors of simulated electrons indicate different energy losses. Dielectric tubes are shown in green.

positive, thereby providing a stabilizing force for the radial motion of a witness particle. This is a distinct improvement in comparison with the case of the rectangular dielectric waveguide [15,18]. A restoring transverse force $\sim$12.5 MeV/m on a typical 5 GeV witness electron at $z = 3500\ \mu$m gives a betatron period of stable oscillation of $\sim$0.92 m. Further studies have shown that the peak of this focusing transverse force tracks the motion of the longitudinal force accelerating peak as the drive bunch moves along the channel. Also, we find that it occurs even when the dimensions of the structure are altered in important ways. It appears to be caused by the quenching wave disturbance that originates at the input end of the structure. The second feature shown in the PIC simulation results is the strong influence of the quenching wave at distances beyond one period of the accelerating field, a result that is absent in the analytical formulation.

Though the electric and magnetic fields are strong on the surface of the drive bunch, the transverse force acting on the peripheral electrons is small because of their high relativistic factor. The maximum of the force acting on the drive bunch electrons is approximately the same as the force acting on the accelerated electrons. Therefore the transverse displacement of drive bunch particles will be insignificant. In Fig. 19, the front view (vertical projection onto the output end face plane) of the drive bunch electrons at the time when the bunch head is near the exit from the dielectric structure is shown. Notice that no particles have contacted the dielectric walls and the transverse profile of the bunch does not differ from the profile at the cathode.

We have also studied a six-zone structure where we use three annular vacuum channels. The inner one contains the witness bunch, the outer one contains the drive bunch, and the middle one is empty. This structure can provide a larger transformer ratio ($\sim$ 15) via a stepwise increase of longitudinal field that can occur at each dielectric shell.

VI. EXCITATION OF A TWO-CHANNEL COAXIAL STRUCTURE BY A BUNCH TRAIN

In principle, a periodic sequence of electron bunches can be used to increase the accelerating field amplitude [19,20]. In a dielectric-lined structure operating in a single-mode excitation regime, the wakefields of a train of bunches spaced by the period of the wake wave are superimposed linearly. As a result, the excited field grows proportionally to the number of bunches. However, the negative influence of the quenching wave in longitudinally bounded dielectric structures restricts the number of bunches that can increase the overall wakefield amplitude by such superposition [4]. The greater the group velocity of wake wave, the more considerable is the interference by the quenching wave. When we decrease the thickness of the dielectric tubes or reduce their dielectric permittivity, the group velocity of the excited waves increases and the region of uncomplicated wakefield operation is narrowed. As shown in the previous section, this region of excitation of the dielectric structure by a single bunch can be as small as the distance to the first wakefield maximum. Therefore, in such a structure, using a sequence of drive bunches would not support a buildup of a larger accelerating field amplitude unless a much longer structure is provided.

We now study a different structure to demonstrate the possibility of coherent addition of wakefields in a coaxial two-channel accelerating structure that is to be excited by a train of periodically spaced bunches. The dielectric tubes in it are made from alumina, and this accelerating structure is designed for a frequency of the operating mode (E_{02} wave) of $\sim$30 GHz. The group velocity of the excited oscillations is less than the corresponding group velocity of waves in the THz structure investigated above. Therefore, the quenching disturbance lags further behind the leading drive bunch and so one can expect a coherent field addition of a short train of bunches; the structure and bunch parameters are listed in Table II.

In Fig. 20 we show the dependence of the longitudinal electric field in the accelerating channel axis versus distance from the center of the first bunch. The structure is energized by a sequence of four bunches. These results are calculated by using the analytical expressions of Sec. III, which do not include the quenching wave effects. The bunch spacing is taken to be the period of the E_{02} mode, and as one would expect, the amplitude of the E_{02} mode increases linearly with distance from the first bunch and its amplitude after the fourth bunch is greater by 4 times than amplitude of the E_{02} mode after the first bunch. The composite field also grows from bunch to bunch. But, because of the considerable amplitude of the E_{01} mode,

TABLE II. Parameters for a GHz two-channel coaxial wakefield accelerator module using alumina dielectric tubes.

Frequency of the E_{02} design mode	28.092 GHz
External radius of outer coaxial dielectric shell r_4	14.05 mm
Inner radius of outer coaxial dielectric shell r_3	13.51 mm
External radius of inner coaxial dielectric shell r_2	3.18 mm
Accelerating channel radius (inner radius of inner coaxial dielectric shell) r_1	2.0 mm
Relative dielectric constant of dielectric shells ε	9.8
rms bunch length σ_z (Gaussian charge distribution)	1 mm
Outer drive bunch radius (box charge distribution) r_{b2}	10.39 mm
Inner drive bunch radius r_{b1}	6.39 mm
Bunch energy	14 MeV
Bunch charge	50 nC

the rate of rise of the composite field is less than linear. After the fourth bunch the accelerating gradient is about 50 MeV/m; use of a single bunch results in a maximum value of accelerating gradient of ~19 MeV/m.

For comparison with these analytical results, in Fig. 21 we show the results of a PIC simulation of the excitation of this coaxial dielectric structure by the same bunch train. From the head of the bunch train, the accelerating gradient amplitude grows almost linearly as we move away from the wakefield front. Just after the last (fourth) drive bunch, the gradient reaches a maximum of 47.4 MeV/m, and then begins to decrease because of destructive interference between the wakefield and the slower-moving quenching wave disturbance. The accelerating gradient from a single bunch at the first field maximum is 16.3 MeV/m. Thus, there is a good correspondence between the analytical calculation and the PIC simulation for the value of the accelerating gradient maximum. For the PIC simulation, there also is a nearly linear buildup of field amplitude behind the front edge of the wakefield. A likely explanation is that the E_{01} wave has a greater group velocity than the E_{02} mode and, consequently, it is not being enhanced much by the subsequent bunches.

In the previous section we showed from a PIC simulation of the excitation of a THz coaxial dielectric structure by a single bunch that the transverse force in the vicinity of an accelerating field maximum in the witness bunch channel is focusing (see Fig. 18). As seen in Fig. 21, this excellent property can also occur when the GHz structure is excited by a bunch train. At the maximum of accelerating field ($z = 127.7$ mm), the value of the focusing force acting on a witness electron that is located at a distance of 0.98 mm from the axis is 1.68 MeV/m. We have found in

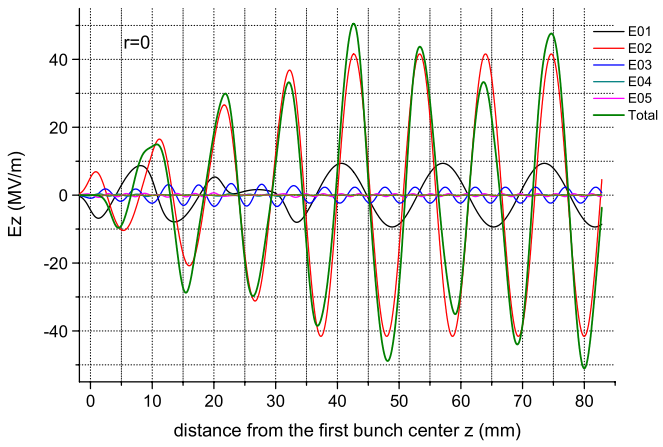

FIG. 20. (Color) Results of analytical computations of axial profiles of the longitudinal composite field (green line) and longitudinal fields of the E_{0m} modes (labeled as E_{0m}) excited by the train of four bunches along the center of the accelerating channel. Drive bunches move from right to left and the center of the first bunch is located at $z = 0$. Bunch spacing is about 10.7 mm.

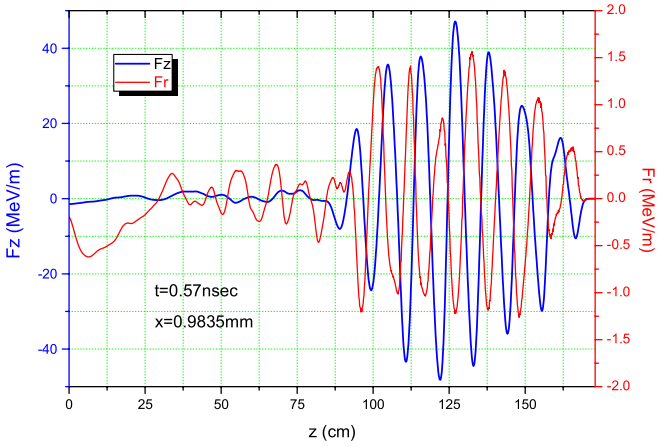

FIG. 21. (Color) Results of PIC simulations of axial (blue line) and transverse (red line) forces acting upon an electron versus z, at $r = 0.98$ mm from the central axis in a witness bunch channel. The coaxial structure is excited by the train of four bunches. Drive bunches move from left to right. The head of the first bunch is located at $z \sim 174$ mm. Bunch spacing is 10.7 mm. The cathode length is 3 mm, the length of dielectric tubes is 173 mm, and the length of the extra vacuum gap is 10 mm.

subsequent simulations that it is possible to adjust the difference of phase between the longitudinal and transverse forces at a maximum of an accelerating field by making a small change of the bunch-repetition period.

The transverse forces acting on the electrons of the drive bunches (as well as for the case where the dielectric structure is excited by a single bunch) are insignificant and do not increase progressively from a leading bunch to a following bunch. For example, at the time $t = 0.57$ nsec the inner edge electrons (at $x = 6.32$ mm) of the second drive bunch experience a maximum defocusing transverse force ~ 0.44 MeV/m, the third bunch ~ 0.71 MeV/m, and the fourth bunch ~ 0.63 MeV/m. At such values of deflecting forces the trailing drive bunch electrons should travel a longitudinal distance ~ 60–70 cm before they begin to strike the walls of the inner dielectric tube. In Fig. 22, the front view of electrons in the fourth drive bunch near the output end of the dielectric structure is shown. It is seen that the cross-section location of the bunch electrons nearly replicates the cathode outline. Their transverse displacement is insignificant and these numerical simulations have found even less displacement than the linear estimates above. The investigation of the radial dynamics of all bunches has shown that the greatest radial displacement is suffered by electrons in the third bunch (although this is comparable with those of the last bunch). Such dependence proves also to be true for the longitudinal distribution of radial forces at the surfaces corresponding to the initial internal and external radii of a bunch. Though these particles are in a smaller braking field, the maximum of the defocusing force acting on these peripheral electrons is greater than the force acting on the particles of the fourth bunch.

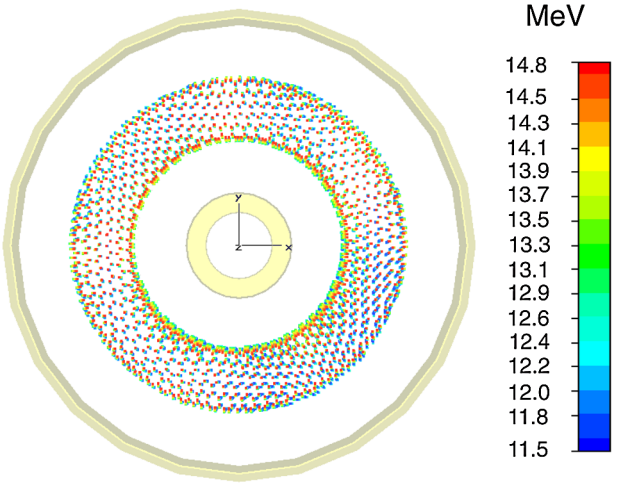

FIG. 22. (Color) Front view of the last bunch in a train of four bunches after 0.67 nsec following injection of the first bunch. The head of this bunch is located at 170 mm from the structure input. Different colors of simulated electrons indicate different energy losses. Dielectric tubes are marked with yellow color.

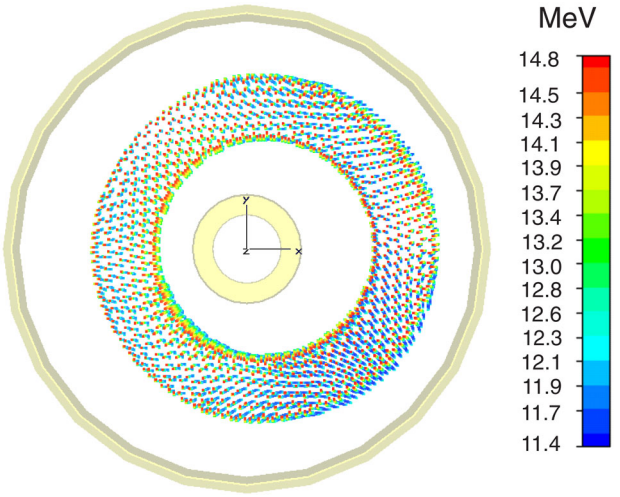

FIG. 23. (Color) The same case as in Fig. 22, but for bunches which are displaced initially by 1 mm to the right from the structure axis.

The off-centered drive bunch causes a deflecting force on the axis of the witness channel amounting to somewhat more than the focusing force, so in practice a somewhat smaller offset would be necessary to assure stable motion of the witness bunch.

Thus, the flat radial profile of the axial electric field $E_z(r)$ allows the bunch train to move stably for long distances. For additional study of the radial and azimuthal stability of the drive bunches, we investigated their dynamics when the initial position of their centers was displaced from the structure axis. In Fig. 23 the front view of particles of the fourth bunch is shown at the same time as for the case of the train of the centered bunches (Fig. 22). The offset of all four bunches is 1 mm. As in the case of the train of the centered bunches, the radial displacement of particles of the last bunch is insignificant. Comparing the energy distributions of electrons in Figs. 22 and 23, it is possible to see a much more nonuniform distribution with azimuthal angle. If in the case of the centered bunches an azimuthal inhomogeneity develops owing to the discreteness of the initial distribution of macroparticles on a spatial grid, in the case of the off-centered bunches, the excitation of the higher of the azimuthal modes should be facilitated by the initial nonuniform distribution of a charge along the azimuth. But we find that in both cases, an energy modulation of particles has not led to a significant development of transverse instability of the bunches. Numerical study of the drive bunch motion is limited by computing power, and thus these results may not be applicable for bunch motion over a long distance.

A problem with using the multiple drive bunch train technique in general is that the drag forces increase on the trailing bunches, and this might complicate the design of a staged collider. In our example, the average drag force on the first drive bunch is ~ 2.4 MeV/m, whereas the drag on the fourth bunch is ~ 7.1 MeV/m. However, deploying a

multiple drive bunch is a useful option if the charge available for a single drive bunch is limited for technical reasons. In that case the sum total of the charge in the multiple bunch train would be the same as that of the single bunch, and the aggregate drag would be approximately the same.

VII. DISCUSSION

A coaxial, two-channel, dielectric-loaded cylindrical structure has been studied using analytic theory with numerical examples, as well as a numerical simulation using the PIC solver of the CST PARTICLE STUDIO code, for the purpose of gaining understanding of a possible new high-gradient accelerator based on dielectric wakefield acceleration principles. The analytic theory takes the assumption of a structure that is infinitely extended along the axis, whereas the PIC simulation includes the effect of injection of charge bunches into a finite length of structure. The effects of the latter are important, because the quenching waves emitted by the necessary open input boundary condition move with a group velocity that is a large fraction of the speed of light in cases where the dielectric loading is slight, and thereby cause interference with the Cherenkov wakefields that trail the drive bunch with relativistic electron bunch speed. This interference is substantial because the quenching waves have amplitude comparable to the Cherenkov wakefields, as they must cancel the latter at the input boundary. Good agreement between the results of analytic theory and the PIC simulation has been obtained in the spatial region where both can apply.

A small, but not excessively small, structure has been examined for suitability as a linear accelerator of electrons (or positrons). Two-channel coaxial operation can achieve a gradient exceeding 1 GeV/m with a transformer ratio ~ 8, and possibly higher, in an optimized design, by using a single annular 6 nC, 5 GeV drive bunch to excite the structure. A trailing witness bunch in the second, central channel can thereby be accelerated stably to high energy using several modules that could be precisely fabricated and aligned. Radially uniform axial electric fields in the two vacuum channels permit a uniform drag (for the drive bunch) or acceleration (for the witness bunch) on all the particles in these bunches, and allow both types of bunches to move appreciable distances without distortion or wall contact. Stable transverse motion of the witness bunch particles should permit the preservation of bunch shape during acceleration without the use of external focusing structures. Use of a short train of drive bunches to enhance performance has been found to be practical when the quenching wave effects can be offset by choice of design parameters. A cathode structure that emits a ring-type bunch of charge has been studied in the past, in connection with a wakefield transformer experiment [21].

In the structure described in this paper, the lateral walls of the coaxial structure are lined with a suitable dielectric that has demonstrated ability to withstand high electric stress and resist wall surface charge buildup. (We have found that the dielectric need not be the same for each cylindrical wall.) A DWFA having microwave-scale dimensions that uses drive bunches of several MeV energy might support the inner dielectric cylinder with a low-Z metallic foil, through which the annular drive bunch can pass with negligible energy loss or structural damage to the foil. In that case, a wall thickness ~ 200 μm of aluminum might be suitable. (We point out that the entry boundary condition we used for the PIC simulation was a metallic one, namely, zero radial and azimuthal electric fields at $z = 0$). For a small high-gradient structure having millimeter-scale transverse dimensions, the supporting ''foil'' might be a carbon nanotube fabric having thickness ~ 25 μm and good electrical conductivity. Support of the inner dielectric tube inside a lengthy accelerator module might require the periodic use of an adjustable supporting carbon nanotube filament. Answers to questions regarding the utility and durability of such materials and the techniques to maintain precise alignment in a coaxial DWFA, as also the matter of production of an annular drive bunch with adequate charge, require a significant research and development effort and are beyond the scope of this study.

We compare the results obtained here with our study of the two-channel *rectangular* DWFA [15]. The cylindrical and rectangular configurations share many common advantages, such as the separated bunch lines, the enhanced transformer ratio, and the continuous coupling of energy from the drive bunch to the witness bunch. However, in order to obtain useful gradients, the rectangular structures cannot be tall, and therefore it suffers from significant deflecting forces that act upon both the drive bunches and the witness bunches. Furthermore, the accelerating gradients are smaller for rectangular units than for the cylindrical ones, the latter benefiting from the $r = 0$ point of symmetry. While it is possible to position a witness bunch at an axial position behind the drive bunch where the axial gradient is large and the transverse force is comparatively small in the rectangular unit [15], nevertheless these transverse forces do vary along the length of the witness bunch and this will result in bunch distortion as the bunch traverses the accelerating module. In contrast, the cylindrical structure provides a stabilizing transverse force for the witness bunch, a gift, surprisingly enough, of the quenching waves.

Recently [22], analysis was published for wakefields on a four-zone coaxial structure energized by an infinitesimally thin ring drive bunch, without consideration of the quenching wave.

ACKNOWLEDGMENTS

This research was supported by U.S. Department of Energy, Office of High Energy Physics, Advanced Accelerator R&D.

[1] C. Wang and J. L. Hirshfield, Phys. Rev. ST Accel. Beams **9**, 031301 (2006).
[2] S. Y. Park and J. L. Hirshfield, Phys. Rev. E **62**, 1266 (2000).
[3] I. N. Onischenko, D. Yu. Sidorenko, and G. V. Sotnikov, Phys. Rev. E **65**, 066501 (2002).
[4] T. C. Marshall, N. I. Onischenko, and G. V. Sotnikov, in *Advanced Accelerator Concepts: 11th Workshop*, edited by Vitaly Yakimenko, AIP Conf. Proc. No. 737 (AIP, New York, 2004), pp. 698–707.
[5] A. Sessler and G. Westenskow, in *Handbook of Accelerator Physics and Engineering*, edited by A. W. Chao and M. Tigner (World Scientific, New Jersey, 2002), pp. 46–48.
[6] J. P. Delahaye, ''The Compact Linear Collider (CLIC) Study,'' CERN Particle Physics Seminar, http://clic-study.web.cern.ch/CLIC-Study/Presentations/20050421.pdf.
[7] E. Chojnacki, W. Gai, P. Schoessow, and J. Simpson, in *Proceedings of the IEEE 1991 Particle Accelerator Conference (APS Beams Physics)* (IEEE, Piscataway NJ, 1991), Vol. 5, pp. 2557–2559.
[8] M. E. Conde, W. Gai, R. Konecny, J. Power, P. Schoessow, and P. Zou, in *Advanced Accelerator Concepts: Eighth Workshop*, edited by W. Lawson, C. Bellamy, and D. F. Brosius, AIP Conf. Proc. No. 472 (AIP, New York, 1998), pp. 626–634.
[9] C. Jing, W. M. Liu, W. Gai, J. G. Power, and T. Wong, Nucl. Instrum. Methods Phys. Res., Sect. A **539**, 445 (2005).
[10] L. Schachter, R. L. Byer, and R. H. Siemann, Phys. Rev. E **68**, 036502 (2003).
[11] A. M. Altmark and A. D. Kanareykin, Tech. Phys. Lett. **34**, 174 (2008).
[12] M. C. Thompson, H. Badakov, A. M. Cook, J. B. Rosenzweig, R. Tikhoplav, G. Travish, I. Blumenfeld, M. J. Hogan, R. Ischebeck, N. Kirby, R. Siemann, D. Walz, P. Muggli, A. Scott, and R. B. Yoder, Phys. Rev. Lett. **100**, 214801 (2008).
[13] We observe that formerly a matrix approach was applied to derive the dispersion equation of a stratified Bragg fiber [14]. The transfer matrices determined there connect fields in two adjacent layers at the same boundary, on the left and to the right of it. The definition of transition matrices used in Ref. [1] allows one to derive a much more compact form of the dispersion equation.
[14] P. Yeh, A. Yariv, and E. Marom, J. Opt. Soc. Am. **68**, 1196 (1978).
[15] G. V. Sotnikov, I. N. Onishchenko, J. L. Hirshfield, and T. C. Marshall, Probl. At. Sci. Technol., Ser. Nucl. Phys. Investigations **49**, 148 (2008).
[16] T. C. Marshall, G. V. Sotnikov, S. V. Shchelkunov, and J. L. Hirshfield, in *Advanced Accelerator Concepts: 13th Workshop*, edited by Carl B. Schroeder, Wim Leemans, and Eric Esarey, AIP Conf. Proc. No. 1086 (AIP, New York, 2009), pp. 421–426.
[17] Hereafter we will analyze (for the reasons which will be clear from following section) only the first maximum of an accelerating field.
[18] G. V. Sotnikov, T. C. Marshall, S. V. Shchelkunov, A. Didenko, and J. L. Hirshfield, in Advanced Accelerator Concepts: 13th Workshop (Ref. [16]), pp. 415–420.
[19] I. N. Onishchenko, V. A. Kiseljob, A. K. Berezin, G. V. Sotnikov, V. V. Uskov, A. F. Linnik, and Ya. B. Fainberg, in *Proceedings of the 1995 Particle Accelerator Conference* (IEEE, New York, 1995), pp. 782–783.
[20] C. Jing, A. Kanareykin, J. G. Power, M. Conde, Z. Yusof, P. Schoessow, and W. Gai, Phys. Rev. Lett. **98**, 144801 (2007).
[21] M. Bieler, W. Bialowons, H.-D. Bremer, F.-J. Decker, H.-Ch. Lewin, P. Schütt, G.-A. Voss, R. Wanzenberg, and T. Weiland, http://accelconf.web.cern.ch/AccelConf/e88/PDF/EPAC1988_0967.PDF; also, F.-J. Decker, W. Bialowons, M. Bieler, H.-D. Bremer, H.-C. Lewin, P. Schütt, G.-A. Voss, R. Wanzenberg, and T. Weiland, http://accelconf.web.cern.ch/AccelConf/e88/PDF/EPAC1988_0613.PDF.
[22] Wanming Liu and Wei Gai, Phys. Rev. ST Accel. Beams **12**, 051301 (2009).

Improved ramped bunch train to increase the transformer ratio of a two-channel multimode dielectric wakefield accelerator

G. V. Sotnikov[1,2,*] and T. C. Marshall[2,3,†]

[1]*NSC Kharkov Institute of Physics and Technology, 61108 Kharkov, Ukraine*
[2]*Omega-P, Inc., New Haven, Connecticut 06511, USA*
[3]*Columbia University, New York, New York 10027, USA*

(Received 29 October 2010; published 11 March 2011)

Here we show a possibility of applying the ramped drive bunch train (RBT) technique to a two-channel coaxial dielectric wakefield accelerator (CDWA). For numerical research we study a 28 GHz structure with two nested alumina cylindrical shells having these diameters: outer shell, OD = 28.1 mm, ID = 27 mm; inner shell, OD = 6.35 mm, ID = 4.0 mm. The structure is to be excited by a train of four annular bunches having energy 14 MeV and axial rms length 1 mm; the total charge of bunches is 200 nC. In the case of equally charged drive bunches, spaced apart by the principal wakefield wavelength 10.67 mm, we obtained transformer ratio $T = 3.4$. If the bunch charge is increasing as the ratio 1:3:5:7 and the bunches are spaced by one and one-half wavelengths, we obtained $T = 3.8$. We found that if the charge ratios are 1.0:2.4:3.5:5.0 and the spaces between the bunches are 2.5, 2.5, and 4.5 wakefield periods, then T increases strongly, $T \sim 20$. The RBT also can be used successfully in a high gradient THz CDWA structure. A particle-in-cell simulation shows that the four drive bunches can move without appreciable distortion.

DOI: 10.1103/PhysRevSTAB.14.031302 PACS numbers: 41.75.Ht, 41.75.Lx, 41.75.Jv, 96.50.Pw

I. INTRODUCTION

Dielectric wakefield accelerator devices have become an attractive alternative to conventional metallic-structure elements used for electron/positron linear colliders [1]. In dielectric wakefield accelerator (DWA) devices, a high energy drive bunch or train of drive bunches sets up a wakefield via Cherenkov radiation; some of this energy is then transferred to a trailing bunch positioned to receive axial accelerating force. Recent interest in this concept has been rekindled by a finding that dielectrics can withstand very high fields (>1 GeV/m) for the short times involved in the passage of charged bunches along the dielectric-lined channel [2]. However, other than the possibility to develop high accelerating gradients, an accelerator should have other advantages, such as an attractive transformer ratio.

Transformer ratio (**T**), which is a measure of the efficacy by which energy provided by a drive bunch is transferred to a bunch that is to be accelerated in a DWA structure, is generally <2 in a collinear device, namely, one in which the drive bunch and the bunch to be accelerated (''witness'' bunch here) travel along the same path [3–6]. The **T** is customarily defined to be the ratio of the peak accelerating field set up by a drive bunch to the average energy loss per unit charge of particles in the drive bunch [3,4]. On the other hand, some authors [7–10] use the ratio of the maximum energy gain of the witness bunch to the maximum energy loss of the drive bunch. There are two ways to increase the **T**. The first has been to use a train of drive bunches that have a certain programmed charge and spacing determined by a simple algorithm [7,8,10,11] to drive wakefields in a collinear device: this is termed a ''ramped bunch train'' (RBT). This method has been tried experimentally with modest success [7,8], and it is most suitable when the drive bunch can excite a single mode in the device. Another technique is to separate the drive and witness bunch channels: this has been done successfully at CLIC [12] and at the Argonne Wakefield Accelerator facility [13,14]. Our recent effort to develop a two-channel wakefield accelerator structure that encloses both channels in one assembly [1] has found that a $\mathbf{T} \sim 5$–6 can be obtained in a coaxial DWA configuration (CDWA) in which the drive bunch is annular and is centered on the axis of a second accelerating channel that carries a witness bunch (see Fig. 1). This configuration has been found to transport a short train of drive bunches, as well as the witness bunch, satisfactorily [1]. Comparison of **T** for the ramped bunch train to that of the single drive bunch is a satisfactory indication of any improvement of **T**. In this paper our attention is directed to improving the transformer ratio for the CDWA device.

An example will show how the performance of an accelerator is affected by the transformer ratio. In a certain dielectric wakefield structure, let us suppose a 14 MeV

*sotnikov@kipt.kharkov.ua
†tcm2@columbia.edu

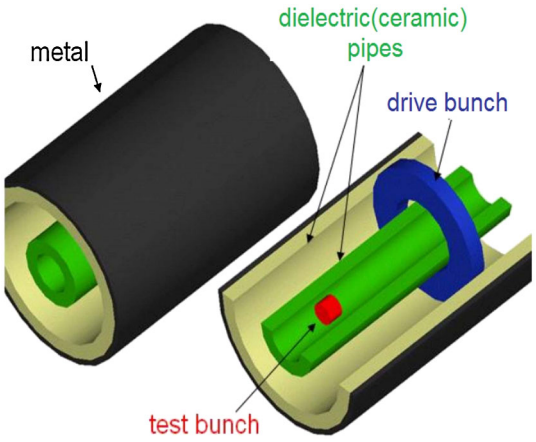

FIG. 1. Schematic of the CDWA structure, showing a single annular drive bunch followed by an accelerated witness bunch that moves along the axis.

drive bunch sets up a gradient of $\mathbf{G} = 50$ MeV/m for the witness bunch and $\mathbf{T} = 4$. A drive bunch electron, which should then lose energy at the rate of 12.5 MeV/m, can travel no more than 1.12 m, and the witness bunch electron will gain 56 MeV. Now suppose that the gradient accelerating the witness bunch that is set up by a ramped drive bunch that has the same energy in the same structure is only $\mathbf{G} = 28$ MeV/m, but $\mathbf{T} = 20$. In that case, the drive bunch can travel 10 m (stability issues permitting) and the witness bunch will gain 280 MeV. (The numbers for this illustration are based on examples in the next section.) This example, which omits the influence of beam loading, illustrates the trade-off between **T** and **G**: the higher-**G**/lower-**T** case leads to a shorter active length, but 5 times the number of drive beam segments, while the higher-**T**/lower-**G** case implies a longer active length but fewer drive beam segments. Thus, other than high accelerating gradients, a two-beam accelerator should have a suitably high transformer ratio, so as to minimize the number of drive beam segments needed to achieve a given final test beam energy.

In the following, we find that it is possible to combine the RBT technique with the two-channel CDWA structure to improve **T**. In evaluating our results in a useful form, we take the definition of **T** to be the ratio of the peak accelerating field acting on the witness bunch to the maximum energy loss of any of the drive bunches. We can compare our results for the four-bunch train with the **T** for a single bunch having the aggregate charge of all the drive bunches in the RBT. The ratios of bunch charges within the drive bunch train and the spacing between the bunches that optimize the result is specific to the structure being studied, but we find a considerable improvement in **T** can be obtained. This is potentially a useful method to optimize the design of a collider that uses CDWA modules. In what follows, we shall take bunch parameters modeled on those obtained at the AWA facility (Table I); this facility can provide a single 50 nC bunch, but for computational purposes we assume that four 50 nC bunches can be provided with arbitrary delays.

II. WAKEFIELD ANALYSIS OF RAMPED DRIVE BUNCH TRAINS

The computations were done using a particle-in-cell code, PIC SOLVER of the CST PARTICLE STUDIO being a part of the CST STUDIO SUITE 2010 bundle. Boundary conditions for PIC simulations were tangential electric fields are zero at metal surface of the waveguide and the input boundary of the unit, and output boundary is open to free space. The code computes fields, and changes in particle energy and position as the bunches move.

A factor that affects the practicality of the scheme we study is the group velocity of the Cherenkov radiation generated by the drive bunches as they enter the structure aperture [15]. Because of this factor the Cherenkov wakefield is nonzero in the region defined by the approximate inequality $(t - t_0)v_g \leq z \leq (t - t_0)v_0$, where t_0 is entry time of the first bunch in the structure, t is current time, v_0 is bunch velocity, and v_g is the group velocity of

TABLE I. Parameters used for the study of a two-channel CDWA (alumina dielectric).

Design mode	28.092 GHz
External radius of outer coaxial cylinder	14.05 mm
Inner radius of outer coaxial waveguide	13.512 mm
External radius of inner coaxial cylinder	3.175 mm
Accelerator channel radius (inner radius of inner coaxial cylinder)	2.0 mm
Relative dielectric constant ε	9.8
Bunch axial rms dimension $2\sigma_z$ (Gaussian charge distribution)	2.0 mm
Full bunch length used in PIC simulation	5 mm
Outer drive bunch radius (box charge distribution)	10.34 mm
Inner drive bunch radius	6.34 mm
Bunch energy	14 MeV
Total bunch charge	200 nC
Number of bunches	4

the resonance wave. Within this region, the envelope of a Cherenkov signal is about constant. The plane $z^{gr} = (t - t_0)v_g$ is the trailing edge of the wakefield. This edge moves behind the electron bunch at the group velocity v_g. In this plane, the fields from the number $N_b^{\max} = (t - t_0)(v_0 - v_g)/\Delta z_0 + 1$ of bunches will be added [16], where Δz_0 is the distance between the adjacent bunches. Everything said here is true in the case of excitation of a single resonant mode in the approximation of rigid bunches. For investigation of multimode excitation with different values of group velocities of excited modes and for a self-consistent account of energy losses of bunch particles, a full numerical simulation is required.

We now turn to the computation of some examples, where we change the drive bunch train to improve **T**. The first example (Fig. 2) shows the axial wakefield trailing a *single* 50 nC drive bunch, measured on the axis of the unit (along which the witness bunch moves) and along a line parallel to the axis halfway between the outer and inner radii of the drive bunch annulus. Here and in the next figures, axial distance z is counted starting from the injection plane of the first bunch. From this we conclude the **T** for this structure is 3.6, calculated as the ratio of maximum accelerating wakefield on the central axis of the structure (see blue curve) to the maximum decelerating wakefield at the drive bunch, $z = 168$ mm, along the center line behind the drive bunch (see red curve). It is correct to infer **T** from the wakefield behind the annular drive bunch (as shown in Fig. 2) because the transverse profile of the wakefield mode amplitudes is very nearly flat [1] across the radius of the drive bunch channel; this is caused by the large relativistic factor, even for 14 MeV. One should observe also that the wakefields are much diminished for $z < 100$ mm: this shows that the superposition of wakefields is limited to a zone behind the drive bunch depending

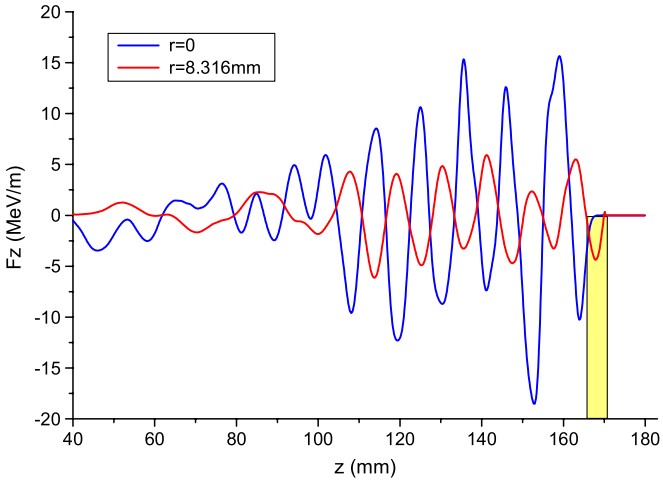

FIG. 2. Axial force from wakefields set up by a single 50 nC, 14 MeV drive bunch in the CDWA structure described in Table I. The head of the drive bunch is located at $z = 171$ mm and the bunch travels from left to right.

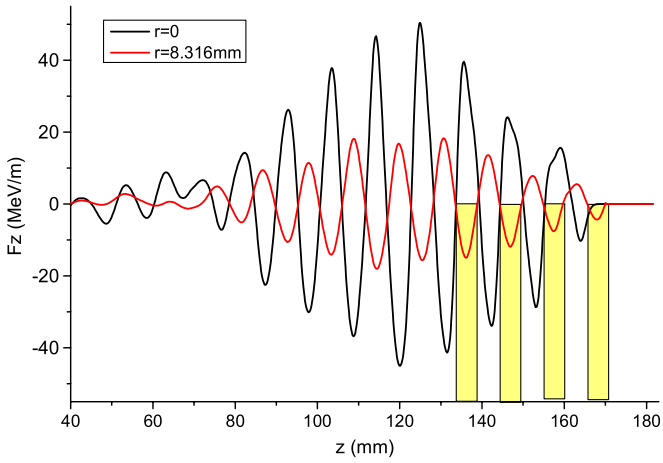

FIG. 3. Axial wakefields set up by four equally charged 50 nC, 14 MeV drive bunches.

on the length of the structure and the group velocity of the waves set up by the passage of the drive bunch into the structure [1,15,16].

We now set up a train of drive bunches. Figure 3 displays the wakefields set up by four equally charged 50 nC drive bunches, spaced apart by the wakefield wavelength of the principal mode (10.66 mm). The **T** calculated from the last drive bunch is 3.4, essentially unchanged from the single bunch case. This choice achieves the maximum accelerating gradient 50 MeV/m for the witness bunch, which in this example can be located at $z = 125$ mm. This choice of bunch train does not improve **T**.

In Fig. 4, we change the distribution of charge among the bunches so that the ratios of bunch charge increases [7] from the first to the last bunch as 1:3:5:7. The **T** is 3.3. The conclusion thus far is that a train of multiple bunches having this variable charge, but with constant spacing of one wakefield period, does not improve **T**. In this and the

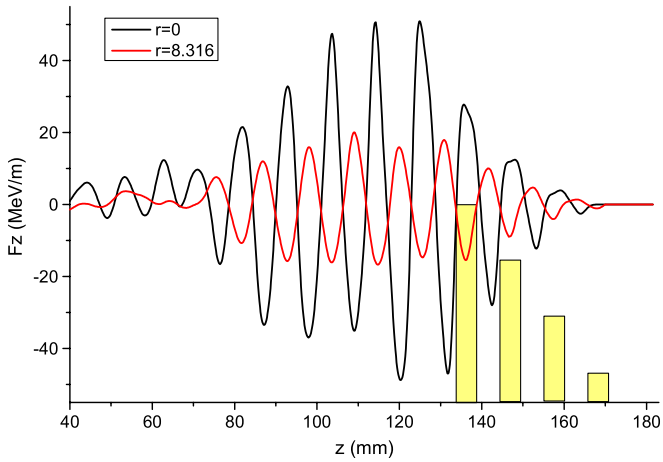

FIG. 4. Same as for Fig. 3, but now the bunch charge is increased as the ratio of odd numbers.

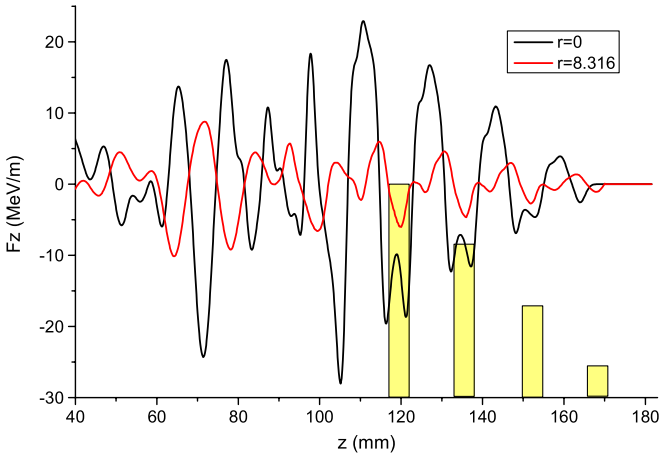

FIG. 5. Axial wakefields excited by a ramped bunch charge of drive bunches spaced by 1.5 wakefield wavelengths.

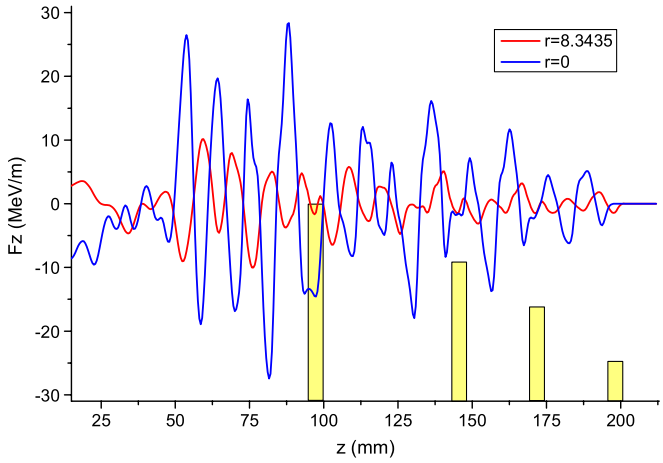

FIG. 6. In this example the bunch charges and spacings vary so as to enhance **T**.

following examples, the total bunch charge for the four drive bunches is fixed at 200 nC.

In Fig. 5, the spacing of the bunches is changed to be one and one-half wakefield periods [7,17], but the bunch charge ratio is the same as for Fig. 4. The axial wakefield force is reduced, but that is to be expected, as this arrangement no longer provides maximum decelerating force for each bunch. The **T** is now 3.8: thus, the suggested algorithm of bunch charge ramping and spacing [7,17] is not generally helpful [18], most likely because of the multimode behavior of the wakefields excited by this choice of drive bunches.

We next determine if there is some other choice of drive bunch charges and spacings that will improve **T**, but yet result in a potentially sizable wakefield amplitude. To obtain an improved transformer ratio we proceed from the following, which is strictly proved for the collinear single-mode device: wakefields with maximum transformer ratio are generated by drive bunches whose particles lose the same energy [11,17]. From this statement it follows that for a train of point bunches with repetition period equal to a half wavelength (or one and a half wavelengths), to obtain the maximum transformer ratio the bunch charge should rise from head to tail in the train as the ratios of odd integer numbers. For the Gaussian longitudinal density of a bunch, the charge of the nth bunch should change according to the relation [17] $Q_n = Q_1[1 + T(n-1)]$, where Q_1 is the charge of the first bunch, and **T** is the transformer ratio of a single bunch. In the case of a multimode device, such a simple formula does not exist; therefore to obtain desirable locations of bunches and values of their charges it is necessary to run simulations, the number of which is equal to the number of bunches in the train. First, a calculation with one bunch is carried out, a location of the maximum of an accelerating field in the drive bunch channel is determined, and at this location the second bunch is placed and a new calculation of structure excitation is performed. At the location of the second bunch, the superposition is such that the field there becomes decelerating. Then, each subsequent drive bunch is to be located at the maximum of the accelerating field from the prior bunches, and the charge of the nth bunch is set according to the formula $Q_n = Q_1[1 + T_{n-1}]$, where T_{n-1} is the transformer ratio after the $(n-1)$st bunch. An answer to the goal of improved transformer ratio is provided by the result shown in Fig. 6. In this example the computation is run out to a greater distance, 201 mm to the front edge of the first drive bunch. The spaces between the bunches are, respectively, approximately 2.5, 2.5, and 4.5 wakefield periods, and the charge ratios are 1.0, 2.4, 3.5, and 5.0; again, maintaining the constant total drive bunch charge at 200 nC. The **T** from the last bunch is 17, a factor of 5 times as large as the **T** for the simple four-bunch train of equal charges spaced by one wakefield period. Notice the peak wakefield amplitude following the fourth drive bunch is only 28 MeV/m, down from 50 MeV/m in

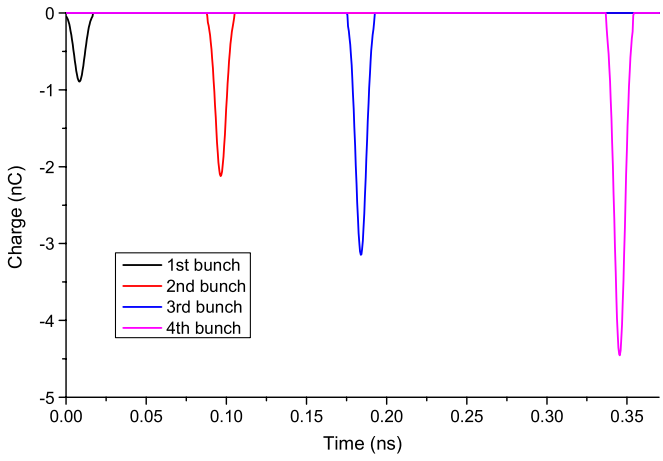

FIG. 7. Spacing and charge, emitted per one computation time step ($\Delta t = 4.4 \times 10^{-4}$ ns), of the four drive bunches used for the computation of wakefields shown in Fig. 6.

Figs. 3 and 4. This prescription for the drive bunch charge and spacing was obtained by striving for uniform drive bunch deceleration, which means that this arrangement should extract more energy from the entire drive bunch train than that, e.g., shown in Fig. 3. A graph of the four drive bunches, showing their relative charges, Gaussian shape, and spacing, is provided in Fig. 7. This example establishes that a considerable enhancement of **T** is possible in the multimode CDWA system using a flexible RBT method. The more complex algorithm (in comparison with [7,17]) for the bunch charge distribution and bunch locations is related to the multimode excitation of the CDWA. Of course, for single-mode structures, the conventional algorithm applies.

The nonuniform spacing of these drive bunches may present a problem for the accelerator system used to prepare them. However, the first three bunches are uniformly spaced, and the transformer ratio of the second bunch is 7.9, and after the third bunch it is 10.6. Thus, an experimental test of this method is feasible. The four drive bunches in the example of Fig. 6 each experience nearly the same decelerating force (~ 1.5 MeV/m).

A natural question arises about the robustness of this method of optimization of the transformer ratio, namely, its sensitivity to fluctuations in charge distribution between the bunches or changes in the distances between the bunches. To answer this question, we performed a series of computations in which the ratio of the last bunch charge Q_4 to the first bunch charge Q_1 was varied, while the other parameters of the bunch train, including total charge, were fixed. The results of computations are shown in Fig. 8. A maximum transformer ratio of 18.6 is achieved for the charge ratio $Q_4/Q_1 = 4.8$. Decreasing the optimal charge ratio by 10%, the transformer ratio falls to a value of 17. Increasing the optimal charge ratio by 10%, transformer ratio falls to a value 13.8. Thus, we can conclude that 20% uncertainty in the RBT charge distribution does not cause a catastrophic change of the transformer ratio. From these computations we find also the accelerating gradient is even less sensitive to the charge fluctuations. For the same 20% range of the charge variation the value of the accelerating gradient changes from 26.7 to 29.5 MeV/m.

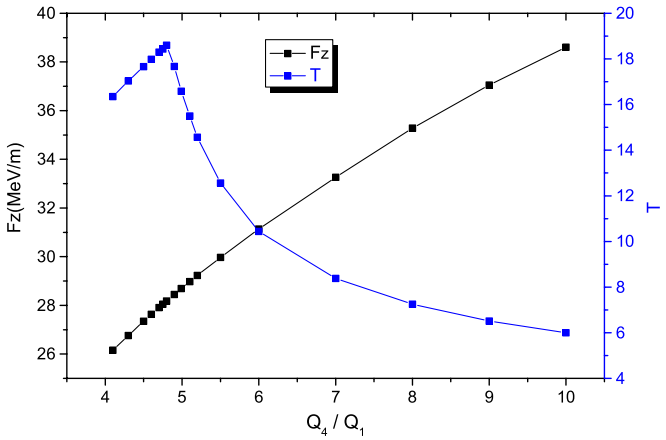

FIG. 8. Transformer ratio (blue symbols) and accelerating gradient (black symbols) versus the ratio of the last bunch charge to the first bunch charge. The other parameters of the bunch train and the CDWA are the same as in Fig. 6.

Finally, we have studied the applicability of the ramped drive bunch train for four bunches to a high gradient THz CDWA structure [19]. Here the question is whether the removal of wakefields due to the group velocities phenomena will permit the superposition of wakefields from the train of delayed drive bunches, because the THz structure is very lightly loaded with dielectric and so the wave group velocity is very close to the particle velocity. It turns out that indeed all four drive bunches do not completely outrun the back front of the Cherenkov radiation in the short distance that we can study here. However, the back front of the wavefields does drop back significantly from each bunch of the train, enough so that one may locate the following bunch so as to engage the desirable effect of wakefield superposition and also find an enhanced **T**. Thus, the RBT technique could find application in small THz collider-type structures. An example of this is shown in Fig. 9 for a diamond dielectric CDWA structure that has a radius ~ 0.8 mm and a design frequency of 0.44 THz, where it can be seen that the wakefield amplitude builds up progressively behind the four drive bunches. For comparison, the four 5 GeV drive bunches with charges totaling 6 nC here set up a peak longitudinal wakefield amplitude ~ 300 MeV/m with $T = 17$, which is to be compared with a wakefield ~ 500 MeV/m with $T = 5.5$ from a single 6 nC bunch [1].

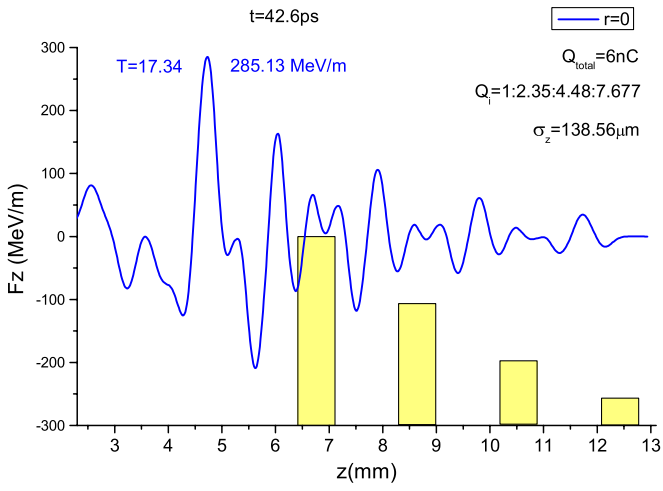

FIG. 9. Wakefield amplitude buildup from a four-drive bunch RBT in a THz CDWA. The bunch energy is 5 GeV, and the total charge Q, bunch rms size σ_z, **T**, and charge ratios are displayed on the graph. The head of the first drive bunch is located at $z = 12\,771$ μm. The bunch spacing is approximately 1890 μm and the bunch length parameter is $\sigma_z = 139$ μm. The bunches move from left to right.

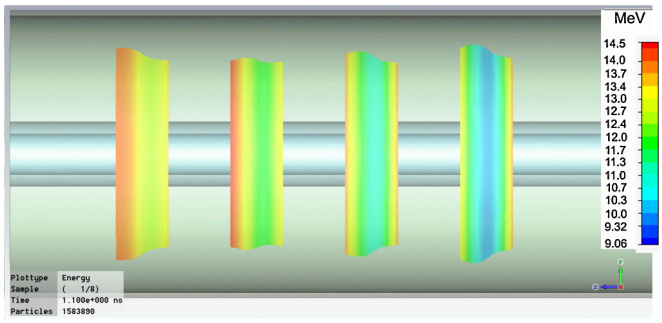

FIG. 10. Right side view of four drive bunches, initially centered on the structure axis, moving from right to left, along a CDWA structure specified in Table I. The color scale on the right shows the energy of the particles. These drive bunches are spaced apart by one period of the design mode, 10.67 mm and have moved 1.1 nsec.

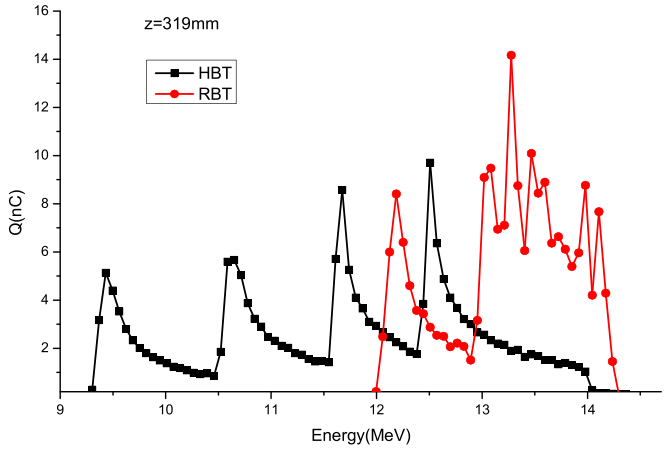

FIG. 11. Distribution functions of drive bunch particles after traveling 319 mm for the HBT (black symbols) and for the RBT (red symbols). The leftmost peak of the distribution function of the RBT is determined by the fourth bunch.

III. MOTION OF DRIVE BUNCH TRAINS

We begin by studying the motion of four drive bunches along the CDWA; the PIC code was run 1.1 nsec (33 cm) as the four drive bunches move along the structure, as specified in Table I. The drive bunches have equal charge and they are equally spaced by the period of principal wakefield mode. For this case, axial profiles of the wakefield were presented in Fig. 3. Figure 10 shows that at the end of travel, the drive bunches have moved with only slight distortion, which on further study is found to be a slight expansion/contraction of bunch diameter, symmetrically patterned around the azimuthal direction. Furthermore, it has been found displacement of the bunch by 1 mm from the axis of symmetry does not set up deflecting motions of the drive bunch train in this distance either [1]. Computational limitations preclude following the drive bunch train further, but this result establishes that, at least for this geometry, the motion of the drive bunches is approximately stable. Study of multi-GeV RBT stability for an accelerator having lengthy sections remains to be done.

From the energy scale given at the right side of Fig. 10 it follows that the maximum energy loss of bunch particles is ~5 MeV; this coincides with estimates obtained from the maximum decelerating force (~ 15 MeV/m) acting on the fourth drive bunch (see Fig. 3). A more precise value of 4.7 MeV and more detailed information about the energy distribution of all particles in the homogeneous bunch train (HBT) case of Fig. 3 is presented in Fig. 11 (black symbols and line). The four peaks on the distribution function correspond to the four drive bunches located in the linearly increasing retarding field. The average energy loss of all particles is 2.36 MeV. For comparison, in this figure is shown in red the energy distribution function of the ramped bunch train (Fig. 6) case. The average energy loss for the RBT is 0.76 MeV. Therefore, the travel distance of the RBT train should be greater by 3.1 times. The accelerating gradient for the RBT case is smaller, by a factor ~1.8, than the acceleration gradient for the HBT case. From these numbers we find that the energy gain of a test bunch in the RBT case will be greater by a factor 1.7 than the corresponding energy gain for the HBT. It should be noted that this number can be improved if we can reduce the unexpected energy loss of fourth bunch.

We now compare the results of Figs. 10 and 11 with a similar study for a cylindrical collinear DWA structure, specified in Table II. Essentially the structure has the same radius and outer alumina cylindrical shell as our CDWA

TABLE II. Parameters used for study of a cylindrical dielectric-lined collinear DWA.

Design mode	~23.7 GHz
External radius of dielectric tube	14.05 mm
Inner radius of dielectric tube	13.512 mm
Relative dielectric constant ε	9.8
Bunch axial rms dimension $2\sigma_z$ (Gaussian charge distribution)	2.0 mm
Full bunch length used in PIC simulation	5 mm
Drive bunch radius (box charge distribution)	5 mm
Bunch energy	14 MeV
Total bunch charge	200 nC
Number of bunches	4

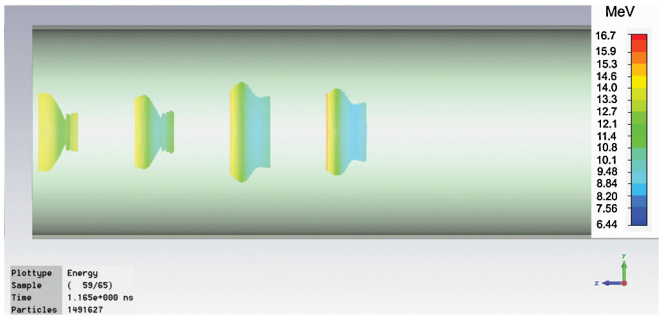

FIG. 12. Right side view of four drive bunches, initially centered on the structure axis, moving from right to left, along a cylindrical collinear DWA structure specified in Table II. The color scale on the right shows the energy of the particles. These drive bunches are spaced apart by one period of the design mode and are shown after 1.16 nsec of travel.

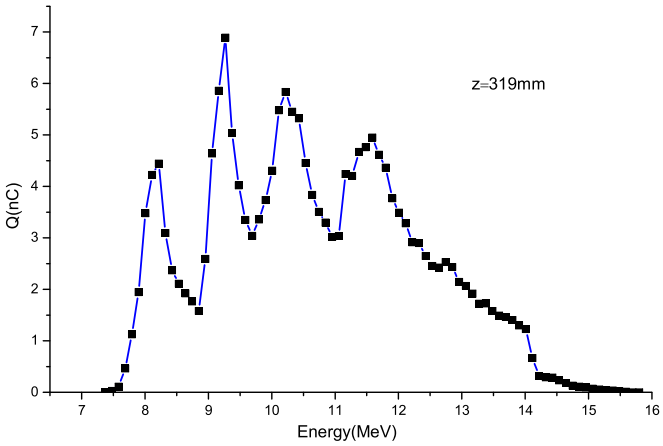

FIG. 13. Distribution function of HBT particles after traveling 319 mm in the cylindrical collinear DWA structure.

structure, but the central coaxial dielectric cylinder has been removed and the drive bunches are now cylindrical ''pills'' having radius 5 mm that have the same charge and energy as the annular drive bunches in Table I. Drive bunches are spaced apart by the wakefield wavelength of the principal mode (12.64 mm). Figure 12 shows the drive bunches at 1.16 nsec. It is apparent that the distortion of the drive bunches in the cylindrical collinear structure is more severe than in the CDWA structure. The field solutions in the cylinder are not the same as in the CDWA, so this result should not be surprising. These computations show that one must be cautious in assuming that the drive bunches move without significant changes in form. However, for purposes of this study of the CDWA, we believe it is fair to state that the drive bunches evidence minor modification of shape in the 20 cm (0.67 nsec) of travel that we used in the examples used in Sec. II.

The distribution function for the homogeneous bunch train for the cylindrical collinear DWA structure is shown in Fig. 13. Comparing this plot with the similar plot in Fig. 11, one concludes that the energy spread of the drive bunch particles in the CDWA device is significantly less than in the collinear cylindrical DWA device. The average particle energy loss at the bunch location $z = 319$ for the cylindrical collinear device is 3.36 MeV, i.e., greater by $\sim$1.5 times than in the coaxial device, although the accelerating gradient after the bunch train is almost the same. Thus, the CDWA appears to be the preferred device for using the RBT technique.

IV. DISCUSSION

By choosing a flexible algorithm for the charges and spacings of a short train of drive bunches that excite wakefields in a multimode dielectric wakefield accelerator, we have found that a considerable increase of the transformer ratio can be obtained. Furthermore, the use of such a programmed train of drive bunches permits the designer to *control* the transformer ratio independently of the dielectric structure parameters. The procedure for obtaining the best transformer ratio relies on the principle of having all drive bunches decelerate uniformly, but the use of numerical methods to obtain the result permits the designer to adapt the principle to the details of wakefield generation by the drive bunch train, such as the excitation of more than one wakefield mode. The method appears to be suitable for handling smaller structures that can generate very high acceleration gradients. The concept described here is limited to instantaneous excitation of a nonresonant (smooth) dielectric-lined waveguide by a train of only a few bunches.

While the motion of the bunch train could be studied numerically for 14 MeV bunches traveling only 33 cm, in this distance no breakup or deflection of the bunch train was found for the CDWA. An instability would be expected to affect the last drive bunch more than the first, which was not found to happen.

ACKNOWLEDGMENTS

This research was supported by the U.S. Department of Energy, Office of High Energy Physics, Advanced Accelerator R&D. The authors thank Professor J. L. Hirshfield for his advice concerning this work.

[1] G. V. Sotnikov, T. C. Marshall, and J. L. Hirshfield, Phys. Rev. ST Accel. Beams **12**, 061302 (2009).
[2] M. C. Thompson *et al.*, Phys. Rev. Lett. **100**, 214801 (2008).
[3] R. D. Ruth, A. W. Chao, P. L. Morton, and P. B. Wilson, Part. Accel. **17**, 171 (1985).
[4] A. W. Chao, *Physics of Collective Beam Instabilities in High Energy Accelerators* (Wiley, New York, 1993).
[5] G. A. Voss and T. Weiland, Report No. DESY M-62-10, 1982.

[6] K. L. F. Bane, P. B. Wilson, and T. Weiland, in *Physics of High Energy Particle Accelerator*, AIP Conf. Proc. No. 127 (AIP, New York, 1985), p. 875.
[7] C. Jing, A. Kanareykin, J. G. Power, M. Conde, Z. Yusof, P. Schoessow, and W. Gai, Phys. Rev. Lett. **98**, 144801 (2007).
[8] C. Jing, J. G. Power, M. Conde, W. Liu, Z. Yusof, A. Kanareykin, and W. Gai, *AAC: Fourteenth Workshop*, edited by S. Gold and G. Nusinovich, AIP Conf. Proc. No. 1299 (AIP, New York, 2010), p. 348.
[9] K. L. Bane, P. Chen, and P. B. Wilson, IEEE Trans. Nucl. Sci. **32**, 3524 (1985).
[10] J. T. Seeman, IEEE Trans. Nucl. Sci. **30**, 3180 (1983).
[11] P. Schutt, T. Weiland, and V. M. Tsakanov, Probl. At. Sci. Technol., Ser. Nucl. Phys. Invest. **7**, 12 (1990).
[12] J. P. Delahaye, CERN Particle Physics Seminar, http://clic-study.web.cern.ch/CLIC-Study/Presentations/20050421.pdf.
[13] E. Chojnacki, W. Gai, P. Schoessow, and J. Simpson, in *Proceedings of the IEEE 1991 Particle Accelerator Conference (APS Beams Physics)* (IEEE, Piscataway, NJ, 1991), Vol. 5, pp. 2557–2559.
[14] M. E. Conde, W. Gai, R. Konecny, J. Power, P. Schoessow, and P. Zou, in *AAC: Eighth Workshop*, edited by W. Lawson, C. Bellamy, and D. F. Brosius, AIP Conf. Proc. No. 472 (AIP, New York, 1998), p. 626.
[15] I. N. Onishchenko, D. Yu. Sidorenko, and G. V. Sotnikov, Phys. Rev. E **65**, 066501 (2002).
[16] V. A. Balakirev, I. N. Onishchenko, D. Yu. Sidorenko, and G. V. Sotnikov, J. Exp. Theor. Phys. **93**, 33 (2001).
[17] S. S. Vaganyan, E. M. Lasiev, and V. M. Tsakanov, Probl. At. Sci. Technol., Ser. Nucl. Phys. Invest. **7**, 32 (1990) (in Russian).
[18] Algorithm used in [7,17] for the increasing of the transformer ratio is correct, but its applicability is limited by single-mode structures.
[19] T. C. Marshall, G. V. Sotnikov, and J. L. Hirshfield, *AAC: Fourteenth Workshop*, edited by S. Gold and G. Nusinovich, AIP Conf. Proc. No. 1299 (AIP, New York, 2010), p. 336.